ABSTRACT

Title of Document: MECHANISMS UTILIZED BY *NEISSERIA GONORRHOEAE* TO PERSIST IN THE HUMAN CERVICAL EPITHELIUM: SIGNALING, INVASION, INTRACELLULAR SURVIVAL, AND ESCAPE

Samuel Earl Bish, Doctor of Philosophy, 2007

Directed by: Daniel C. Stein
Professor, Department of Cell Biology and Molecular Genetics

The obligate human pathogen *Neisseria gonorrhoeae* (gonococci) causes the sexually transmitted disease gonorrhea. Interactions between gonococci and human cervical epithelial cells that promote bacterial invasion and post-invasion survival were examined. The data showed that gonococci activated MAPK signaling in cervical epithelial cells prior to invasion. Gonococci triggered prolonged ERK phosphorylation (possibly through EGFR signaling), which could facilitate gonococcal invasion. Furthermore, gonococci expressing lacto-*N*-neotetraose LOS decreased JNK activation and elicited lower IL-8 production from host cells compared to variants expressing lactosyl LOS. I propose that gonococci can manipulate MAPK signaling to facilitate invasion into cervical epithelial cells and to evade the innate immune response.

To investigate gonococcal invasion, I expressed β-lactamase on the outer membrane of gonococcal strain FA1090 to generate the reporter strain FA1090 Φ(*bla-iga'*). Utilizing a β-lactamase reporter assay, I demonstrated that FA1090 Φ(*bla-iga'*) only invaded a subpopulation of cervical epithelial cells. Nonviable FA1090 Φ(*bla-iga'*) did not invade host cells and failed to recruit F-actin to sites of adherence. Viable

gonococci required pili expression but not Opa expression to invade susceptible host cells. These data suggest that viable gonococci elicit invasion-promoting interactions with host cells not triggered by nonviable gonococci.

Finally, the data demonstrated that gonococci realize different intracellular fates after entry into cervical epithelial cells. I developed a tannic acid survival assay to show that intracellular gonococci survived within host cells. Intracellular survival did not require catalase or the NfsB nitrogen reductase. A subpopulation of gonococci could escape from cells back into the extracellular milieu. Gonococci utilized an exocytosis pathway to escape after invasion that was blocked by treating cells with tannic acid, but not cytoskeletal inhibitors.

I propose a working scenario whereby gonococci undergo cycles of invasion into and escape from a susceptible subpopulation of cervical epithelial cells. Gonococci that survive within host cells may represent bacteria that progress into deeper host tissues to disseminate to secondary sites. Escaping gonococci could invade into other host cells and are well-positioned for transmission to another host. Gonococci interact with the cervical epithelium through invasion, intracellular survival, and escape to establish bacterial persistence in the female host.

MECHANISMS UTILIZED BY *NEISSERIA GONORRHOEAE* TO PERSIST IN THE HUMAN CERVICAL EPITHELIUM: SIGNALING, INVASION, INTRACELLULAR SURVIVAL, AND ESCAPE.

By

Samuel Earl Bish

Dissertation submitted to the Faculty of the Graduate School of the
University of Maryland, College Park, in partial fulfillment
of the requirements for the degree of
Doctor of Philosophy
2007

Advisory Committee:

Professor Daniel C. Stein, Chair
Professor Michael Co Ma
Professor David M. Mosser
Professor Wenxia Song
Professor Richard C. Stewart

Dedication

This work is dedicated to my parents (Dale and Kathleen Bish) and to my grandparents (Earl, Katherine, William, and Mary Lou)—the people who taught me the values of hard work, a strong moral character, a steadfast faith, and a genuine respect for other people.

Acknowledgements

I would like to thank my advisor, Dr. Dan Stein, for your guidance, support, and patience on both scientific and career matters. I thank you for your hard work and determination through both the prosperous and difficult time periods in our laboratory. I also thank you for allowing me to travel to Oslo, Norway; Cairns, Queensland, Australia; and Wintergreen, VA for beneficial scientific conferences and unforgettable experiences. I also appreciate how you balance your scientific career and family life to achieve success in both areas. Thank you to my co-advisor, Dr. Wenxia Song, for your technical expertise, scientific advice, and positive encouragement. I would also like to thank Dr. David Mosser for your guidance and support and your leadership in the forward advancement of infectious disease research at the University of Maryland. I would also like to thank Dr. Richard Stewart for your guidance and excellent teaching ability. Also, thank you to Dr. Michael Ma for your willingness to serve as my dean's representative.

Professionally, I thank the many people beyond my committee and advisors who assisted me in progressing through graduate school. To the Stein lab, you are not only my colleagues, but more importantly my friends: Julie, Ellen, Karen, Mark, Clint, Adriana, Chris, Meredith, Derek, Hwalih, Azy, Anne, Esteban, Kathryn, Dr. Andrzej Piekarowicz, and Dr. J. MacLeod Griffiss. Among them, I would like to provide a special thanks to Julie for allow me to collaborate on your manuscript and to Karen for your helpful discussions and critiques of my research and writing. Also, a special thanks to Dr. Piekarowicz and Dr. Griffiss for your helpful science discussions and encouragement. Furthermore, I would like to thank members of the Song lab (Nandini, Segun, Shruti, Sara, Vonetta, and Katie), Mosser lab (Sean, Anni, Justin, Suzanne, Tricia, Chuck, Dalit,

Maria-Chiara, Xia, and Shanjin), and the Hutcheson lab (Mike, Nate, Jamie, Liliana, and James). I would also like to thank Dr. Ann Smith and Dr. Patty Shields for your teaching support and general encouragement throughout graduate school. Thank you to Dr. Dina Sigano and Dr. Melissa Maderia from the NCI and Mark Kenyon from the University of Maryland Career Services for your professional career advice and guidance. I would like to thank the CBMG staff, especially Nancy Williams for your encouragement and Ruth Mausolf for your hard work in helping our lab function and for your friendly attitude.

I would also like to thank those individuals who provided technical support. Thank you to Dr. Susan Pierce for allowing me to access the flow cytometry facility at the NIAID and thank you to Dr. Song for arranging this access. Thank you to Dr. Robert Brown, Amy Beaven, and the personnel at Zeiss Microimaging, Inc.—Jen Malloy, Ruth Redman, Elise Shumsky, and Dan Stevens—for assistance and expertise in microscopy.

Beyond the scientific arena of graduate school, I would like to acknowledge the positive distractions that provided enjoyment and needed balance during graduate school. Thank you to the Pittsburgh Steelers for the Super Bowl XL Championship and the University of Maryland men's basketball team from the 2002 National Championship. Thank you to all the members of the CBMG Fantasy Football League, the CBMG intramural basketball team, and all the participants in our March Madness fun for the competition and fun social interactions. Thank you to the SportsTalk 980 radio personalities, especially the Sports Reporters Andy and Steve, for providing entertainment during all those hours at the lab bench and while sitting in traffic getting to and from school.

I would like to acknowledge and thank all of the additional people in my life that helped guide me emotionally, spiritually, and caringly with their love and/or friendship during these years. Thank you to Sean, Rachel, Noah, and Charlie Conrad not only for providing me with a residence during most of my graduate school years, but also for including me as a part of your family life. I will be forever grateful for your friendship and the sacrifices you made for me. A special thanks to Sean for all of those conversations at the dinner table when we just refused to let each other give up on our goals and for being someone I consider one of my best friends. Also, thank you to John and Rosemary Russ for providing me with housing and your friendship in the later stages of graduate school. I would like to thank all of my friends at Derwood Bible Church for your guidance, wisdom, and friendship—Pastor Steve and family, Pastor Colin and family, Pastor Todd and family, Pastor Scott and family, Pastor Pete and family, Pastor John and family, Jim and Kate, Jason and Donna, Josh and Jen, Travis, InShil, Chris, Liz, Tim, Trisha, Vicki, Colleen, Nate, Laura, Joyce, Ryan P., Danielle, Dustin and Beverly, Ryan B., Brittany, Mike and Carol. A special thanks to Mike and Carol for being like second parents during these years and your continued willingness to open your home to me. Also, a special thanks to Dustin, Ryan, and Brittany for treating me like another brother; I consider all three of you among my best friends and thank you Dustin for all of those encouraging conversations that helped me persevere through these years. I would also like to thank Mandy for your willingness to always see the good in me and your steadfast belief in me. To all of my friends, I want you all to know I appreciate all you have done for me.

Finally, I want to thank my family for loving me and believing in me with unwavering consistency. To my brother Nathan and sister-in-law Jessica, thank you for your support. Nathan, I thank you for your level-headed approach to life that I have always looked up to and I admire the man you have become. I am proud to be your brother. To my dad and mom, Dale and Kathleen, I would not have made it through this journey without those weekly phone calls and your constant prayers. I thank you for your immeasurable sacrifices over the years to allow me to have opportunities to grow and achieve. You are great parents and I am so fortunate that you are my parents. I love you.

Table of Contents

List of Tables

List of Figures

List of Abbreviations

3-deoxy-D-*manno*-2-octulosonic acid……...…KDO

acid sphingomyelinase……..ASM

activator protein 1……..…AP-1

adenosine triphosphate……...ATP

ampere(s)……..…..Amp

antibody…….……Ab

antigenic variation……....AV

arbitrary units…….…..AU

asialoglycoprotein receptor……..ASGP-R

bacterial lysate……..…BL

base pairs……...bp

beta-lactamase…….……Bla

bovine serum albumin……BSA

Campylobacter jejuni…….....CJ

carbon dioxide…….CO_2

carcinoembryonic antigen cellular adhesion molecules……...……CEACAM

colony forming units……..CFU

complement receptor 3……...CR3

contact regulatory element of *Neisseria*……....….CREN

cephalosporin core linking 7-hydroxycoumarin to fluorescein……..……..CCF2

cytidine-5'-monophospho-N-acetylneuraminic acid……..……..CMP-NANA

cytosolic nucleotide oligomerization domain (proteins)……..……..NOD

degrees Celsius……...^{o}C

deoxyribonucleic acid……...DNA

dimethyl sulfoxide……..……DMSO

disseminated gonococcal infections……....DGI

enzyme-linked immunosorbent assay……..…ELISA

epidermal growth factor receptor……..…EGFR or ErbB1

extracellular signal regulated kinase…….…….……ERK

fetal bovine serum……...FBS

filamentous actin…….F-actin

final concentration…….fc

globular actin…….G-actin

gonococcal uptake sequence…….…….GUS

gravity……..*g*

heparan sulfate proteoglycans…….HSPG

high performance liquid chromatography……...HPLC

hour(s)……..h

immunoglobulin……..Ig

immunotyrosine inhibitory motif……..ITIM

immunotyrosine activating motif…….ITAM

interleukin……..IL

intracellular survival……ICS

invasion media……..IM

Jun-N-terminal kinase…….JNK

kilobase(s)……..……kb

kilodalton(s)……...…….kDa

lacto-n-neotetraose…….…..LnNT

laser scanning confocal microscopy……...LSCM

lipooligosaccharide……..……...LOS

lipooligosaccharide glycosyl transferase……...lgt

Luria-Bertani…….LB

lysosomal associated membrane protein……..…LAMP

microgram(s)……..µg

microliter(s)……µl

micrometer(s)……µm

micromolar……...µM

milligram(s)…...……...mg

milliliter(s)…….ml

millimeter(s)...…….mm

millimolar……mM

minute(s)……..min

mitogen-activated protein kinase……MAPK

molar……...M

molecular weight……MW

multiplicity of infection……..MOI

myeloperoxidase……....MPO

myosin light chain kinase……...…MLCK

N-acetyl galactosamine…….……GalNAc

naladixic acid resistant……...Nal^R

nanogram(s)...……ng

nanometer(s)...……..nm

Neisseria gonorrhoeae, gonococci, or gonococcal……..GC

nitric oxide……...…NO

nonsialylated…….....NS

nuclear factor-kappaB.……....NF-κB

opacity-associated proteins…….……Opa

optical density……..OD

oxygen gas…….O_2

pathogen-associated molecular patterns……...……...PAMP

phase variation……...…PV

pelvic inflammatory disease……....PID

penicillin G……...PenG

phosphate-buffered saline……...PBS

phosphatidylinositol-3-kinase…….……...PI3K

phosphatidylinositol-3-phosphate……...…PI3P

phosphatidylinositol-4,5-bisphosphate……...PIP_2

phosphocholine-phospholipase C…….…PC-PLC

phospholipase D…….PLD

pictogram(s)…..……pg

pili……....P

p-nitrophenyl phosphate……...PNPP

polymerase chain reaction……..PCR

polymorphonuclear cells……...PMN

polyvinylidene difluoride……..……..…….PVDF

porin B 1A……...…….Por B

primary human urethral epithelial cells……....PHUEC

protein 21 activated kinase…….PAK

protein 38……p-38

protein kinase C……..PKC

reactive nitrogen intermediates……...RNI

reactive oxygen intermediates…….……ROI

revolutions per minute…….rpm

ribosomal S6 kinase 1……..RSK1

rifampicin resistant…….Rif^R

room temperature……..RT

second(s)……...sec

secretory……...……Sec

sexually transmitted disease……...STD

sialylated……..…S

sodium dodecyl sulfate polyacrylamide gel electrophoresis……..SDS-PAGE

spectinomycin resistant……$Spec^R$

standard deviation……..…SD

standard error of the mean…….SEM

streptavidin-alkaline phosphatase……...SAP

streptomycin resistant…….Sm^R

tannic acid…….TA

toll-like receptor…….TLR

translocated intimin receptor……..…Tir

Tris-borate-EDTA……..TBE

Type III-secretion system…….TTSS

tumor necrosis factor alpha….……..……...TNFα

uncomplicated gonorrhea……...……..UG

units…….U

volts……..……V

wavelength……...λ

Introduction

Background and Significance

Neisseria gonorrhoeae (gonococci, or GC) is an obligate human pathogen that causes the venereal disease gonorrhea. People with GC infections are also commonly co-infected with *Chlamydia trachomatis* and are predisposed to increased HIV transmission (148, 169, 213, 306). According to recent statistics from the Center for Disease Control and Prevention, gonorrhea is the second most common notifiable and sexually transmitted disease (STD) in the United States (1, 306). Nearly 340,000 cases were documented in 2005—the first increase in the incidence of gonorrhea since 1999—and an estimated 600,000 new GC infections occur each year (1, 306). Cephalosporins are the only remaining class of drugs recommended to treat gonorrhea. The rise in fluoroquinolone resistant GC has eliminated this class of antimicrobials as a recommended treatment (1). GC are facultative anaerobes that are classically identified in infected individuals as Gram-negative diplococci within neutrophil-containing exudates (133, 306). GC express variable surface components and do not generate a productive adaptive immune response, which have prevented the development of a suitable vaccine to prevent GC transmission.

GC disease remains a major source of morbidity in the male and female genital tracts and many of the clinical symptoms and outcomes of disease are gender-specific. GC usually infect the male urethra or the female cervix, but they are capable of colonizing almost any mucosal surface, including the nasopharynx, conjunctiva of the eye, fallopian tubes, and rectum. Around 90% of men develop uncomplicated gonorrhea (UG) 2-5 days after GC exposure and realize few secondary complications after treatment

(270). UG is a symptomatic disease characterized by local inflammation where neutrophils migrate to the site of infection to phagocytose GC and generate proinflammatory cytokines that damage the surrounding tissues (69). Tissue damage in the male urethra leads to the characteristic symptoms of GC disease in men—dysuria and the mucopurulent discharge of mucosal epithelial cells and neutrophils (239, 304).

In women, GC may cross the mucosal barrier by triggering bacterial-mediated endocytosis (invasion) into cervical epithelial or endothelial cells (69, 73, 261, 266, 288-290). Invasion into host cells protects GC from components of the innate and humoral immune system to help GC avoid symptom elicitation (190, 192). Often in women, GC invade at a low-level without generating a substantial inflammatory response or creating recognizable symptoms (asymptomatic) during the initial stages of disease (306). Asymptomatic women do not realize they are infected and fail to seek treatment allowing GC to spread to secondary sites (62). GC can ascend into the normally sterile upper reproductive tract, including the fallopian tubes and uterus, to elicit severe tissue destruction, scarring, and chronic inflammation that leads to secondary complications, such as pelvic inflammatory disease (PID), ectopic pregnancy, salpingitis, and/or infertility (62, 119, 172, 202). GC can also transcytose through epithelial tissues into subepithelial regions where they encounter phagocytes (261). On rare occasions, GC can reach the bloodstream, become serum resistant, and disseminate throughout the body (291). Women are more susceptible to these disseminated gonococcal infections (DGI) that can lead to gonococcal arthritis, septicemia, or bacteremia in 1-3% of infected individuals (37, 52).

Role of Antigenic and Phase Variation in GC Pathogenesis

Phase variation (PV), turning on and off the expression of genes in response to environmental cues or due to mistakes in replication, and antigenic variation (AV), modifying the amino acid sequence/structural appearance of cellular components, provide GC with mechanisms to modify their cell surface. In other words, progeny derived from a single GC ancestor will be a mixed population of surface variants since each GC has the potential to express a unique combination of surface molecules due to PV and AV. GC can modulate the expression of several surface proteins, glycoproteins, and glycolipids by PV and/or AV. The generated variability allows GC to interact with various host cell types and take advantage of new environments encountered during infection. PV and AV result in GC expressing a repertoire of surface ligands that can bind to a variety of host cell receptors on different cell types (188, 190). Surface modifications due to PV and AV also permit GC to mimic host structures and avoid recognition by pathogen associated molecular pattern (PAMP) receptors, such as toll-like receptors (TLR) and cytosolic nucleotide oligomerization domain (NOD) proteins, in order to evade immune surveillance and persist in host tissues (190, 197). Pili, opacity proteins (Opa), and lipooligosaccharide (LOS) are three major GC surface components that undergo PV and AV and play important roles in adherence, invasion, intracellular fate, and innate immune evasion.

GC Interactions with Epithelial Cells

A. Overview of GC-Epithelial Cell Interactions and Host Defense Against Infection

Upon transmission to a new host, GC encounter mucosal epithelial cells, an initial barrier of innate immune defense. Epithelial cells provide protection for underlying tissues and allow for secretion and absorption exchanges with the external environment. They can be ciliated or nonciliated, simple or stratified, and are classified into three general shape categories—columnar, cuboidal, and squamous. GC seem to preferentially colonize nonciliated mucosal epithelial cells, such as those found in the female cervix, endometrium, and fallopian tubes (177).

Our understanding of GC infection of human cells is derived from clinical human challenge, the estradiol-treated mouse model, and tissue culture cell models that support gonococcal interactions *in vitro*, including primary human organ or cell cultures and transformed cell lines (137, 250). When GC are transmitted to a new female host, cervical epithelial cells represent one of the initial cell types encountered and a primary location for GC to establish infection (232). In the data presented here, I primarily utilized the ME180 cervical carcinoma cell line as a model for GC infection of the cervical epithelium. ME180 cells were originally isolated from an omental metastasis in a patient exhibiting a rapidly spreading cervical carcinoma (276). This cell line maintains many of the morphological characteristics found in a typical differentiated epithelial layer, including desmosomes, tonofilaments, and epidermal filaments (277), suggesting these cells bear close resemblance to normal cervical epithelial cells. ME180 cells support GC attachment and invasion and are capable of proinflammatory cytokine production, which mimic the cellular responses to GC infections in primary cervical and endometrial cells (35, 42, 78, 104, 146, 266). Ultimately, natural human challenge studies in women are not possible due to the ethical restrictions imposed by the asymptomatic

and disseminating nature of GC disease in women. Therefore, I cannot be certain that the pathogenicity displayed by GC during infection of ME180 cells will completely reflect natural infections (60). However, several of the virulence factors GC utilize to infect ME180 cells, including pili, Opa, and LOS, have been shown to contribute to infection in human challenge studies with men, primary cell models, and other immortalized cell lines that support GC infection (42, 106, 138, 234, 253). Overall, ME180 cells can serve as a suitable model to investigate various aspects of GC infection of the human cervical epithelium.

From in vitro models, such as ME180 cells, research has demonstrated that GC infection of epithelial cells occurs in several stages—initial attachment, intimate adhesion to the plasma membrane, invasion into the cell, intracellular survival and persistence, and transcytosis to the subepithelium or escape back into the extracellular environment (Fig. 1). At each stage, GC must overcome the innate immune responses of host tissues and initiate signaling pathways in epithelial cells to orchestrate continued progression of the infection. GC establish persistence within the host at a low level where they do not elicit a profound proinflammatory response, yet are still transmitted readily within the population.

B. Adherence: Attachment and Intimate Adhesion

Pili or fimbriae represent the most common adhesin utilized by pathogens, including GC, to make initial contact with host cells. Some bacteria possess nonpilus adhesins to secure attachment to cells. In general, one class of these adhesins bind to extracellular matrix components and include fibronectin binding proteins, collagen

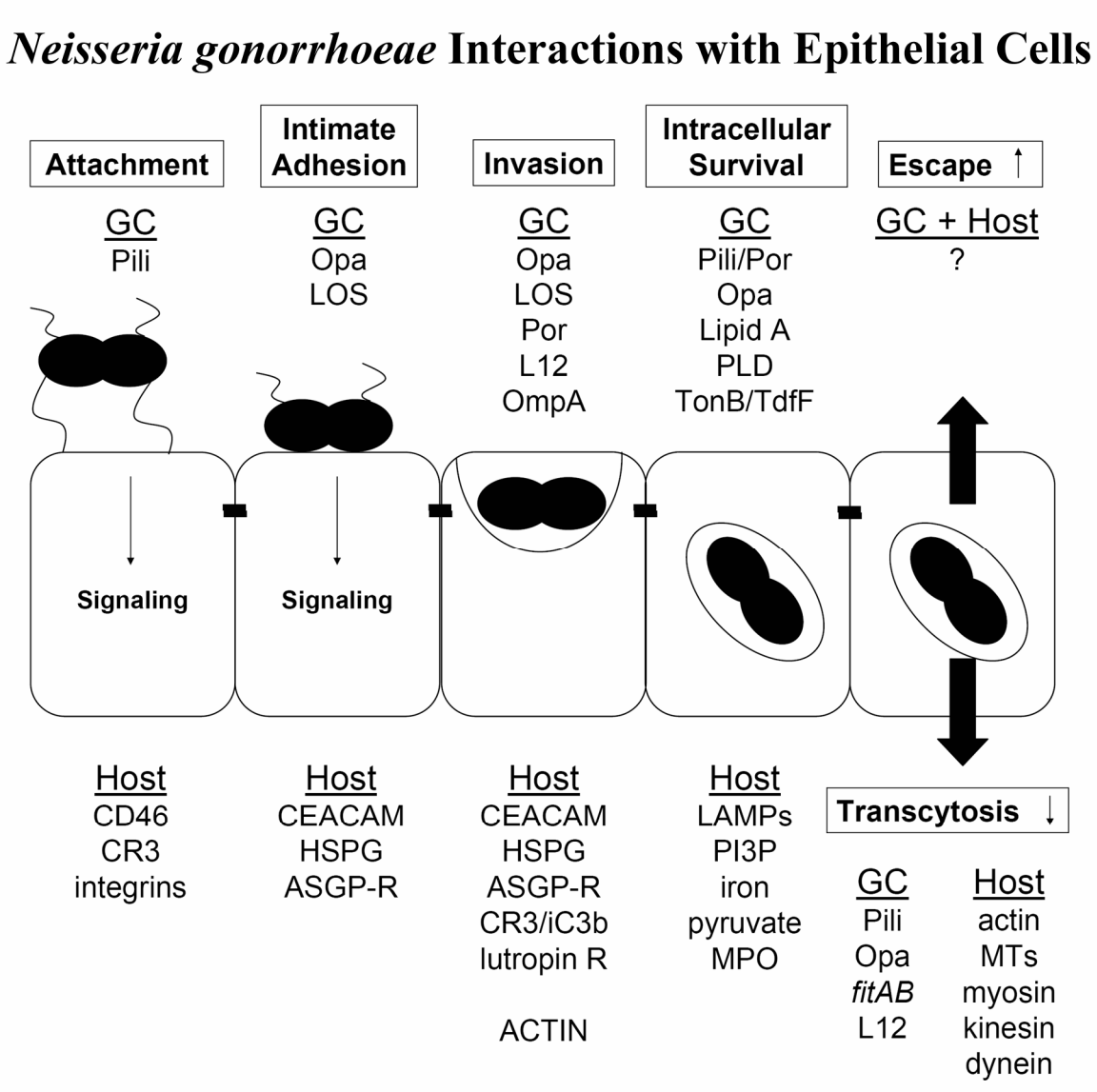

Figure 1—GC pathogenesis of the epithelial cell barrier. Shown are the different stages of GC interaction with epithelial cells. Factors listed under (GC) indicate GC virulence factors utilized to accomplish each process. Factors listed under (Host) indicate host cell factors GC interact with or manipulate during each process. GC = black diplococci, pili = irregular-shaped thin lines, epithelial cells = white rectangular boxes, cell tight junctions = small black boxes adjoining adjacent epithelial cells to indicate the polarized nature of an epithelial cell barrier. GC initial attach to the apical side of the epithelial cells and transcytose towards the basolateral membrane.

binding proteins, or M proteins from pathogenic *Streptococci* and *Staphylococci* spp. (31, 139, 256). Other adhesins include autotransporter proteins, such as the BabA protein in *Helicobacter pylori* or other surface expressed proteins, like Opa, with adhesive domains that bind to cellular receptors, such as integrin, cadherin, or selectin family molecules (9, 27, 223). In a unique case, enteropathogenic and enterohemorrhagic *E.coli* (EPEC and EHEC) encode for Tir, the translocated intimin receptor for their intimin adhesin, both of which are part of a TTSS. Once injected into the host, the Tir effector protein integrates into the plasma membrane where it binds intimin (150). In some cases, these bacterial adhesins induce host cell receptor phosphorylation and downstream signaling to recruit additional receptors, signaling molecules, and cytoskeletal proteins to the adherence site. This bacterial-directed recruitment can generate further host-pathogen adhesions and prepares cells to internalize the adherent bacteria.

In order to colonize mucosal epithelial cells, GC must attach to the cell surface. Epithelial cells possess a variety of defense mechanisms to prevent bacterial adherence. A flowing layer of mucus covers these cells, washing bacteria away before they can establish ligand-receptor interactions (47, 171). The mucoid layer also contains mucin, secretory IgA antibodies, and secreted antimicrobial molecules, such as defensins, cathelicidins, lysozymes, and phospholipases that can disrupt bacterial membrane integrity or block pathogen access to the cell surface (171, 232). Furthermore, GC must contend with normal commensal flora, like *Lactobacillus* spp. and *Enterococcus* spp., for attachment sites, especially in the female reproductive tract (232). GC that are able to overcome these defenses, must deal with pathogen-associated molecular pattern PAMP molecules, such as TLRs, that recognize bacterial components, such as LPS,

peptidoglycan and deoxyribonucleic acid (DNA), from a variety of pathogens (8, 134). Binding these receptors triggers signaling pathways within epithelial cells that lead to the activation of transcription factors, such as nuclear factor-kappaB (NF-κB) and activator protein-1 (AP-1), and the expression of genes involved in defense responses. Part of this response includes the increased production of proinflammatory cytokines and chemokines. GC are known to elicit different levels of tumor necrosis factor alpha (TNFα), IL-1, IL-6, and IL-8 secretion from a variety of epithelial cell types, which results in tissue damage and the recruitment of phagocytes (3, 134, 311). Neutrophils and macrophages can engulf and destroy adherent GC, but some studies show a subset of GC may survive inside these cell types [for review see (239)] (168).

GC that overcome these extracellular innate defense mechanisms can make initial contact with the apical side of epithelial cells via their type-IV pili—long, filamentous protein appendages extending from the GC cell surface composed of individual pilin protein subunits (32, 274). GC possess several silent pilin genes (*pilS*) copies that can recombine into the pilin expression locus (*pilE*) to mediate AV (193, 194, 257). AV creates morphologically and immunologically distinct pilus structures that may allow GC to adhere to a greater variety of cell types and evade the immune response (29, 144, 243).

GC utilize their type-IV pili-associated PilC adhesin to attach to the CD46 receptor on epithelial cells (147, 241, 243). GC can also adhere to epithelial cells with pili in the absence of cellular CD46 expression via complement receptor 3 (CR3) or integrins (68, 72, 152, 153), but these interactions are less well-characterized. Binding these receptors stimulates signal transduction pathways in mucosal epithelial cells. Pili trigger CD46 phosphorylation by the Src-family kinase c-Yes and the influx of calcium into the

host cell cytosol (146, 166). Pili-mediated signaling also triggers the accumulation of cortical plaques, which contain actin, actin-associated proteins, tyrosine phosphorylated proteins, and Opa receptors, that cluster beneath sites of gonococcal contact with host cells to facilitate gonococcal adherence and invasion (147, 166, 185, 187). GC retract pili powered by the ATPase motor protein, PilT (189). PilT-mediated retraction triggers the phosphatidyl inositol-3-kinase (PI3K)/Akt signaling pathway in epithelial cells and blocking this retraction-induced signaling inhibits subsequent GC invasion (167). Retractile forces also enhance mitogen-activated protein kinase (MAPK) activation during the early stages of infection and cause epithelial cells to release CD46 into the extracellular milieu (86, 123). GC twitching motility is driven by pilus retraction (189), which may allow GC to spread out or migrate as a microcolony on the cell surface and engage additional host receptors (117).

After making initial contact with host cells, GC establish more intimate adhesion with host cells through additional GC ligand-host cell receptor interactions. Most GC surface factors responsible for establishing intimate GC adhesion to epithelial cells also direct bacteria-mediated endocytosis (invasion) and are discussed in the next subsection. GC form microcolonies of tightly-associated bacteria on the surface of most nonphagocytic cells. GC microcolonies are formed through Opa-LOS interactions on neighboring GC and bacterial growth over time (24). GC also recruit host cell factors, such as kinases, adaptor molecules, and actin-associated factors to the adherence site to promote intimate adhesion, microcolony forming interactions, host cell signaling, and invasion (67, 117, 167, 185). Microcolonies may provide protection for GC sequestered in the core of the formation from antimicrobial molecules and phagocytes.

C. Invasion: Mechanisms and Signal Transduction

Bacterial pathogens possess a diverse array of strategies to invade into nonphagocytic cells. The specifics of each pathway involve different host cell and bacterial factors that interact to orchestrate internalization, but overall invasion mechanisms can be divided into three general categories. Direct penetration occurs when a microorganism, like *Borrelia burgdorferi* or *Clostridium perfringens*, crosses the epithelial barrier due to a puncture, such as a tick-bite that delivers the pathogen into a subepithelial region, or an indirect injury to the tissue (121). Other bacteria utilize TTSS to inject effectors directly into the host cell cytosol where they interact with signaling molecules and actin cytoskeletal components. Bacteria utilizing this strategy invade by a "trigger" mechanism whereby the effectors provoke membrane ruffling. Those pathogens lacking TTSS gain entry by binding their invasin proteins to host cell receptors, which then triggers invasion-promoting signal transduction pathways that culminate in actin reorganization. Bacteria are internalized via a "zipper" mechanism where microvilli elongations surround and engulf the pathogen (50, 79).

MAPKs are activated by some invasive pathogens and are linked to cytoskeletal rearrangements. Tang, *et al*. were the first group to link MAPK activation to the invasion of epithelial cells when they demonstrated that extracellular signal regulated kinase-2 (ERK-2) inhibition reduced *Listeria monocytogenes* invasion into HeLa cells via the internalin-E-cadherin "zipper" pathway (278). Since then, combinations of p38, Jun-N-terminal kinase (JNK), and/or ERK signaling have been shown to contribute to invasion by many pathogens. For example, *Yersinia* spp. use the Inv or YadA invasin proteins to

invade epithelial cells via integrin receptors by activating several kinases, including the MAPKs (74, 249). Furthermore, JNK inhibition prevented *Neisseria meningitidis* internalization through integrin receptors (264). Some type-III secretion effectors (Sops and Sips) from *Salmonella enterica* serovar Typhimurium act as nucleotide exchange factors to manipulate actin-associated proteins, such as Cdc42 and Rac, in their "trigger" pathway. Blocking Cdc42 activation prevents the activation of downstream MAPK signaling in this pathway (39, 105, 114).

GC invasion occurs when GC penetrate into the epithelial cells via a dynamic "zipper" phagocytosis/internalization orchestrated by both bacterial and host cell factors (186). GC invade epithelial cells as a potential way to gain protection from extracellular immune defenses and persist in the host tissues. The fact that GC gain entry into host cells to attempt to establish a niche in host tissues demonstrates the importance of invasion in GC pathogenesis. Multiple gonococcal surface factors can interact with the cervical epithelial cell surface to facilitate GC invasion (162, 176). Pili, in conjunction with one or more gonococcal invasins (Opa, LOS, or Por, iC3 surface deposition), can coordinate host cell signaling modifications to drive host actin cytoskeleton polymerization beneath the site of adherence to form microvilli elongations that internalize GC (72, 84, 94, 98, 107, 243, 274, 295).

Opa proteins mediate intimate contact between the gonococcal surface and the surface of epithelial, endothelial, and phagocytic cells and facilitate host cell invasion (162, 176). An individual GC can express any combination of 0-11 different Opa proteins (18, 19, 25). Expression of each Opa is regulated by the pentameric CTCTT repeated sequence in the leader peptide portion of each protein sequence and AV occurs when *opa*

loci undergo homologous recombination with each other (273). Each Opa forms a β-barrel in the GC outer membrane that contain eight membrane spanning regions and three distinct extracellular variable domains that determine receptor specificity (18, 28).

Two different classes of Opa proteins, Opa_{CEA} and Opa_{HSPG}, can bind carcinoembryonic antigen cellular adhesion molecules (CEACAM) and heparan sulfate proteoglycans (HSPG), respectively, to trigger uptake into different cell types (40, 112, 162, 290, 293). Opa-HSPG interactions activate a tyrosine phosphorylation pathway involving phosphocholine-phospholipase C (PC-PLC) and acidic sphingomyelinase (ASM). During these processes, the secondary messengers diacylglycerol and ceramide are released to trigger many host cell responses, including the recruitment of F-actin and other tyrosine phosphorylated proteins to the site of colonization (61, 93, 94). GC can invade epithelial cells using either the syndecan-1 or syndecan-4 members of the HSPG family. Engaging these receptors can also recruit protein kinase C (PKC), phosphatidylinositol-4,5-bisphosphate (PIP_2), syntenin, and CASK to mediate GC entry (81). The extracellular matrix proteins vitronectin and fibronectin can bridge interactions between Opa_{HSPG} and epithelial cell integrin receptors to promote invasion by triggering a signaling pathway that involves PKC (61, 66, 67, 89, 289).

Opa-dependent invasion through CEACAM binding leads to activation of different cellular factors. GC infection of epithelial and endothelial cells triggers the upregulation of CEACAM1 expression by activating NF-κB, which allows for increased Opa_{CEA}-mediated binding to these cells (204, 205). GC invasion via CEACAM1, 5, or 6 in transfected epithelial cells occurs via a macropinocytosis-like Rac1/Cdc42-independent mechanism that is not blocked by kinase inhibitors and may not involve

actin recruitment (20, 26, 179). However, disrupting the cholesterol-rich lipid rafts that contain these CEACAM receptors at the cell membrane blocks GC uptake, indicating that membrane organization is important for GC invasion (251). GC binding to CEACAM3 transfected cells triggers Src kinase phosphorylation of the immunotyrosine activating motif (ITAM) on CEACAM3 (180). Downstream signaling to PI3K and Rac1/Cdc42 provokes actin rearrangements and GC entry (20, 26).

GC can invade cervical epithelial cells that do not express CEACAM and only a single member of the Opa protein family can bind HSPG (275, 290, 292). GC can initiate alternate ligand-receptor interactions to promote invasion into epithelial cells by Opa-independent mechanisms. Defined LOS structures contribute to increased adhesion and host cell invasion in an Opa^- background (106, 196, 266). LOS is a primary component of the GC outer membrane that displays AV and PV (177). The LOS core is composed of a lipid A core linked to two 3-deoxy-D-*manno*-2-octulosonic acid (KDO) molecules and heptose core sugars. Extending from the core unit are chains of O-polysaccharides that are shortened in comparison to the repeating O-antigen subunits found in the LPS of most Gram-negative bacteria. LOS biosynthesis occurs via the sequential addition of monosaccharide subunits to a grown LOS chain by LOS glycosyltransferase (*lgt*) genes. Some *lgt* genes (most notably *lgtA*, *lgtD*, and *lgtC*) undergo PV and expression is controlled by homopolymeric tracts of guanines within their coding regions (53, 92). These repeated nucleotide stretches promote slip-strand mispairing during replication to shift the reading frame of *lgt* RNA (92). Lgt PV allows a single GC to simultaneously produce multiple antigenically distinct LOS structures on its cell surface. These structures

can mimic host glycosphingolipids and blood group antigens to prevent an effective host antibody response against a single LOS structure (6, 33, 85, 99, 254, 287).

The nonsialylated lacto-*N*-neotetraose (LnNT) LOS glycoform and the galNAc-LnNT LOS structure allow GC to bind and invade into epithelial cells in the presence or absence of Opa (140, 266, 287). The LnNT and galNAc-LnNT α-chain LOS structures are synthesized by the Lgt enzymes derived from the *lgtABCDE* gene cluster (92). Deletion of the *lgtD* gene (Δ*lgtD*) prevents the addition of the terminal galNAc to the α-chain, which truncates LOS expression at the LnNT glycoform. Deletion of the *lgtA* gene (Δ*lgtA*) further truncates the α-chain to a lactosyl structure devoid of both LnNT and galNAc-LnNT. GC expressing the LnNT LOS glycoform can bind to the asialoglycoprotein receptor (ASGP-R) to mediate entry into primary human urethral epithelial cells (PHUEC) by a clathrin-dependent mechanism (106, 228, 229). GC expressing polylactosaminylated LOS structures can bind to galectin-3, a lectin binding receptor on cervical epithelial cells, that may lead to invasion (141). Furthermore, the lipid A portion of LOS serves the site of complement factor C3 deposition on the GC surface where it is subsequently converted to iC3b (71). iC3b-bound GC can utilize porin and pili to coordinate a joint interaction with CR3 on primary cervical epithelial cells to trigger invasion (71, 72). This invasion mechanism involves activation of myosin light chain kinase (MLCK), PIP_2, and GC phospholipase D (PLD)-dependent activation of Akt, but not PI3K (70).

Porin (Por) can also mediate GC invasion in an Opa-independent manner through pathways distinct from the CR3 pathway. Porin is the most abundant GC outer membrane protein and is phase invariable (143, 145). GC can be characterized by their expression of

one of two different porin subtypes—PorB 1A or PorB 1B. GC that express PorB 1A are more invasive (160, 288). In low phosphate environments, PorB IA-mediated invasion requires clathrin-coated pit formation, actin rearrangement, and Rho GTPases and may involve direct translocation of Por into the epithelial cell membrane (160, 242, 288).

Other GC factors also contribute to invasion, but the molecular mechanisms for these invasion pathways have not been as well-characterized. The L12 ribosomal protein, OmpA-like protein, and some RpoH-regulated genes all confer invasive phenotypes on Opa^- GC into various epithelial and endometrial cell types (65, 260, 268).

GC utilize a variety of receptor-mediated invasion pathways to enter epithelial cells. Specific kinases, such as PKC and Src, appear to associate with these receptors to transmit signals to downstream components. However, the downstream kinases and transcription factors activated through GC-receptor binding and how they are linked to the actin cytoskeleton are less understood. Signaling through the Opa-HSPG invasion pathway leads to the release of diacylglycerol and ceramide from the membrane, which are linked to actin reorganization (61, 93, 94). Opa-CEACAM3 interactions in phagocytes activate Src-family kinases, p-21 activated kinase (PAK), and JNK and trigger the Rac-1 GTPase to mediate actin rearrangements for phagocytosis (110, 113). However, a similar Src/PAK/JNK/Rac-1 pathway has not been demonstrated in epithelial cells. GC also activate the transcription factors NF-κB and AP-1 (through JNK) to mediate pro-inflammatory cytokine production and increased intercellular adhesion molecule-1 (ICAM-1) expression (135, 210, 211). A direct connection between MAPK activation, cytoskeletal reorganization, and GC invasion into epithelial cells has not been established.

D. Intracellular Survival, Transcytosis, and Host Cell Exit

Intracellular pathogens can utilize multiple methods simultaneously to sustain their ICS. Bacteria can induce anti-inflammatory cytokines, such as IL-10, to counteract the pro-inflammatory immune response or trigger increased expression of anti-apoptotic factors to prevent clearance via cell death (22, 23, 121, 199). Many organisms possess siderophores, scavenger receptors, or iron-binding proteins to acquire essential nutrients from the host to prevent starvation (49, 238). Intracellular pathogens also possess diverse strategies for dealing with phagolysosomes. *Shigella flexneri* and *Listeria monocytogenes* are two species that escape from the vacuole into the host cytosol by utilizing pore-forming toxins to breach the phagosome membrane (88). Another strategy is to prevent the bacteria-containing vacuole from fusing with lysosome. *Salmonella* spp. secrete effectors that interfere with vesicular trafficking to disrupt vacuole maturation (82, 116). Other pathogens, like *Mycobacterium tuberculosis*, institute vacuolar remodeling whereby they prevent acidification and acquisition of lysosomal markers to create a less harsh environment within the bacteria-containing compartment (44).

Host epithelial cells can call upon multiple intracellular defense mechanisms to prevent the intracellular survival (ICS) of invading pathogens. Cytokines produced by epithelial cells can alert phagocytes to travel to infection sites to engulf both bacteria and infected cells (234, 235). Infected cells can undergo apoptosis, thereby limiting the ability of the pathogen to spread to neighboring cells (220). Epithelial cells can sequester essential nutrients, such as iron, to starve internalized microorganisms to prevent their growth and proliferation (279). The intracellular PAMP recognition receptors, NOD proteins, can recognize bacterial peptidoglycan and trigger defense responses (87, 131).

Epithelial cells can also directly kill bacteria within the phagolysosome (297). The overall effectiveness of these host defenses against GC remains questionable. Infected individuals fail to generate a substantial adaptive immune response against GC, which is characterized by a lack of GC antigen presentation to develop immunological memory in order to prevent subsequent reinfections (115). GC can establish chronic asymptomatic infections, especially in women, by evading the innate immune response and persisting at a low-level in the reproductive tract (270, 302).

Following invasion, GC can survive inside epithelial cells long enough to transcytose to the basolateral cell membrane and enter a subepithelial compartment or return to the extracellular lumen by exiting through the apical side of the cell (51, 181, 261). GC within epithelial cells can escape the innate defenses of the external milieu and the underlying phagocytes to facilitate their spread to secondary sites of infection or generate systematic, disseminated disease (63, 202). Weel, *et al*. demonstrated the existence of two subpopulations of GC inside epithelial cells—intact GC maintaining membrane integrity and morphologically disintegrated GC. Preventing phagolysosome fusion and acidification blocked the destruction of the susceptible subpopulation (297, 298), indicating GC need to avoid degradation in the lysosome to promote ICS. GC can stimulate calcium-mediated signaling responses in epithelial cells that may facilitate ICS by modifying phagolysosomal properties. Pili and Por can trigger calcium ion influxes into the epithelial cell cytosol to instigate the exocytosis of lysosomal associated membrane protein-1 (LAMP-1) and reduce levels of other lysosome components [LAMP-2, lysosomal acid phosphatase, and CD63] prior to gonococcal invasion (11, 16, 206, 298). The GC IgA protease can cleave LAMP-1 at the plasma membrane to help

delay phagolysosome maturation and promote intracellular survival (10-12, 111, 173, 224, 225). However, loss of LAMP-1 function may not be sufficient to achieve GC ICS. A recent study indicated that GC displayed increased ICS in host cells deficient in both LAMP-1 and LAMP-2, but not in cells lacking only one of the two components (21). Finally, investigations have revealed intact GC in the host cytosol not surrounded by a vacuolar compartment (203).

GC expressing Opa_{CEA} that invade epithelial cells via CEACAM3, but not CEACAM1, show evidence of increased PI3K activation and greater recruitment of LAMP-2 (26). Thus, the increased ICS of GC that invade via CEACAM1 may be explained by their ability to inhibit phagolysosome maturation events in host cells. Invasion via CEACAM3 leads to phosphatidylinositol-3-phosphate (PI3P) accumulation on GC-containing phagosomes—a maturation step that allows the phagosome to acidify and acquire lysosomal markers. During invasion through CEACAM1, only a portion of the phagosomes accumulate PI3P, which may allow GC to survive in some vacuoles (26).

GC also utilize other surface factors to avoid intracellular killing. GC must acquire iron for ICS and require the expression of TonB and TdfF for intracellular iron acquisition. Other GC iron binding proteins, including the transferrin binding proteins TbpA and TbpB, the lactoferrin binding protein LbpA, the siderophore FetA, and the hemoglobin receptor HpuAB, can all bind cellular iron sources, but are not yet known to play a role in GC iron utilization inside host cells (34, 164, 183, 284). GC can also use Opa proteins to bind to pyruvate kinase in order to utilize intracellular pyruvate for growth when nutrients are scarce within host cells (303). GC also possess enzymes, such catalase, peroxidase, and nitrogen reductases that may help them confront reactive

oxygen or nitrogen intermediates within the intracellular environment (7, 109, 122, 184). In addition, Por has been implicated in inhibiting host myeloperoxidase (MPO) activity to prevent hypochlorous acid formation and late cytoplasmic granule fusion following phagolysosome formation (175).

Instead of surviving within epithelial cells, some GC can progress to additional locations within the host. GC can transcytose through an epithelial cell monolayer towards the basolateral membrane without disrupting monolayer integrity (91, 186). L12 expression permits fast GC monolayer crossing potentially via a paracellular route (269). Expression of pili and Opa-CEACAM interactions assist GC traversal through an epithelial cell barrier as does the expression of two genes, *fitA* and *fitB*, of unknown function (120, 186, 293). GC transcytose through epithelial cells along actin microfilaments and microtubules by utilizing the motor activity of myosin, kinesin, and dynein (294). GC can exit through the basolateral side of the epithelial cell into subepithelial tissues and the bloodstream where they encounter phagocytes and complement (261). To evade complement and become serum resistant, GC bind the complement inhibitory factor H with Por or C4-binding protein or sialylate their LOS (217, 233). GC can also re-emerge into the extracellular environment by escaping through the apical membrane where they are positioned to be transmitted to a new host or invade nearby cells (51, 203).

Specific Aims and Approaches

This study was designed to investigate how *N. gonorrhoeae* manipulate the cervical epithelium to establish infection and persist in the female reproductive tract. The central hypothesis of this work is that GC utilize their repertoire of virulence factors to trigger host responses that allow the bacteria to invade into and survive within human epithelial cells. Through this dissertation I have explored host cell signaling pathways activated by GC in the early stages of infection, GC factors that contribute to host cell invasion, methods to improve the quantification of GC invasion, and the post-invasion fates of GC inside cervical epithelial cells.

Research in the Stein laboratory is focused on determining how GC elicit different disease outcomes in the male and female host, including understanding what factors contribute to the asymptomatic nature of GC disease in women. Mucosal epithelial cells represent the initial host cell barrier of defense against infectious agents and the first cell type encountered by most GC. GC colonize these cells to establish infection and penetrate this barrier to spread to additional tissues. Though GC are known to invade into various epithelial cells via multiple mechanisms, we do not understand the importance of each pathway in natural human infections, including which invasion pathways lead to greater disease severity. Furthermore, few links have been made between entry pathways that lead to GC survival versus those pathways that result in intracellular killing. This study identifies both host and bacterial factors involved in the invasion process and quantifies their impact on host cell entry and the cytokine response. This work also investigates the different strategies employed by GC to survive after invasion. I propose

that the specific interactions between GC and epithelial cells contribute to the varying outcomes of gonococcal disease.

In this study, I developed a tissue culture cell model to examine GC adherence, invasion, and intracellular survival. I utilized a main cervical epithelial cell line, ME180 cells, and a second endometrial cell line, Hec1B cells, both of which have been shown to be susceptible to GC infection (38, 98, 266, 275). Invasion and survival assays where cells were incubated with different GC variants expressing different surface profiles or at different MOI for various time periods represent the foundational approach for most experiments in this work. After infection, host cells, host cell lysates, or recovered bacteria were analyzed to reveal different aspects of GC pathogenesis.

Aim 1: Little is known concerning the GC-induced signaling pathways that lead to invasion after receptor binding. I identified receptor-associated kinases and downstream kinases activated by GC prior to invasion by challenging ME180 cells with different surface variants over time. I discussed the potential role of each kinase in invasion. I also examined the role of the GC-activated kinase JNK in bacterial induced IL-8 production.

Aim 2: The number of GC that actually invade epithelial cells and the percentage of cells that are susceptible to this invasion are unclear. I constructed a β-lactamase expressing GC to quantify the number of ME180 cells in a GC-infected population that are invaded and determine the relative contribution of pili expression, Opa expression, and GC viability to the invasion process. I also examined the ability of different agents to inhibit invasion or improve invasion quantification methods.

Aim 3: The intracellular fate of GC inside epithelial cells (survival, killing, or proliferation) remains controversial. I developed a tannic acid-based survival assay to quantify GC intracellular survival levels and the number of GC expressing different surface profiles that escape/re-emerge from ME180 cells. I also analyzed a potential mechanism of GC escape.

Materials and Methods

Bacterial Strains, Cell Lines, Plasmids, and Reagents. *Neisseria gonorrhoeae* strain FA1090 was obtained from Dr. W.M. Shafer (Emory University, Atlanta, GA). FA1090 was a cervical isolate from a patient with a disseminated gonococcal infection; it is streptomycin resistant (Sm^R) and is sensitive to both ceftriaxone and ciprofloxacin (45, 140). *Neisseria gonorrhoeae* strain MS11 mKC (referred to as MS11) was obtained from Dr. J.M. Griffiss (University of California at San Francisco, San Francisco, CA) and MS11Δ*opa* is a derivative of MS11 mKC that is genetically incapable of expressing Opa proteins. *Neisseria gonorrhoeae* strain F62 was obtained from P.F. Sparling (University of North Carolina, Chapel Hill, NC). Strain F62Δ*lgtD* is a derivative of F62 that expresses LnNT α-chain LOS as its predominant LOS structure due to a deletion in *lgtD* (266). F62Δ*lgtA* is a derivative of F62 that expresses lactosyl α-chain LOS due to a deletion in *lgtA* (266). Commensal organisms *Neisseria sicca* 342 and *Neisseria subflava* 44 were obtained from H. Feldman (SUNY at Albany, Albany Medical Center, Albany, NY). In all procedures, GC and commensal *Neisseria* strains were grown overnight (~18 h) at 37°C, 5% CO_2 on GCK agar (Becton Dickinson, Sparks, MD) plus 1% Kellogg's supplement unless otherwise stated (300). Penicillin G (75 ng/ml) was added to GCK agar plates (GCK PenG) for maintenance of Bla-expressing GC strains. Colonies were selected as Pil^+Opa^+, Pil^-Opa^+, Pil^+Opa^-, or Pil^-Opa^- based on their light refraction phenotype under a dissecting microscope. For analyses with nonviable organisms, bacteria were killed by incubation with 2 mg/ml gentamicin sulfate (BioWhittaker/Cambrex Biosciences, Walkersville, MD) followed by overnight storage at 4°C as described previously (218). The cloning strain *Escherichia coli* DH5α *mcr*$^-$

[mcrA (mrr-hsdRMS-mcrBC) was obtained from New England Biolabs (Beverly, MA) and maintained on Luria-Bertani (LB) agar (US Biologicals, Swampscott, MA). Plasmids pFT180 (271), pK18 (230), and pK18UP (246) have been described previously. ME180 cells, a human cervical epidermal carcinoma cell line (HTB-33; American Type Culture Collection [ATCC], Manassas, VA), were maintained in RPMI 1640 (Gibco/Invitrogen, Grand Island, NY) supplemented with 5% fetal bovine serum (FBS) (HyClone, Logan, UT), 1% penicillin-streptomycin (Pen-Strep) solution (Gibco/Invitrogen), and 10 μM Hepes (Mediatech, Herndon, VA). Hec1B cells, an endometrial adenocarcinoma cell line derived from the female uterus (HTB-113; ATCC) were obtained from K.V. Swanson (University of Maryland, College Park, MD) and maintained in Minimal Essential Media-Alpha Media with GlucoMax® (Gibco/Invitrogen) supplemented with 10% FBS, 1% Pen-Strep, and 10 μM Hepes. In all procedures, seeding and incubating tissue culture cells alone or tissue culture cells infected with bacteria occurred at 37^{o}C, 5% CO_2 unless otherwise stated. All chemicals used in this study were reagent grade or better and were obtained from Sigma Aldrich (St. Louis, MO) unless otherwise specified (for reagents utilized see Table 1).

Statistical Analysis. All graphical data were prepared using GraphPad Prism version 3.00 for Windows (GraphPad Software, Inc., San Diego, CA). For data derived from three independent experiments each performed in triplicate, the error bars represent the standard error of the mean (SEM). For all other experiments, the error bars represent the standard deviation (SD). In experiments where the statistical significance between two data sets were analyzed, a p-value was determined by performing a two-tailed unpaired

Table 1. Reagents and Buffers Used in This Study

Solution	Composition
Bacterial Culturing and Transformation	
Kellogg's supplement	6.8 mM glutamine, 2.1mM $Fe(NO_3)_3$, 0.04 mM thiamine pyrophosphate, 2.22 M glucose
GCK agar	GC[1] media base containing 5 g/L agar and 1% Kellogg's supplement
GCP	1.5% proteose peptone 3, 0.1% soluble starch, 7.3 mM KH_2PO_4, 23 mM K_2HPO_4, 85.5 mM NaCl, pH 7.4
GC broth	GCP, 1% Kellogg's supplement, 0.042% $NaHCO_3$
GC transformation broth	GCP, 1% Kellogg's supplement, 10 mM $MgCl_2$, 0.042% $NaHCO_3$
Cell Culturing	
Penicillin-Streptomycin	10 mg/ml streptomycin sulfate, 1000 U/ml Penicillin G in DMEM[2]
ME180 cells IM[3]	5% FBS[4], 0.5% Kellogg's supplement, and 10 mM Hepes in RPMI
Hec1B cells IM	10% FBS, 0.5% Kellogg's supplement, and 10 mM Hepes in MEM-Alpha Media with GlucoMax®
serum-starved IM	0.5% FBS, 0.5% Kellogg's supplement, 10 μM Hepes in RPMI
serum-free IM	0.5% Kellogg's supplement, 10 μM Hepes in RPMI
Trypsin	0.05% trypsin/0.53 mM EDTA
PBS	14.6 mM KH_2PO_4, 17.1 mM NaCl, 81mM Na_2HPO_4, pH 7.4, (dilute 1:10)
Saponin	10% saponin in PBS
Lysate Collection	
NP-40 lysis solution	1% NP40, 20mM Tris-Cl, pH 7.5, 150mM NaCl, 1mM $MgCl_2$, 1mM EGTA, 10μg/ml leupeptin and aprotinin protease inhibitors, 50 mM NaF, 1mM Na_3VO_4
NP-40 buffer	1% NP40, 20mM Tris-Cl, pH 7.5, 150mM NaCl, 1mM $MgCl_2$, 1mM EGTA
LOS[5] lysis buffer	2% SDS[6], 4% β-mercaptoethanol, 10% glycerol, 1M Tris [pH 6.8], bromophenol blue

SDS-PAGE[7]

resolving gel solution	25% 0.99 M Tris [pH 8.8], 0.1% SDS, X% of 37.5:1 acrylamide/bis-acyrlamide stock [40% acrylamide/bis-acrylamide, 2.67 C] depending on the gel percentage, bring to volume with HPLC grade-water, degassed for 10 min, 0.1% APS[8] and 0.001% TEMED added after degassing)
stacking gel solution	25% 0.5 M Tris [pH 6.8], 12.5% acrylamide/bis-acrylamide stock, 0.1 % SDS, 61% HPLC-grade water, degassed for 10 min, 0.1% APS and 0.001% TEMED added after degassing
1X running buffer	25 mM Tris, 192 mM glycine, 1% SDS
2X loading buffer	50% glycerol, 5% SDS, 0.25M Tris-Cl pH 6.8, 0.04% 2-mercaptoethanol, 25μg/ml bromophenol blue

Gel Staining

Coomassie Blue	Coomassie Brilliant Blue R-250
Coomassie Blue destain	50% methanol, 40% HPLC-grade water, 10% glacial acetic acid
Fixing solution	30% ethanol, 10% glacial acetic acid, 60% HPLC-grade water
Silver Stain	0.8 g $AgNO_3$ in 4 ml HPLC-grade water added dropwise to: 1.4 ml NH_4OH, 0.1 g NaOH, 25 ml HPLC-grade water
Developing solution	50 μg/ml citric acid, 0.019% formaldehyde

Western/Immunoblotting

1X transfer buffer	25mM Tris, 192mM glycine, 15% methanol, pH 8.2
wash buffer	1X PBS/0.05% Tween-20
blocking solution	Western wash buffer, 1% fish skin gelatin
Stripping buffer	62.5mM Trizma base, 2% SDS, 100mM 2-mercaptoethanol, pH 6.7

ELISA

Capture Ab[9] solution	2 μg/ml Ab, 0.1 M Na_2HPO_4, pH 9.0 with HCl
ELISA wash buffer	0.05% Tween-20, 1X PBS, pH 7.4
Detection Ab solution	1 μg/ml Ab, 10% FBS in ELISA wash buffer
SAP[10] solution	1:1000 SAP, 10% FBS in ELISA wash buffer

PNPP[11] substrate solution	one 5 mg PNPP tablet dissolve in 5 ml (0.24 mM $MgCl_2 \cdot 6H_2O$, 9.6% diethanolamine, pH 9.8) prepared just prior to use

Antibody Purification and Labeling

Starting Buffer	100 mM Tris, 100 mM NaCl, pH 7.5
Elution Buffer	100 mM glycine, pH 2.5
Neutralization Buffer	1 M Tris, pH 8.0
Bicarbonate solution	1M $NaHCO^3$, pH 8.3
Spin column buffer	2 mM sodium azide in PBS

Immunofluorescence

blocking solution	10% FBS and 10 μM glycine in 1X PBS
permeabilization solution	0.1% Triton X-100, 10% FBS, 10 mM glycine in 1X PBS

Molecular Cloning and Agarose Gel Electrophoresis

10X ligase buffer	0.5M Tris-HCl [pH 7.8], 0.1M MgCl2, 10mM ATP, 500 μg/ml BSA
1X TBE buffer	89 mM Tris-HCl [pH 8.0], 89 mM boric acid, 2mM EDTA
loading dye	5% glycerol, 0.05% Orange G

Nitrocefin Hydrolysis Assay

PE buffer	0.1 M phosphate buffer, 1 mM EDTA, pH 7.0

---

1 GC = gonococci

2 DMEM = Dulbecco's minimal essential media

3 IM = invasion media

4 FBS = fetal bovine serum

5 LOS = lipooligosaccharide

6 SDS = sodium dodecyl sulfate

7 PAGE = polyacrylamide gel electrophoresis

8 APS = ammonium persulfate

9 Ab = antibody

10 SAP = streptavidin-alkaline phosphatase

11 PNPP = p-nitrophenyl phosphate

t-test with a 95% confidence interval using GraphPad Prism version 3.00 for Windows. To analyze the statistical difference between the subpopulation of ME180 cells invaded by Pil^+Opa^+ and Pil^+Opa^- FA1090 Φ(*bla-iga'*) in Figure 15A, only experiments were greater than 10% of the ME180 cell population were invaded by GC were chosen for analysis. Data where the means were determined to be statistically different/significant were denoted by (*), (**), or (***) depending on the strength of the statistical data.

LOS Sialylation. GC strain F62Δ*lgtD* was grown overnight and resuspended to a Klett of 40 in GCP solution containing 1% Kellogg's supplement and 0.042% $NaHCO_3$. 1 ml of GC was transferred into a 10 ml polypropylene tube and 50 µl of 1 mg/ml CMP-NANA added. (A corresponding tube for each trial was grown without CMP-NANA as a negative control for sialylation.) The tubes were incubated for 4 h in a rotation shaker at 37°C and then added directly to ME180 cells for signaling assays described below. LOS was extracted from one set of tubes to test for LOS sialylation via Tris-Tricine SDS-PAGE analysis described below.

Signaling Assays. ME180 cells were seeded in serum-starved invasion media (IM) in 6-well tissue culture plates (5×10^5 cells/well) or 100 mm diameter (100 mm) tissue culture plates (1×10^7 cells/well). ME180 cells were incubated for ~60 min in serum-free IM prior to incubation with GC, *N. sicca* 342, *N. subflava* 44, or inert bovine serum albumin (BSA)-coated microspheres/beads at a MOI of 10. Fluoresbrite® YG carboxylated microspheres (1 µm) were coated with BSA using the carbodiimide kit and sterilized with 70% ethanol rinsing according to the manufacturer's instructions (Polysciences, Inc.,

Warrington, PA). Prior to their addition to ME180 cells, the beads were resuspended in RPMI similar to bacteria.

After incubation, the tissue culture plates were placed on an ice bath and washed three times with ice-cold PBS (pH 7.4). Lysates were collected by adding 100 µl (6-well) or 250 µl (100 mm plates) of NP-40 lysis solution to each well, scraping the cells from the plates with a cell scraper, and pipetting the lysate into microcentrifuge tubes. The lysates were placed on ice for 20-30 min, vortexed briefly every 7 min, centrifuged at 4^{o}C for 30 min at 12000 rpm, and the supernatants transferred to a new microcentrifuge tube and stored at -80^{o}C.

LOS Preparation from GC. LOS was prepared using the procedure of Hitchcock and Brown (118). GC were grown overnight and resuspended in GCP to Klett 100. An aliquot (1 ml) was transferred to a microcentrifuge tube and centrifuged for 3 min at 12000 rpm. Supernatants were removed via aspiration and 50 µl lysis buffer and 10 µl proteinase K (2.5 mg/ml) added. Samples were boiled for at least 60 min at 60^{o}C and diluted 1:25 in lysis buffer after boiling. Aliquots (10-15 µl) of each LOS sample were run on Tris-Tricine/SDS polyacrylamide gels and silver stained to detect LOS bands as described previously (283). Images were acquired using the Gel Doc XR transilluminator (Biorad) and processed using Quantity One 1-D analytical software version 4.6.1 (Biorad).

Protein Concentration Assay (Bradford Assay). Lysates were diluted 1:5 in NP-40 buffer and 10 µl of diluted lysate was added to a 96-well plate in triplicate. Different concentrations of BSA (0.5, 0.4, 0.25, 0.1, 0.05 µg/µl) were added to the 96-well plate in

duplicate as protein concentration standards. To each well, 200 µl of Biorad Protein Assay reagent (diluted 1:5) was added, samples were incubated 20-30 min at room temperature (RT), and analyzed on a Labsystems Multiskan Ascent (MTX Lab Systems, Inc., Vienna, VA) 96-well plate reader at $\lambda = 595$ nm. A standard protein concentration curve ($OD_{595\ nm}$ [y-axis] vs. concentration (µg/ml) [x-axis]) was generated for the BSA samples using GraphPad Prism 3.0. By comparing the $OD_{595\ nm}$ readings for each lysate to the BSA standard curve, the protein concentration of each lysate was determined and equilibrated in NP-40 buffer.

SDS-PAGE and Western Blot. SDS-PAGE gels of varied concentration (10%-15%, 4-15% gradient, or 4-20% gradient) were purchased precast from Biorad or were manually cast as described previously (244). Lysates were diluted with 2X loading buffer in a 1:1 ratio, boiled for 5 min, and centrifuged for 2 min at 12000 rpm. Unpolymerized acyrlamide was removed from the lanes, lysates were loaded, and the gels electrophoresed at 0.01Amp/gel at room temperature until the dye front reached the bottom of the gel. Gels were analyzed by: (1) Coomassie blue staining (2) silver staining (3) Western/immunoblotting. For Coomassie blue staining, the gels were stained overnight with mild shaking at RT according to the procedure of Maniatis (244). Gels were destained and images were acquired on a Gel Doc XR ultraviolet transilluminator (Biorad) and processed using Quantity One 1-D analytical software version 4.6.1 (Biorad). For silver staining, the gels were fixed, incubated with a silver nitrate solution, washed, and the bands visualized in developing solution as described previously (244). For Western blotting experiments, samples were processed through a SDS-PAGE gel, the

gel equilibrated in transfer buffer, and the proteins transferred to a PVDF membrane (Osmonics). (The PVDF membrane was prepared by immersing the membrane in methanol, rinsing with HPLC-grade water and equilibrating in transfer buffer). Proteins were transferred onto the PVDF membrane via wet, horizontal transfer at 100 V for 60 min at 4^{o}C.

The PVDF membrane was incubated in blocking solution overnight at RT. The membrane was washed and incubated in primary antibody (Ab) solution (Ab in blocking solution) for 90 min at RT. (A list of primary Ab used in this study and their appropriate secondary Ab is found in Table 2). After washing, membranes were incubated in secondary Ab solution (secondary Ab-IgG-HRP conjugate in PBS/0.5% gelatin) for 60 min at RT followed washes. Membranes were developed with luminal/peroxide Western Lightning^{TM} Chemiluminescence Reagent Plus (Perkin Elmer, Boston, MA) and exposed to blue autoradiography film (Marsh Bioproducts, Rochester, NY). To normalize for actin loading controls, membranes were incubated in stripping buffer for 45 min at 50^{o}C, washed thoroughly with wash buffer and reprobed for actin protein detection following the procedure listed above.

IL-8 Enzyme-Linked Immunosorbent Assays (ELISA). ELISA experiments were performed to detect human interleukin-8 (IL-8) secretion from ME180 cells. ME180 cells were seeded in 24-well tissue culture plates (1 x 10^5 cells/well) overnight in serum-starved IM. ME180 cells were pre-incubated in serum-free IM and GC were prepared and added to ME180 cells as described in the signaling assays above. ME180 cells were incubated with GC or purified LOS (purified according to the Westphal and Jann hot-

Table 2. Antibodies Used in This Study

Primary Antibody	(Isotype)	Secondary Antibody
Mouse α-phosphotyrosine 4G10	($IgG_{2bκ}$)	Goat α-mouse IgG_{2b}-HRP
Rabbit α-phospho ERK 1/2	(IgG)	Goat α-rabbit IgG-HRP
Rabbit α-phospho JNK	(IgG)	Goat α-rabbit IgG-HRP
Rabbit α-phospho p38	(IgG)	Goat α-rabbit IgG-HRP
Rabbit α-phospho EGFR [Tyr 1173]	(IgG)	Goat α-rabbit IgG-HRP
Rabbit α-β-actin	(IgG)	Goat α-rabbit IgG-HRP
Rabbit α-phospho PKCα [Thr 638]	(IgG)	Goat α-rabbit IgG-HRP
Rabbit α-human phospho Bad [Ser 136]	(IgG)	Goat α-rabbit IgG-HRP
Rabbit α-phospho Akt/PKB [Thr 308]	(IgG)	Goat α-rabbit IgG-HRP
Rabbit α-phospho Src [Tyr 418]	(IgG)	Goat α-rabbit IgG-HRP
Mouse α-human IL-8	($IgG_{2bκ}$)	
Mouse α-human IL-8 [biotinylated]	(IgG_{2b})	

phenol method) for 24 h in serum-free IM (299). Culture supernatants were collected, centrifuged at 12000 rpm for 5 min, and the supernatants transferred to new microcentrifuge tubes. Leupeptin and aprotinin protease inhibitors (fc 10 μg/ml) were added to each supernatant and supernatants were stored at -20^{o}C (short-term storage) or -80^{o}C (long-term storage). In JNK inhibition experiments, anthra[1,9-cd]pyrazol-6(2H)-one (SP600125) (Biosource, Camarillo, CA), a JNK 1,2,3 inhibitor, was added to ME180 cells at various concentrations 30 min prior to the addition of GC (15).

Sandwich ELISA were performed according to the protocols provided by BD Pharmigen (San Diego, CA) and all IL-8 Ab and recombinant standards were purchased from BD Pharmigen. Briefly, to a non-sterile 96-well plate, 50 μl of mouse anti-human IL-8 $IgG_{2b\kappa}$ capture Ab solution was added to every well to be tested for the presence of IL-8. The plate was sealed with parafilm and stored overnight at 4^{o}C. For all other incubations, the outgoing solution was decanted, the wells washed with ELISA wash buffer, and incubated in the incoming solution at RT. Wells were blocked with 10% FBS in PBS for 30 min. 100 μl of the appropriate supernatant or IL-8 recombinant protein standard was added to each well for 4 h at RT or overnight at 4^{o}C. (Standards were prepared by resuspending the stock solution to 4000 pg/ml in RPMI and performing 1:2 serial dilutions from 4000 pg/ml—7.8 pg/ml). IL-8 in the wells was detected by adding 100 μl of biotinylated mouse anti-human IL-8 IgG_{2b} Ab solution for 60 min. 100 μl of streptavidin-alkaline phosphatase (SAP) (Southern Biotech, Birmingham, AL) solution was added to each well for 30 min. 100 μl p-nitrophenyl phosphate (PNPP) substrate (Southern Biotech) solution was added to each well. The plate was immediately covered with aluminum foil and checked periodically for detection of yellow color production in a

linear range in the wells containing standards. At the appropriate time (~ after 15-30 min), the plate was analyzed at λ = 405 nm using a Labsystems Multiskan Ascent 96-well plate reader (MTX Lab Systems, Inc.). Similar to the Bradford Assay above, a standard curve ($OD_{405\ nm}$ vs. protein concentration) was developed for the IL-8 standards using GraphPad Prism 3.0 and the protein concentration of each supernatant was derived from their $OD_{405\ nm}$ by comparison to the standard curve.

Goat anti-GC IgG Polyclonal Antibody Purification. All steps in this procedure were performed at 4^{o}C unless otherwise stated. Agarose anti-goat IgG beads were washed with 20 ml of starting buffer and centrifuged at 1000 rpm for 10 min three times. The beads were resuspended in 60-80 ml of starting buffer and slowly packed into an 8 mm diameter column. The beads were allowed to settle and the buffer was eluted. Crude goat serum containing anti-GC polyclonal Ab (Alpha Diagnostics, Inc., San Antonio, TX) was centrifuged at 10000 rpm for 10 min and the supernatant was diluted 1:2 in starting buffer. The Ab solution was added to the column and the liquid was eluted until all the Ab solution was added to the column. (The elutant was saved since some Ab did not bind due to column saturation.) Starting buffer was added to the column and elutant was collected in 2 ml increments. Each elutant was shaken to test for the generation of bubbles (an indication that non-specific proteins are still bound to the column) and no more starting buffer was added to the column once no more bubbles were observed. Elution buffer was added to the column and 2 ml fractions of elutant were collected in polypropylene tubes containing 200 µl of neutralization buffer. The absorbance of each fraction was measured spectrophotometrically at λ = 280 nm and all fractions with an

OD_{280nm} above 0.2 were pooled together for protein concentration. The column was cleaned with 10 ml of elution buffer and 20 ml of starting buffer and stored in starting buffer containing azide at 4°C. 2 ml of purified Ab was added to a Centricon® reservoir capped with a collection vial. Samples were centrifuged at 3000 rpm for 30 min in an SS-34 rotor and the filtrate was discarded. These steps were repeated until all purified Ab was bound to the filter matrix. The Centricon® tube was inverted and the new bottom of the tube was capped with a retention vial and centrifuge at 2500 rpm for 5 min. The recovered liquid was resuspended in 50% glycerol solution and the concentration of the recovered protein was measured using the Bradford assay.

Conjugation of Chromophores to Purified Antibody. Purified goat anti-GC Ab was conjugated to Oregon green 488 using the FluoReporter® Oregon Green 488 Protein Labeling Kit (Molecular Probes/Invitrogen). Briefly, 200 µl of Ab and 20 µl of bicarbonate solution were transferred to a reaction tube. In a separate tube, 500 µg of reactive Oregon green 488 dye (warmed to RT) was resuspended in 50 µl DMSO. Dye solution was stirred into the Ab solution for 60 min at RT protected from light based on the following equation:

$$\mu l \text{ of dye solution} = [(\text{Ab concentration})(0.2)/MW](509)(100)(MR)$$

where MR = 15 or 20 if the purified Ab concentration is 1-3 mg/ml and MR = 10 or 15 if the purified Ab concentration is 4-10 mg/ml) and MW = the molecular weight of the Ab. Near the end of the labeling incubation, the column buffer was drained from a spin

column (containing a 30000 MW exclusion resin) and the spin column was placed in a 2 ml collection tube. The column was centrifuged at 1100 x *g* for 3 min and the collected liquid was discarded. The labeling reaction was centrifuged at 12000 rpm for 5 min and the supernatant was added dropwise to the spin column to allow the labeled Ab to absorb onto the resin. The spin column was placed in a collection tube and centrifuged as described above. The conjugated Ab present in the collection tube was aliquoted and stored at -20^{o}C.

Immunofluorescence Microscopy Analysis. In general, ME180 cells were seeded on circular silicate glass coverslips (13 mm diameter x 0.13 mm—0.17 mm thick (Gold Seal, Eric Scientific Company, Portsmouth, NH)) in 24-well plates overnight. GC were added to wells and incubated for various lengths of time. Cells were washed with IM and once with PBS. Cells were fixed for 20 min with 4% paraformaldehyde (Electron Microscopy Sciences, Ft. Washington, PA) and treated with blocking solution for 5 min prior to staining. GC and host cells were stained on ice covered from light (unless otherwise stated).

To determine the cellular distribution patterns of GC on ME180 cells, extracellular adherent GC were stained with the Oregon green 488 conjugated goat anti-GC Ab (100 µg/ml) on ice for 60 min. Cells were washed with PBS and treated with a permeabilization solution for 5 min at RT. F-actin was stained with Alexa Fluor 546-labeled phalloidin (4 U/ml) (Molecular Probes/Invitrogen) in the permeabilization solution on ice for 60 min. In F-actin inhibitor studies, ME180 cells were pretreated for 90 min with various concentrations of cytochalasin D prior to staining. In all procedures

following staining, cells were washed with PBS, fixed with 2% paraformaldehyde, and mounted on glass slides (Fisher Scientific, Pittsburgh, PA) with Gel/Mount (Biomeda, Foster City, CA). Cells were analyzed using laser scanning confocal microscopy (LSCM) (Zeiss LSM 510, Carl Zeiss North America, Thornwood, NY) utilizing the 488 nm and 543 nm excitation lasers.

Gentamicin and Tannic Acid Protection Assays. ME180 or Hec1B cervical epithelial cells were seeded in 6-well tissue culture plates (5 X 10^5 cells/well) or in 24-well plates (1 X 10^5 cells/well) and incubated overnight. Prior to infection, GC strains FA1090, MS11 mKC, F62, F62Δ*lgtD*, and F62Δ*lgtA* were grown on GCK for 16-18 h; FA1090(pFT180) and FA1090 Φ(*bla-iga'*) were grown on GCK PenG for 16 h-18 or 20-22 h, respectively; and *E. coil* strain DH5α was grown 16 h on LB agar. Bacteria were resuspended in GCP to a cell density of 1 x 10^9/ml, added to host cells at the appropriate MOI, and incubated in ME180 cell-IM or Hec1B cell-IM for the designated times. Cells were washed four times with IM (or twice with IM and twice with PBS in wells to be treated with tannic acid [TA]). To quantify the total number of adherent and invasive GC (i.e., cell associated), IM was added to triplicate wells for 2 h. Wells were washed, treated with 1% saponin for 15 min, lysates were collected, and aliquots plated on GCK agar. To quantify the number of invasive GC, gentamicin (200 μg/ml or 500 μg/ml in specified experiments) or TA (0.1%, 0.2%, 0.5 %, or 0.2% 90 min + 1% 30 min in specified experiments) was added 2 h prior to the preparation of ME180 cell lysates. Supernatants were collected to quantify extracellular GC that remain resistant to gentamicin or TA treatment. The number of CFU arising on GCK agar was determined after 36-48 h

incubation. In experiments utilizing potential invasion inhibitors, ME180 cells were pretreated with TA (0.2% for 90 min, then 1% for 30 min) for 2 h, gentamicin (200 μg/ml) for 2 h, or cytochalasin D (3 μM) for 45 min prior to incubation with GC. Cytochalasin D was maintained in wells during the incubation of ME180 cells with GC.

Polymerase Chain Reaction. All PCR reactions were performed using the Expand Long Template PCR Kit (Roche Applied Science, Penzberg, Germany). A series of reactions were prepared in two stock solution tubes. The first tube contained the appropriate forward and reverse primers (200 ng/reaction each) (Integrated DNA Technologies, Coralville, IA), template DNA (usually 1 μl), each of the four nucleotide triphosphates (ATP, TTP, CTP, and GTP) (175 μM each), and HPLC grade water. The second tube contained the appropriate DNA polymerase buffer (875μM) and *Taq* Long Template DNA Polymerase (1.25 U/reaction). An aliquot (22.25 μl) from the first stock tube was added to 8-strip thin-walled PCR tubes (Fisher Scientific, Pittsburgh, PA) and mixed with an aliquot (2.75 μl) from the second stock tube immediately prior to insertion into the thermocycler (MJ Research, Inc., Waltham, MA). PCR conditions were: 95^{o}C for 2 min, 10 amplification cycles (denaturation at 95^{o}C for 30 sec, annealing at the appropriate temperature for 30 sec, and primer extension at 68^{o}C for the appropriate time), then 30 additional amplification cycles with a higher annealing temperature (usually + 5^{o}C) and 20 additional sec added to the primer extension of each cycle, and storage at 4^{o}C in the thermocycler until analysis.

Agarose Gel Electrophoresis. Agarose gels (1%) were prepared in TBE buffer with 10 µl ethidium bromide (10 mg/ml). Agarose gel electrophoresis was performed at constant voltage (100 V) until the loading dye front reached the bottom of the gel. Gels were visualized using a Gel Doc XR ultraviolet transilluminator (Biorad) and gel images were processed using Quantity One 1-D analytical software version 4.6.1 (Biorad).

General Cloning Procedures. Digestion and ligation of bacterial DNA was performed using restriction and ligation enzymes, buffers, and protocols provided by New England Biolabs (Beverly, MA). In general, digestion reactions totaled 20 µl, consisted of template DNA, HPLC grade water, 2 µl of 10X digestion buffer, and 1 µl of restriction enzyme (10-20 U/reaction), and proceeded at 37^{o}C for 2 h or overnight. Ligation reactions totaled 20 µl, consisted of the appropriate molar ratios of template DNA(s), HPLC grade water, 2 µl of 10X ligase buffer, and <1 µl of T4 DNA ligase (~100-200 U/reaction), and proceeded at room temperature for 2 h or 16^{o}C overnight.

Transformation of *E. coli* DH5α. *E. coli* DH5α were made competent for heat-shock transformation using the Inoue method (244). An aliquot of competent *E. coli* DH5α was placed on ice for 10 min and mixed with transforming DNA. After a 2 min heat shock, cells were incubated for 30-45 min in a rotating shaker at 37^{o}C. Transformants were selected on LB agar plates containing the appropriate antibiotic by incubation overnight at 37^{o}C.

GC Transformations. GC were swabbed from GCK agar and resuspended to faint turbidity in sterile GC transformation broth in a polypropylene tube. 1 ml of resuspended GC was transferred to a borosilicate glass tube (Fisher Scientific, Pittsburgh, PA) and mixed with transforming DNA or no DNA (negative control). The transformation mix was incubated in a rotating shaker for 3-4 h at 37^{o}C, plated on selective antibiotic-containing GCK agar, and incubated for 48 h.

The spot transformation was performed using the procedure of Gunn and coworkers (103). Briefly, one isolated P^{+} GC colony was resuspended in 100 µl GCP, 10 mM $MgCl_2$ solution. The GC solution was serial diluted 1:3 (25µl into 50 µl GCP), 10 mM $MgCl_2$ and 1 µl of high concentration (>1 µg/µl) DNA of interest was added to each dilution tube. An aliquot (5 µl of each dilution) was spotted onto GCK agar plates, spots were allowed to dry, and incubated overnight. Isolated colonies were patch plated onto GCK PenG (10 ng/ml) and GCK plates to select for GC transformants possessing the *bla-iga*β gene fusion construct.

Establishing the Reporter Strain, **FA1090 Φ(*bla-iga'*).** The Bla-IgAβ fusion protein was constructed using a gene replacement strategy (see Fig. 11A and Fig. 11B) and was expressed in FA1090 to yield strain FA1090 Φ(*bla-iga'*). FA1090 chromosomal DNA was purified (Wizard Genome DNA kit, Promega, Madison, WI) and the IgA protease gene, *iga*, was amplified by the PCR from FA1090 chromosomal DNA using primers igaβ F2 and igaβ R2. The *iga* PCR product was digested with EcoRI and XbaI and directionally cloned into pK18 forming plasmid pSEB77. The first 3294 bp of the *iga* coding region and an additional 149 bp upstream of the *iga* start codon were deleted

utilizing deletion PCR with primers igaβ del F and igaβ del R. The deletion PCR product was digested with the BamHI and religated onto itself, forming pSEB77Δ (~5200 kb). The *bla* gene was amplified via the PCR from pBR322 using primers bla F and bla R, digested with BamHI and XmaI, and directionally cloned into pSEB77Δ, forming pSEB79. (The *bla* PCR extended from 250 bp upstream of the *bla* start codon through the entire coding region, but excluded the *bla* stop codon.) pSEB79 contains the Φ(*bla-iga'*) gene fusion construct. The Φ(*bla-iga'*) construct was amplified from pSEB79 via the PCR with igaβ F3 and igaβ R3. The resulting PCR product was digested with XbaI and cloned into pK18UP, which possesses the gonococcal uptake sequence (GUS), to form pSEB82. GC strain FA1090 was transformed with pSEB82 utilizing the gonococcal DNA spot transformation procedure. Transformants were selected on GCK agar containing 10 ng/ml PenG and confirmed to possess PenG resistance on 75 ng/ml GCK PenG media. (All primers used in this study are described in Table 3.)

Nitrocefin Hydrolysis Assay. Bla activity was determined using a modified version of a spectrophotometric assay established by O'Callaghan et al. (214) (see Fig. 12A). Briefly, GC were grown overnight at 37^{o}C in GC broth, resuspended to a Klett of 100, and collected by centrifugation for 1 min at 12000 rpm. Culture supernatants were saved. Pellets were resuspended in PE buffer. A 500 μg/ml (1 mM) stock solution of nitrocefin substrate (Calbiochem, LaJolla, CA) was prepared according to the manufacturer's instructions and stored as aliquots at -20^{o}C. Appropriate dilutions of bacteria culture supernatants (overnight broth cultures diluted to Klett 50, centrifuged for 1 min at 12000 rpm, supernatants transferred to a new tube, and diluted in PE buffer for

Table 3. List of Primers Used in This Study

Primers	DNA Sequence (5' to 3')[a]
Bla F	TCCCCCCGGGCCGCATTAAAGCTTATCGATG[b]
Bla R	CGGGATCCCCAATGCTTAATCAGTGAGG[c]
igaβ F2	GCTCTAGACCCGAGATACTGACCAAATG[d]
igaβ R2	CGGAATTCCAAAGGCATTGAGCTGTAGC[e]
igaβ del F	CGGGATCCCCCGGGCTGTTATTCAAGCGAAGATGGGAAGC[f]
igaβ del R	CGGGATCCGTACAGCAAAACAATGTGGAAATTGC[g]
igaβ F3	CCAATGCATCTAGACCCGAGATACTGACCAAATG[h]
igaβ R3	CCAATGCATCTAGAGGCATTGAGCTGTAGCTTTG[i]
Omega F	GACCTGCAGTTGCAAACCCTCACTGATCC[j]
Omega R	CAGTCTGCAGGAGTTAAGCCGCGCCGCGAA[k]
GCKatA F1	TCCCCCCGGGGTGCCTCGTCAGAATAGGAC[l]
GCKatA R1	CCCAAGCTTAATGCCAATACTGATGCGAGG[m]
GCKatA del F1	AAAACTGCAGCGGAAAGCGTATTCGTAACCGG[n]
GCKatA del R1	AAAACTGCAGCCAAGACGATGACGACTACTTCAG[o]

a The underlined sequence represents the restriction enzyme site
b Amplifies *bla* starting 250 bp upstream of *bla* start codon, XmaI site
c Amplifies *bla* starting at the 3' end of *bla* excluding the stop codon, BamHI site
d Amplifies *iga* starting 1095 bp upstream of *iga* start codon, XbaI site
e Amplifies *iga* starting 94 bp downstream of *iga* stop codon, EcoRI site
f Amplifies sequence starting 149 bp upstream of the *iga* promoter and continues upstream of *iga*, BamHI site
g Amplifies the β-domain of *iga* and downstream sequence, BamHI site
h Amplifies the Φ(*bla-iga'*) construct from pK18 Φ(*bla-iga'*) starting upstream, XbaI site
i Amplifies the Φ(*bla-iga'*) construct from pK18 Φ(*bla-iga'*) starting downstream, XbaI site
j Amplifies the Ω_{Spec} cassette from pHP45 starting upstream, PstI site
k Amplifies the Ω_{Spec} cassette from pHP45 starting downstream, PstI site
l Amplifies *katA* starting 1090 bp upstream of *katA* start codon, XmaI site
m Amplifies *katA* starting 1280 bp downstream of *katA* stop codon, HindIII site
n Amplifies sequence starting 62 bp upstream of *katA* start codon and continues upstream of *katA*, PstI site
o Amplifies sequence starting 259 bp upstream of *katA* stop codon and continues downstream of *katA*, PstI site

spectrophotometric reading) or buffer blanks (diluted to a concentration where OD readings fell into a linear range of nitrocefin hydrolysis) were incubated with nitrocefin (fc 50 μg/ml) at RT for 30 min and centrifuged for 1 min at 12000 rpm. Supernatants were collected and transferred to disposable plastic cuvets and the OD at $\lambda = 520$ nm measured. Control samples included PE buffer alone, nitrocefin alone in PE buffer, each GC strain alone in PE buffer, and GC broth in PE buffer. The Bla activity of the FA1090 Φ(*bla-iga'*) pellet was established as 100 arbitrary units (AU) for a selected individual trial (within the triplicate trials). 100 AU of activity is defined as the amount of nitrocefin hydrolyzed in 30 min by 1 x 10^9 FA1090 Φ(*bla-iga'*) in a 1 ml reaction. The enzymatic activity in other pellet samples and culture supernatants were normalized to this reading. In experiments with nonviable GC, prior to analysis, GC were killed with gentamicin and 4^{o}C overnight storage as described previously (218).

Cellular Distribution of CCF2-AM. ME180 cells were seeded in 24-well plates on coverslips overnight as described above, washed with RPMI 1640 containing 10 μM Hepes, and loaded with 1 μM CCF2-AM (Invitrogen/PanVera, Carlsbad, CA) for 90 min at room temperature. Hoechst 33342 (100 ng/ml) (Molecular Probes/Invitrogen) was added for the final 60 min. Cells were washed once with PBS and mounted on glass slides with Gel/Mount. Cells were analyzed using a Zeiss Axioplan 2 fluorescence microscope (Carl Zeiss North America, Thornwood, NY).

Fluorescence-based β-lactamase Reporter Assay. ME180 cells were seeded in 24-well plates on coverslips (for fluorescence microscopy) or in 6-well plates without coverslips

(for flow cytometry) overnight. FA1090 Φ(*bla-iga'*) was grown on GCK PenG overnight, added to the wells at the indicated MOI, and incubated for 6 h (unless otherwise stated). GC culture supernatants were prepared as above and filtered through 0.2 μm Acrodisc Syringe Filter (Pall/Gelman Laboratory, East Hills, NY)] before incubation with host cells. After washing, cells were incubated with 1 μM CCF2-AM for 90 min (for fluorescence microscopy) or 0.25 μM CCF2-AM for 45-60 min (for flow cytometry) at RT covered from light. For microscopic visualization, cells were washed with PBS and coverslips were mounted on glass slides with Gel/Mount. Cells were analyzed using a Zeiss AxioImagerZ1 microscope (Carl Zeiss North America) with excitation at 405 nm and image quality was optimized using AxioVision 4.6 software (Carl Zeiss North America). For flow cytometry analysis, cells were washed with PBS, incubated in trypsin (Mediatech, Herndon, VA) for 15 min at 37^{o}C, and pelleted. Cells were resuspended in 5 ml polystyrene round bottom tubes (12 x 75 mm) (BD Biosciences, Bedford, MA) and centrifuged at 1250 rpm for 5 min at 4^{o}C. Trypsin was decanted and ME180 cells were gently resuspended in PBS and placed on ice covered from light until analysis. Samples were gravity filtered through 30 μm Filcons (Consul T.S., Torino, Italy) immediately prior to analysis. Cells were resuspended in PBS and analyzed using the 405 nm (photomultiplier tube FL6) and 488 nm (photomultiplier tube FL1) excitation lasers on a CyAn ADP flow cytometer (Dako Cytomation, Fort Collins, CO). (Experimental trials for flow cytometry analysis where procedural changes occur, including alterations in the invasion MOI, invasion time course, CCF2-AM concentrations, or CCF2-AM loading time, are indicated in the appropriate figure legends and/or Results subsection.) For experiments utilizing inhibitors, ME180 cells were

pretreated with cytochalasin D (100 μM) for 60 min or latrunculin B (5 μM) for 45 min prior to incubation with GC and the inhibitors were maintained in the media throughout the incubations. Data were analyzed using the Summit 4.1 software (Dako Cytomation).

Establishing the Catalase Deficient Strain, FA1090Δ*katA*. The GC catalase gene (*katA*) was deleted and replaced with a spectinomycin resistance ($Spec^R$) cassette (Ω_{Spec}) using a gene replacement strategy (see Fig. 26A and Fig. 26B) and was expressed in FA1090 to yield strain FA1090Δ*katA*. FA1090 chromosomal DNA was purified (Wizard Genome DNA kit, Promega) and the *katA* gene was amplified by the PCR from FA1090 chromosomal DNA using primers GCKatA F1 and GCKatA R1. The katA PCR product (~3880 bp) was digested with XmaI and HindIII and directionally cloned into pK18 (~2700 bp) forming plasmid pSEB3 (~6550 bp). The first 1254 bp of the *katA* coding region and an additional 62 bp upstream of the *katA* start codon were deleted utilizing deletion PCR with primers GCKatA del F1 and GCKatA del R1 (A GUS is located 77 bp downstream of the *katA* stop codon in the flanking region amplified by GCKatA del R1). The deletion PCR product was digested with the PstI and religated onto itself, forming pSEB3Δ (~5230 bp). The Ω_{Spec} cassette (~1450 bp) was amplified via the PCR from pHP45 (~2340 bp) using primers Omega F and Omega R, digested with PstI, and cloned into pSEB3Δ, forming pSEB5 (~6680 bp). GC strain FA1090 was transformed with pSEB5. Transformants were selected on GCK agar containing 50 μg/ml kanamycin and 50 μg/ml Spec. The lack of catalase activity was confirmed in transformants by adding hydrogen peroxide (10%) dropwise to patch streaks to test for the production of O_2

bubbles. FA1090 was tested with hydrogen peroxide as a positive control. (All primers used in this study are described in Table 3.)

Generating Spontaneous Rifampicin and Naladixic Acid Resistant Mutants of GC. GC strains FA1090 and FA1090Δ*katA* were grown overnight and resuspended to a Klett of 100 in GCP solution. Bacteria (250 µl) were plated on GCK agar containing rifampicin (Rif) (50 µg/ml) or naladixic acid (Nal) (50 µg/ml) and incubated for 48-72 h. Colonies were picked and streaked onto new GCK Rif or GCK Nal plates to confirm that they are Rif^R and Nal^R, respectively.

GC Intracellular Survival and Escape Assays. ME180 cells or Hec1B cells were seeded in 6-well or 24-well tissue culture plates and incubated with GC as described in the gentamicin protection assay above unless otherwise stated. In all survival and escape assays, supernatants and cell lysates were collected at each time point as described in the gentamicin protection assay unless otherwise stated.

To quantify GC adherence, invasion, and intracellular survival under **continuous bactericidal agent treatment**, cells were treated with gentamicin (200 µg/ml or 500 µg/ml) or TA (0.1% or 0.5%) for 2 h post-infection. Wells were washed and treated with the same concentration of gentamicin or TA for 2 and 4 h chase periods. Alternatively, to quantify GC invasion, intracellular survival, and escape with **intermittent bactericidal agent treatment**, survival assays were performed as described above except wells were treated with gentamicin (200 µg/ml) or TA (0.1% or 0.2% 90 min+ 1% 30 min) for 2 h post-infection and then treated with IM during the 2 and 4 h chase periods. After the

chase period, some wells were treated with 0.1% TA for 1 h. To measure GC survival, lysates were collected at each time point and to quantify escape, supernatants were collected at each time point. In experiments where cytoskeletal inhibitors were used, cytochalasin D (3 μM), latrunculin B (1 μM), or nocodazole (35 μM) were added to the gentamicin for the final 15 min of the 2 h post-infection treatment and added during the chase periods. In experiments using **Bla reporter escape assays**, ME180 cells were incubated with $Pil^{+}Opa^{+}$ FA1090 Φ(*bla-iga'*) for 6 h and treated with gentamicin (200 μg/ml) for various lengths of time. Following gentamicin treatment, cells were loaded with 0.25 μM CCF2-AM for 45-60 min and analyzed by flow cytometry as described above.

For competitive intracellular survival assays between FA1090 and FA1090Δ*katA*, ME180 cells were seeded in 6-well tissue culture plates (4×10^5 cells/well). To each well, half of the added GC were FA1090 and the other half were FA1090Δ*katA* as follows: (1) Rif^R FA1090 vs. Nal^R FA1090Δ*katA* or (2) Nal^R FA1090 vs. Rif^R FA1090Δ*katA*. ME180 cells were incubated with 8×10^6 GC/well (4×10^6 FA1090 and 4×10^6 FA1090Δ*katA*) (for assays with a starting MOI 10) or 8×10^8 GC/well (4×10^8 FA1090 and 4×10^8 FA1090Δ*katA*) (for assays with a starting MOI 1000) for 6 h and chased with 200 μg/ml gentamicin (MOI 10 assays) or 500 μg/ml gentamicin (MOI 1000 assays) to test for GC adherence, invasion, and survival in the presence of continuous bactericidal agent treatment as described above. In all TA treated wells, the initial wash after treatment was performed with PBS followed by additional washes with IM. All data was compiled using the GraphPad Prism 3.0.

Gentamicin or TA GC Kill Curve Assays. GC were grown overnight and resuspended in GCP (1 x 10^9/ml). For the gentamicin kill curve assay, GC were diluted (7.5 x 10^7 GC/well) in IM with or without gentamicin in 6-well tissue culture plates. Samples were collected every 20 min over a 2 h period and diluted for viable cell count on GCK. For the TA kill curve assay, GC were diluted (1 x 10^8 GC/well) in PBS plus 1% Kellogg's supplement with or without TA in 6-well tissue culture plates. Samples were collected at 0, 30, 60, 120, and 210 min and diluted for viable cell count on GCK. The number of CFU arising on GCK agar was determined after 36-48 h incubation.

Viability Staining. For viability staining procedures, ME180 cells were incubated with GC in 24-well tissue culture plates as described in the gentamicin protection assay above. Afterwards, ME180 cells were treated with IM, gentamicin (500 μg/ml) in IM, or TA (0.1%) in PBS for 60 min. Cells were washed with PBS, stained for 60 min with SYTO 13 (1-2 μM) (Invitrogen/Molecular Probes) and propidium iodide (250 ng/ml) (Invitrogen/Molecular Probes), and post-fixed and mounted as described in the immunofluorescence microscopy analysis above. In trials without ME180 cells, 5 x 10^8/well GC were incubated in IM or TA and resuspended in SYTO 13/propidium iodide solution. After staining, GC were washed three times with PBS and resuspended in PBS at a concentration of 1.7 x10^7 GC/μl in 30 μl. The entire suspension was streaked onto glass slides, air dried at RT protected from light for 45 min, and heat-fixed to the slide prior to visualization.

TA Disc Diffusion Assay. FA1090 were resuspended to a cell density of 1 x 10^9 GC/ml, diluted (1 x 10^8 GC/ml), and 100 µl of diluted culture was swabbed onto GCK. Blank paper discs (6 mm diameter, Becton Dickinson) were immersed in TA or PBS, removed until no longer dripping with solution, and placed on the FA1090-swabbed GCK plate. Disc-containing GCK plates were incubated for 24 h. Following incubation, the diameter of the each zone of FA1090 growth inhibition generated around each disc was measured from two separate positions on the zone of inhibition.

CHAPTER 1—HOST CELL SIGNALING INDUCED BY *NEISSERIA GONORRHOEAE* PRIOR TO INVASION

Introduction

During host-pathogen interactions, bacteria, such as GC, can bind to cell surface receptors by mimicking receptor ligands. Receptors undergo conformational changes that can lead to receptor autophosphorylation or the recruitment of scaffolding/adapter proteins that possess binding sites for signaling molecules, such as kinases. Kinases mediate phosphorelay transfers from receptors to various internal signaling molecules and amplify signals during these phospho-transfers. A signal initiated at a single receptor can be amplified by kinase activity to trigger an entire signaling cascade [for review see (128)]. Since GC can bind to a variety of host receptors using different GC surface molecules, the order of receptor binding and the number of different receptors bound may influence which host cell signaling pathways are affected, the degree of activation/deactivation of each pathway, and the eventual outcome of infection. GC infections in women are characterized by an initial asymptomatic state and bacterial invasion into subepithelial tissues (270); thus, GC must interact with and signal to cervical epithelial cells in a manner that allows invasion without eliciting inflammatory immune responses.

The MAPK signaling pathways are central regulators of numerous host cell processes, including cell survival, proliferation, differentiation, apoptosis, and stress responses [for review see (41, 240)]. MAPK activation is linked to actin reorganization and elongation of actin microfilaments around GC subsequently encloses the bacteria within the host cell (98, 126). Each MAPK module consists of a MAPK kinase kinase, a

MAPK kinase, and the actual MAPK (ERK, JNK, or p38). All three MAPKs phosphorylate a variety of cytoskeletal proteins, including paxillin by ERK, p38, and JNK; caldesmon by p38; and profilin and p150-spir by JNK (90, 125, 127, 136, 159, 215). MAPK can also trigger downstream kinases, which activate actin-related proteins. ERK can phosphorylate ribosomal S6 kinase 1 (RSK1) or PAK to regulate filamin A, an actin cross linking protein involved in actin rearrangements (286, 305). ERK can also transfer phosphates to MLCK to activate the actin motor protein myosin and increase membrane protrusions (155, 212, 282). Signaling by p38 to MAPKAP 2/3 phosphorylates p16 of the Arp 2/3 actin regulation complex and heat-shock protein 27 to instigate actin polymerization (102, 263). These indirect activation strategies permit signals to be amplified further by these downstream kinases prior to transfer to the actin cytoskeleton. MAPK could also translocate into the nucleus to activate transcription factors to turn on actin-associated genes and cytokine genes to mediate proinflammatory immune responses (240).

Combinations of p38, JNK, and/or ERK signaling have been determined to contribute to invasion by many pathogens, including *N. meningitidis* (75, 77, 124, 157, 249, 264, 278). A connection between MAPK activation and GC invasion into epithelial cells has not been established, but JNK does contribute to GC internalization into phagocytes (110, 113). Opa_{CEA}-expressing GC trigger ASM in monocytes, which leads to increased Src activation, downstream upregulated of JNK phosphorylation, and GC internalization (110, 113). GC pilus retraction was shown to enhance the activation of all three MAPK in T84 epithelial cells and GC were shown to activate JNK in Chang

conjunctiva and HeLa cells to increase activator protein 1 (AP-1) activation and cytokine production (123, 210).

Signaling through the epidermal growth factor receptor (EGFR, or ErbB1) represents a well-known pathway to activate ERK. ErbB1 is activated by binding to ligands directly or through transactivation. During transactivation, ligand binding to G-protein coupled receptors triggers proteases to release growth factors from the cell that can then bind to other receptors, such as ErbB1 (221). Once activated, ErbB1 dimerizes and autophosphorylates using its inherent tyrosine kinase activity. Various signaling molecules, including Grb2, SOS, and Ras are recruited to phosphorylate ErbB1. Ras then signals to a MAPK kinase kinase to initiate a MAPK signaling module (221). Signaling continues through ErbB1 until specific tyrosines on ErbB1 become phosphorylated and recruited phosphatases, such as SHP-1, dephosphorylate the receptor and attenuate the pathway (149). Once GC attach to epithelial cells, they recruit ErbB1 as part of cortical plaque formations (185), suggesting that ErbB1 manipulation is important in GC pathogenesis.

Signaling pathways other than MAPK are also modulated by pathogens, eliciting host cell responses. Bad is a pro-apoptotic factor from the Bcl-2 protein family that binds to Bcl-2 and Bcl-X_L to promote apoptosis (54). Whether GC trigger apoptosis in epithelial cells remains controversial. In a study where GC upregulated anti-apoptotic factors, Bad activation levels were unchanged (23). In studies where GC PorB induced epithelial cell apoptosis, Bad was not investigated. Bad can be phosphorylated by JNK or Akt to promote cell survival by preventing its binding to Bcl-2 and Bcl-X_L (54, 174). Akt is involved in cell cycle regulation, cell survival, and proliferation (259). Previous reports

indicate that GC target Akt activation to enhance entry as part of specific invasion pathways. GC PLD can bind directly to Akt to increase CR3-mediated invasion in primary cervical cells and blocking PI3K/Akt signaling and recruitment to GC microcolonies inhibits epithelial cell invasion (70, 167).

PKC is another signaling molecule linked to bacterial invasion. A signal through PKC can be directed to numerous pathways depending on the cell conditions and the stimulating ligand (208). PKC activation requires an increase in intracellular calcium levels triggered by secondary messengers such as diacylglycerol or inositol-triphosphate (236, 237). Inhibition of PKC blocks internalization of GC and heparin-coated beads through HSPG receptors in HeLa and Hec1B epithelial cells, but not in ME180 cells or Chang conjunctiva cells (59, 61, 81). The interaction of GC pili and Por with A431 epithelial cells also induces elevated cytoplasmic calcium levels suggesting PKC may be activated in these cells (13, 146).

Src represents another family of at least eight kinases involved in a diverse network of cellular functions [for review see (280)]. Several studies indicate GC target Src during host cell invasion via CEACAM receptors. Inhibition of Src kinases inhibits Opa-dependent GC internalization via CEACAM 3 in HeLa cells or the CEACAM 1/ASM signaling pathway in neutrophils (110, 180). Infection with piliated GC also induces phosphorylation of the pilus receptor, CD46 by a specific Src kinase—c-Yes (166). Most of these studies point to a greater role for Src in GC interaction with phagocytes, but the role of Src signaling in epithelial cell invasion is unknown.

In this study, I identified signaling pathways manipulated by GC that may facilitate GC invasion and immune evasion in the ME180 epithelial cell line. Since most

epithelial cells internalize GC 4-6 h after inoculation (98, 261, 266), I focused on GC-host cell signaling transpiring during the first 3 h of infection. I reasoned that signaling events during these early time points would be responsible for the conformational changes in host cell proteins and alterations in host cell gene expression that lead to GC invasion. I followed activation of signaling pathways by performing immunoblots and probing for the phosphorylated forms of each protein of interest. The proinflammatory response of epithelial cells during incubations with GC was measured by detecting IL-8 cytokine production through ELISA. I determined that GC induce MAPK activation in ME180 cells, but do not manipulate Bad, Akt, PKC, or Src-dependent signaling pathways. I identified an unusual prolonged ERK activation profile. ERK was triggered by GC early in infection and extended into time periods where GC are thought to initiate invasion. I also demonstrated that LOS antigenic variation influences JNK activation levels, which in turn, influences host cell proinflammatory cytokine production. My data indicate that GC expressing LnNT LOS may be better equipped for immune evasion. Overall, this study uncovers the fact that GC stimulate MAPK pathways at time points prior to invasion into a susceptible cell line.

Results

Tyrosine phosphorylation changes in ME180 cells induced by interactions with GC.

To determine the host cell signaling molecules GC trigger to mediate invasion, I incubated ME180 cells with strain F62 and monitored changes in protein tyrosine phosphorylation over time in comparison to untreated cells. I identified a ~200 kDa protein that displayed consistent decreased phosphorylation and ~40 kDa protein that showed increased phosphotyrosine levels (Fig. 2A). I performed a similar experiment over a longer time course using strain F62Δ*lgtD*, which does not express the terminal GalNAc on its α-chain LOS, and observed five additional proteins from different trials that exhibited altered tyrosine phosphorylation (Fig. 2B). Each of the identified proteins showed different phosphorylation patterns: some exhibited detectable phosphorylation by as early as 5 min and lost their signal by 30 min (see Fig. 2B, proteins d and e), while other proteins were not activated until 30 min and/or sustain their signal until at least 90 min (see Fig. 2A and Fig. 2B, protein a). These data indicate GC trigger host cell signaling pathway alterations during the early stages of infection leading up to invasion and suggest that changes in LOS structure affect these pathways.

Activation of the ERK pathway in cervical epithelial cells. A critical step in the GC invasion process is the rearrangement of the host actin cytoskeleton. Since the MAPKs have molecular weights near 40 kDa (the approximate size of some of the tyrosine phosphorylated proteins identified in Figure 2) and the MAPKs are associated with proteins involved in actin microfilament and microtubule rearrangement (41), I focused on these proteins.

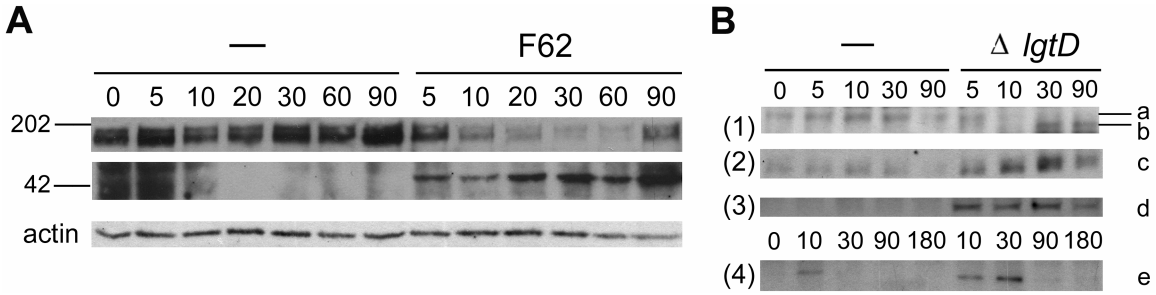

Figure 2—The effect of GC interaction with cervical epithelial cells on protein phosphorylation. Signaling assays were performed by incubating ME180 cells with (A) no GC (-) or F62 or (B) no GC (-) or F62Δ*lgtD*. In panel A, images show two host cell proteins (~200 kDa and ~40 kDa, respectively) with altered phosphorylation levels; actin = loading control. In panel B, proteins a-e represent five proteins with altered phosphorylation levels; (1) ~ 70 kDa (2) ~60 kDa (3) ~ 50 kDa (4) ~40-45 kDa. Protein phosphotyrosine was detected by probing lysates with an anti-phosphotyrosine 4G10 polyclonal antibody; GC used were $P^{+}Opa^{-}$ and time periods = min; data in each panel are representative of at least three independent experiments.

To investigate the signaling pathways that control actin dynamics, I incubated ME180 cells with different GC variants and probed host cell lysates for phosphorylated proteins of interest by immunoblot analysis. GC strains stimulated prolonged activation of ERK. ME180 cells incubated in the absence of GC displayed little or no ERK phosphorylation over the course of the experiments (Fig. 3A, Fig. 3D, and Fig. 3F), indicating that increases in ERK phosphorylation were due to the added bacteria. When commensal *Neisseria* strains *N. sicca* 342 *and N. subflava* 44 were added to ME180 cells, rapid ERK activation was observed during the first 30 min, but this pattern differed from the extended ERK phosphorylation maintained for the entire 3 h time course in host cells incubated with GC strain F62Δ*lgtA* (Fig. 3B). Since ERK phosphorylation was initiated (although in different patterns) by both commensal strains and GC, I determined if the ERK activation was the result of host cell contact with extracellular stimuli, in general. I coated carboxylated microspheres with bovine serum albumin (BSA) and introduced them to ME180 cells. The BSA coated beads were not able to activate ERK over 5 h (Fig. 3C), indicating neisserial factors were triggering ERK and continuous ERK activation was a unique characteristic of the pathogenic GC.

I investigated the potential GC surface factors responsible for the prolonged phosphorylation of ERK. ME180 cells treated with LnNT LOS-expressing F62Δ*lgtD* displayed extensive ERK activation over 3 h regardless of Opa expression (Fig. 3D) and only a slight reduction between 90 min and 3 h in cells infected with nonpiliated derivatives (Fig. 3E). Host cells infected with the lactosyl LOS-expressing F62Δ*lgtA* showed a similar ERK activation profile to F62Δ*lgtD*-infected cells (Fig. 3F-H). Together, these data demonstrate that GC trigger extended robust ERK phosphorylation

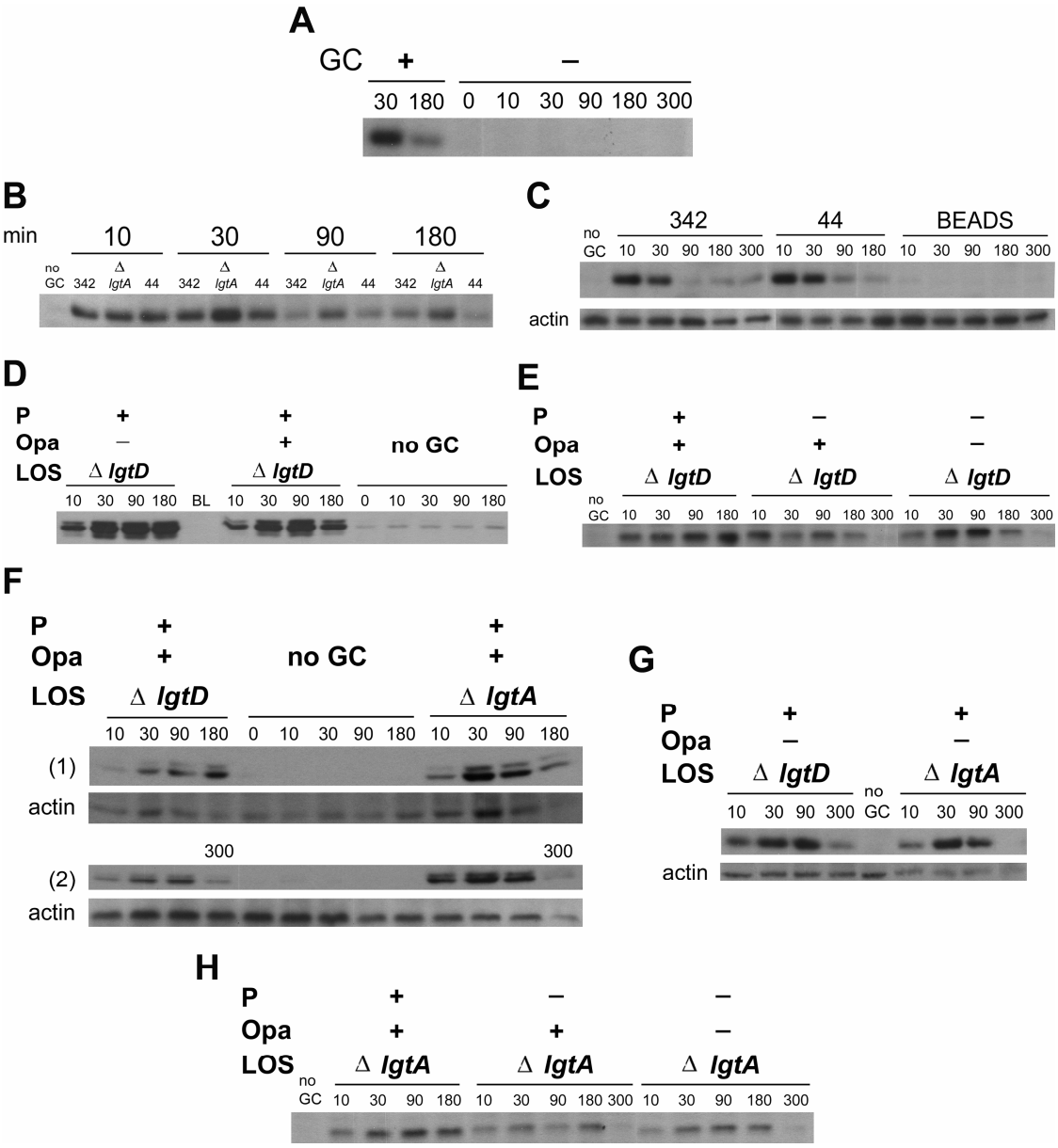

Figure 3—GC trigger extended ERK activation in epithelial cells. Signaling assays were performed by incubating ME180 cells with (A) no GC (-) or $P^{+}Opa^{+}$ F62Δ*lgtA* (+), (B) $P^{+}Opa^{+}$ F62Δ*lgtA* (Δ*lgtA*) or the commensal *Neisseria* strains *N. sicca* 342 (342) or *N. subflava* 44 (44), (C) the commensal strains *N. sicca* 342 or *N. subflava* 44 or bovine serum albumin-coated microspheres (BEADS), (D and E) F62Δ*lgtD* (F and G) F62Δ*lgtD* or F62Δ*lgtA* or (H) F62Δ*lgtA*; data in panels A, D, F, and G representative of at least three independent experiments; panels B and H representative of two independent experiments; panels C and E = single experiment. In each panel, untreated ME180 cells incubated in media alone (labeled [no GC] or [-]) served as negative controls for ERK activation and in selected panels, actin = loading control. ERK phosphorylation was detected by probing lysates with an anti-phospho-ERK 1/2 polyclonal antibody; time periods = min. The image quality of each blot shown was optimized for presentation and equivalent adjustments were made for each lane within a given image.

in epithelial cells for greater than 3 h. Pili expression appears to exhibit an enhanced contribution to ERK activation, but overall alterations in pili, Opa, and LOS expression did not result in strong ERK signal fluctuations. Thus, ERK activation may be provoked by an unidentified GC surface structure or may be activated by several factors in a redundant manner. Regardless, these data suggest a critical role for ERK in GC infection and its activation time course indicates this signaling may be an early step in generating invasion-susceptible host cells.

GC-epithelial cell interactions lead to gradual p38 activation. To determine whether ERK is a specific GC target or if GC activate other MAPK during infection, I incubated ME180 cells with the GC variants utilized to study ERK activation described in Figure 3 and tested host cell lysates for phosphorylation of the stress response kinase, p38. As in Figure 3, ME180 cells incubated in the absence of GC or treated with BSA-coated beads displayed little or no p38 phosphorylation (Fig. 4A, Fig. 4D, Fig. 4F, and Fig. 4I = untreated cells; Fig. 4C = beads), indicating that any p38 phosphorylation would be the results of added bacteria. *N. sicca* 342 *and N. subflava* 44 both activated p38, but their activation pattern varied between experimental trials (Fig. 4B and Fig. 4C). Among the F62 strains examined, all variants exhibited similar patterns of p38 activation. Phosphorylation levels were low over the first 30 min and increased to peak activation at the later 90 min and 3 h time points (Fig. 4D-J). The only observed deviation from this pattern was found when comparing P^-Opa^- F62Δ*lgtD* and P^-Opa^- F62Δ*lgtA*. In this phenotypic background, F62Δ*lgtA* p38 activation peaked by 30 min at a higher degree than F62Δ*lgtD* (Fig. 4H). In all other comparisons, LOS α-chain length, Opa expression,

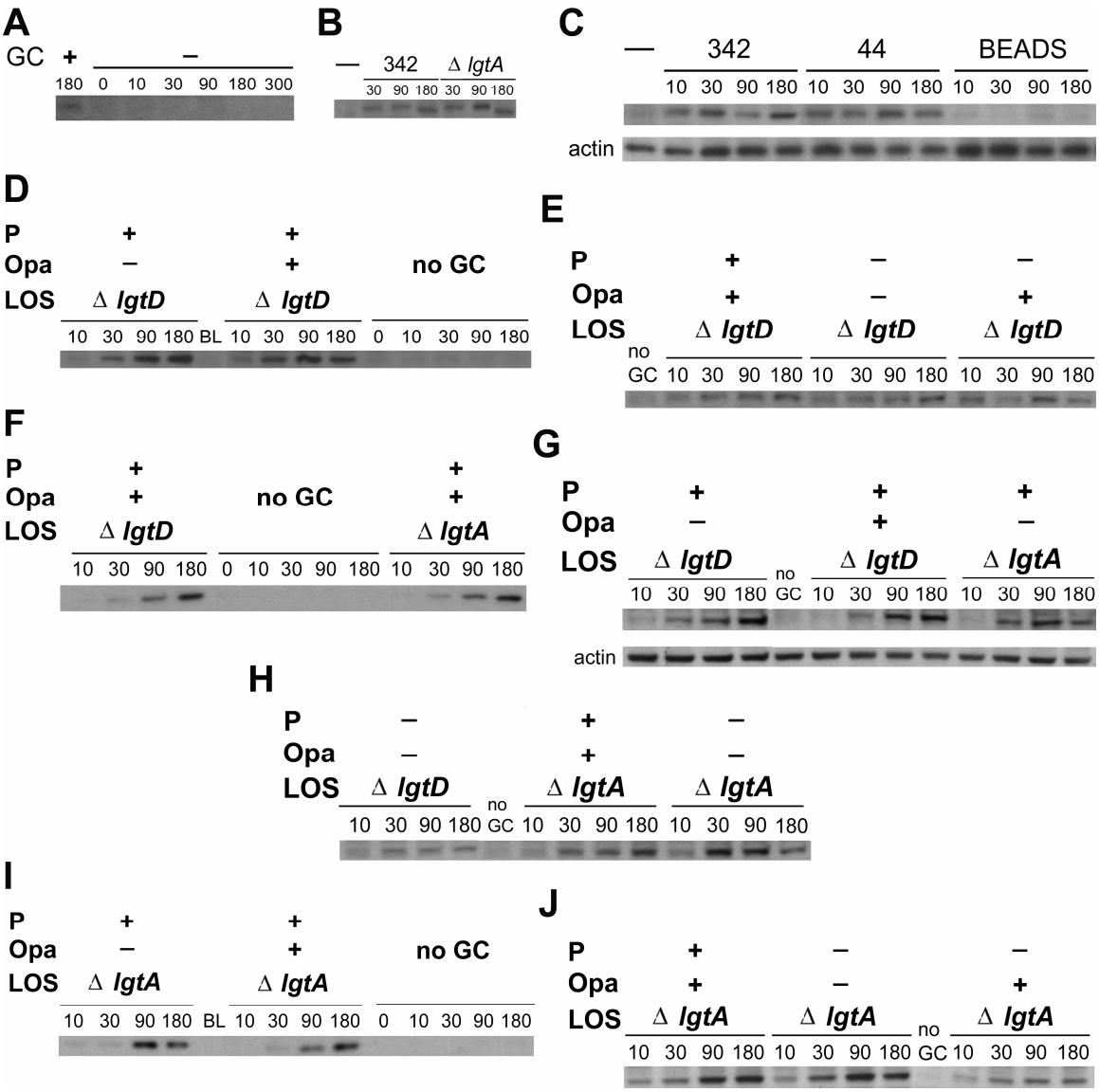

Figure 4—GC elicit prolonged, but delayed, activation of p38. Signaling assays were performed by incubating ME180 cells with (A) no GC (-) or P^+Opa^+ F62Δ*lgtA*, (B) P^+Opa^+ F62Δ*lgtA* (Δ*lgtA*) or the commensal *Neisseria* strain *N. sicca* 342 (342), (C) *N. sicca* 342, *N. subflava* 44 (44), or bovine serum albumin-coated microspheres (BEADS), (D and E) F62Δ*lgtD*, (F-H) F62Δ*lgtD* or F62Δ*lgtA*, or (I and J) F62Δ*lgtA*; data in panels A and D representative of at least three independent experiments; panels B, F, G, and I representative of two independent experiments; panels C, E, and H = single experiment. In each panel, untreated ME180 cells incubated in media alone (labeled [no GC] or [-]) served as negative controls for p38 activation and in selected panels, actin = loading control. p38 phosphorylation was detected by probing lysates with an anti-phospho-p38 polyclonal antibody; time periods = min. The image quality of each blot shown was optimized for presentation and equivalent adjustments were made for each lane within a given image.

and pili expression did not alter the p38 phosphorylation pattern. Overall, these data indicate that p38 activation is downstream in the time course of host cell activation by GC relative to ERK activation. Phosphorylation of p38 is not influenced by LOS, Opa, or pili antigenic and phase variation suggesting p38 activation is not triggered by these invasion-promoting factors, but instead is a general stress response generated by GC.

Influence of GC LOS antigenic variation and Opa expression on JNK signaling. I examined JNK signaling in response to GC during the initial 3 h of infection by incubating ME180 cells with the GC variants utilized to study ERK and p38 activation described in Figures 3 and 4, respectively, and testing host cell lysates for JNK phosphorylation. As seen with other MAPK, ME180 cells incubated in the absence of GC or treated with BSA-coated beads displayed little or no JNK phosphorylation (Fig. 5A, Fig. 5B, and Fig. 5H). The commensals *N. sicca* 342 and *N. subflava* 44 showed a rapid JNK activation profile similar to the commensal-induced ERK signaling (see Fig. 3B). For these strains, the highest phosphorylation levels were observed in the first 30 min, but JNK activation peaked at later time points for GC (Fig. 5C). I also observed that the phospho-JNK antibody recognized multiple JNK isoforms.

To define the GC surface structures responsible for host cell JNK signaling, I incubated ME180 cells with different GC surface variants. In ME180 cells treated with F62Δ*lgtD*, JNK activation peaked at 90 min and was reduced in host cells incubated with an Opa^{+} variant (Fig. 5D). These data suggest Opa expression decreases epithelial cell JNK activation. LOS truncation also influenced the host cell JNK activation profile. JNK phosphorylation levels were elevated and appeared to peak sooner (30-90 min) in ME180

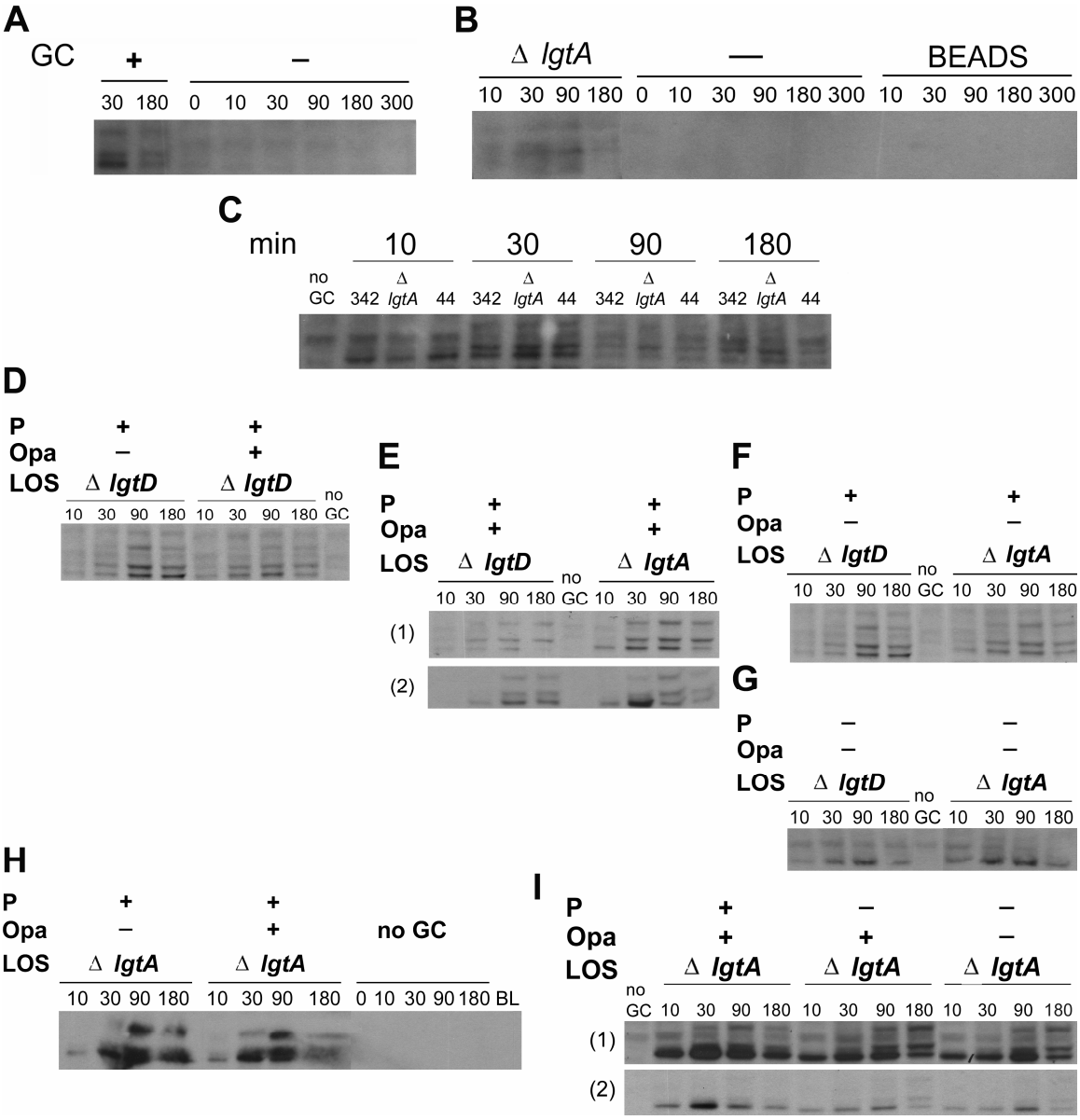

Figure 5—GC activation of JNK. Signaling assays were performed by incubating ME180 cells with (A) no GC (-) or P^+Opa^+ F62Δ*lgtA*, (B) P^+Opa^+ F62Δ*lgtA* (Δ*lgtA*) or bovine serum albumin-coated microspheres (BEADS), (C) P^+Opa^+ F62Δ*lgtA* (Δ*lgtA*) or the commensal *Neisseria* strains *N. sicca* 342 (342) or *N. subflava* 44 (44), (D) F62Δ*lgtD*, (E-G) F62Δ*lgtD* or F62Δ*lgtA*, or (H and I) F62Δ*lgtA*; data in panels A and E representative of at least three independent experiments; panels D, F, G, and I representative of two independent experiments (I = different exposures from the same experiment); panels B, C, and H = single experiment. In each panel, untreated ME180 cells incubated in media alone (labeled [no GC] or [-]) served as negative controls for JNK activation and in selected panels, actin = loading control. JNK phosphorylation was detected by probing lysates with an anti-phospho-JNK 1/2/3 polyclonal antibody; time periods = min. The image quality of each blot shown was optimized for presentation and equivalent adjustments were made for each lane within a given image.

cells incubated with Opa$^+$ F62Δ*lgtA* compared to Opa$^+$ F62Δ*lgtD*-infected cells (90-180 min) (Fig. 5E). In infections with Opa$^-$ and/or P$^-$ F62Δ*lgtD* derivatives, host cell phospho-JNK levels are similar to levels created by the corresponding F62Δ*lgtA* variants (Fig. 5F and Fig. 5G). These data indicate that P$^+$Opa$^+$ F62Δ*lgtD* reduce JNK signaling relative to other variants. Opa expression by piliated F62Δ*lgtA* did not reduce host cell JNK phosphorylation as seen with the LnNT LOS strains above (Fig. 5H). P$^-$ F62Δ*lgtA*-infected cells displayed a lower activation level of the major phospho-JNK isoform at 30 min (Fig. 5I, panel 1), but exhibited a higher degree of activation of the two minor isoforms (characterized by slower migration on SDS-PAGE) at 3 h (Fig. 5I, panel 2). Taken together, these data demonstrate that GC expressing truncated LOS elicit more rapid and intense JNK activation from host cells compared to LnNT LOS-expressing GC in an Opa$^+$ background. GC expressing Opa and LnNT LOS can inhibit and delay JNK signaling in infected host cells, which suggests that preventing a strong JNK activation signal in host cells is advantageous to GC infection.

Role of LOS in inducing IL-8 expression from cervical epithelial cells. One role of MAPK activation is to activate transcription factors to increase expression of proinflammatory cytokine genes. Since epithelial cells secrete proinflammatory cytokines, such as IL-8 and IL-6 in response to GC (78, 80, 108), I determined if increased activation of the JNK pathway influenced ME180 cells to produce more IL-8. I incubated ME180 cells with F62Δ*lgtD* and F62Δ*lgtA* for 24 h, collected culture supernatants and tested for IL-8 expression. P$^+$Opa$^+$ F62Δ*lgtA* triggered greater IL-8 secretion from ME180 cells compared to P$^+$Opa$^+$ F62Δ*lgtD* (p-value = 0.0001), but

treating cells with purified LOS from either strain was not sufficient to elicit IL-8 secretion (Fig. 6A). The difference in IL-8 production appeared to correlate with the difference in JNK activation from host cells incubated with P^+Opa^+ F62Δ*lgtD* or F62Δ*lgtA* in Figure 5E. To determine if the increased JNK activation elicited by F62Δ*lgtA* contributes to greater IL-8 secretion by epithelial cells, I treated ME180 cells with an inhibitor of JNK kinase activity, SP600125, to block further downstream JNK signaling events prior to incubation with F62Δ*lgtD* or F62Δ*lgtA*. In the presence of SP600125, IL-8 production from F62Δ*lgtA*-infected ME180 cells was reduced, but remained higher than IL-8 levels in F62Δ*lgtD*-infected cells, which were not affected by the inhibitor (Fig. 6B). Taken together, these data demonstrate that LnNT LOS expression by GC inhibits IL-8 production from epithelial cells (Fig. 6). IL-8 expression in epithelial cells is triggered by GC-induced signaling through the JNK pathway and at least one other unidentified pathway. GC expressing truncated LOS appear to activate the JNK pathway as an additional stimulus for IL-8 production. LnNT LOS-expressing GC do not signal through the JNK pathway and only activate the unidentified pathway(s) to elicit IL-8 production. Thus, IL-8 production is reduced during infections with LnNT-expressing GC, which may help this variant inhibit recruitment of immune cells, such as neutrophils and macrophages, to infection sites.

Contact with bacterial stimuli reduces ErbB1 autophosphorylation at tyrosine 1173. A previous report showed that the cell surface receptor ErbB1 (185 kDa) was recruited to sites of GC adherence on host epithelial cells (185). Autophosphorylation of ErbB1 at the regulatory site tyrosine 1173 (Y^{1173}) creates a binding site for the SHP-1 phosphatase,

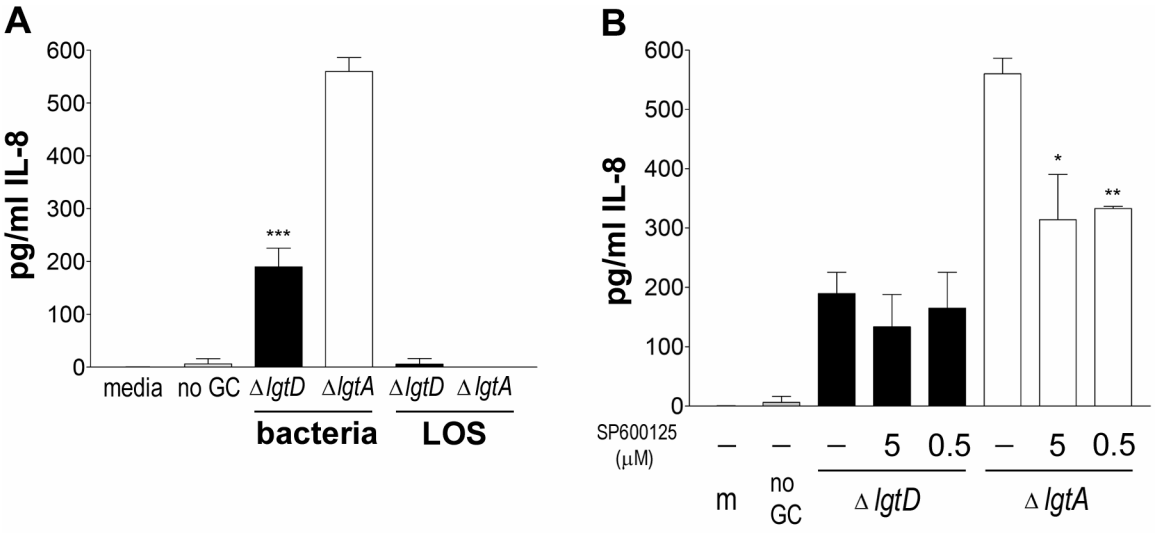

Figure 6—IL-8 production by epithelial cells infected with GC expressing different LOS structures. ELISA were performed by incubating ME180 cells with: (A) F62Δ*lgtD*, F62Δ*lgtA*, or their corresponding purified LOS, or (B) F62Δ*lgtD* or F62Δ*lgtA* in the absence or presence of the JNK inhibitor, SP600125 (30 min pretreatment and maintained throughout incubation); data in panel A are representative of two independent experiments each performed in triplicate (±SD) and panel B = average (±SD) of triplicate trials (-inhibitor) or duplicate trials (+inhibitor) from a single experiment. In panel A, a statistical comparison between IL-8 production from F62Δ*lgtD*-infected cells and F62Δ*lgtA*-infected cells (bacteria) yielded a p-value = 0.0001. In panel B, a similar comparison between F62Δ*lgtA*-infected cells (-inhibitor) and F62Δ*lgtA*-infected cells (+ 5 μM inhibitor) yielded a p-value = 0.0118 and the comparison between F62Δ*lgtA*-infected cells (-inhibitor) and F62Δ*lgtA*-infected cells (+ 0.5 μM inhibitor) yielded a p-value = 0.0014. Cells incubated without GC (no GC) or media incubated without cells or GC (media or m) served as negative controls for IL-8 production. GC used were P^+Opa^+.

which deactivates ErbB1 and prevents signaling to ERK. These factors combined with my finding that GC promote extended ERK activation in epithelial cells (see Figure 3) made this ErbB1 residue an excellent candidate for GC to target for dephosphorylation during infection.

To identify the ~200 kDa host cell protein from Figure 2A that exhibited decreased tyrosine phosphorylation upon incubation with F62, I incubated ME180 cells in the presence or absence of different GC variants as described in Figure 3 and examined ErbB1 phosphorylation. Untreated cells displayed high autophosphorylation at the Y^{1173} regulatory site over the course of the experiments (Fig. 7A and Fig. 7F), indicating that ErbB1 was not activated prior to GC infection. The addition of GC decreased ErbB1 Y^{1173} phosphorylation suggesting GC induced activation of this pathway (Fig. 7A). However, none of the GC surface molecules examined influenced ErbB1 phosphorylation patterns. Lack of pili or Opa expression did not prevent GC-induced Y^{1173} dephosphorylation (Fig. 7B-E), but Y^{1173} autophosphorylation levels tended to recover better at later time points (90 min, 3 h, or 5 h) in ME180 cells incubated with P^- variants (Fig. 7C and Fig. 7E). LOS variation also did not alter ErbB1 dephosphorylation patterns (Fig. 7F-H). Since ErbB1 is not known as a direct receptor for GC, I hypothesized that the physical contact of GC with epithelial cells may be responsible for the observed decrease in Y^{1173} phosphorylation. ME180 cells incubated with *N. sicca* 342 and *N. subflava* 44 showed similar ErbB1 dephosphorylation levels to GC over the first 90 min of infection, but recovered to normal phosphorylation levels similar to P^- GC by 3 h (Fig. 7I and Fig. 7J). Less dramatic Y^{1173} dephosphorylation was also observed in ME180 cells treated with BSA-coated beads (Fig. 7J). Overall, these data indicate that ErbB1 Y^{1173}

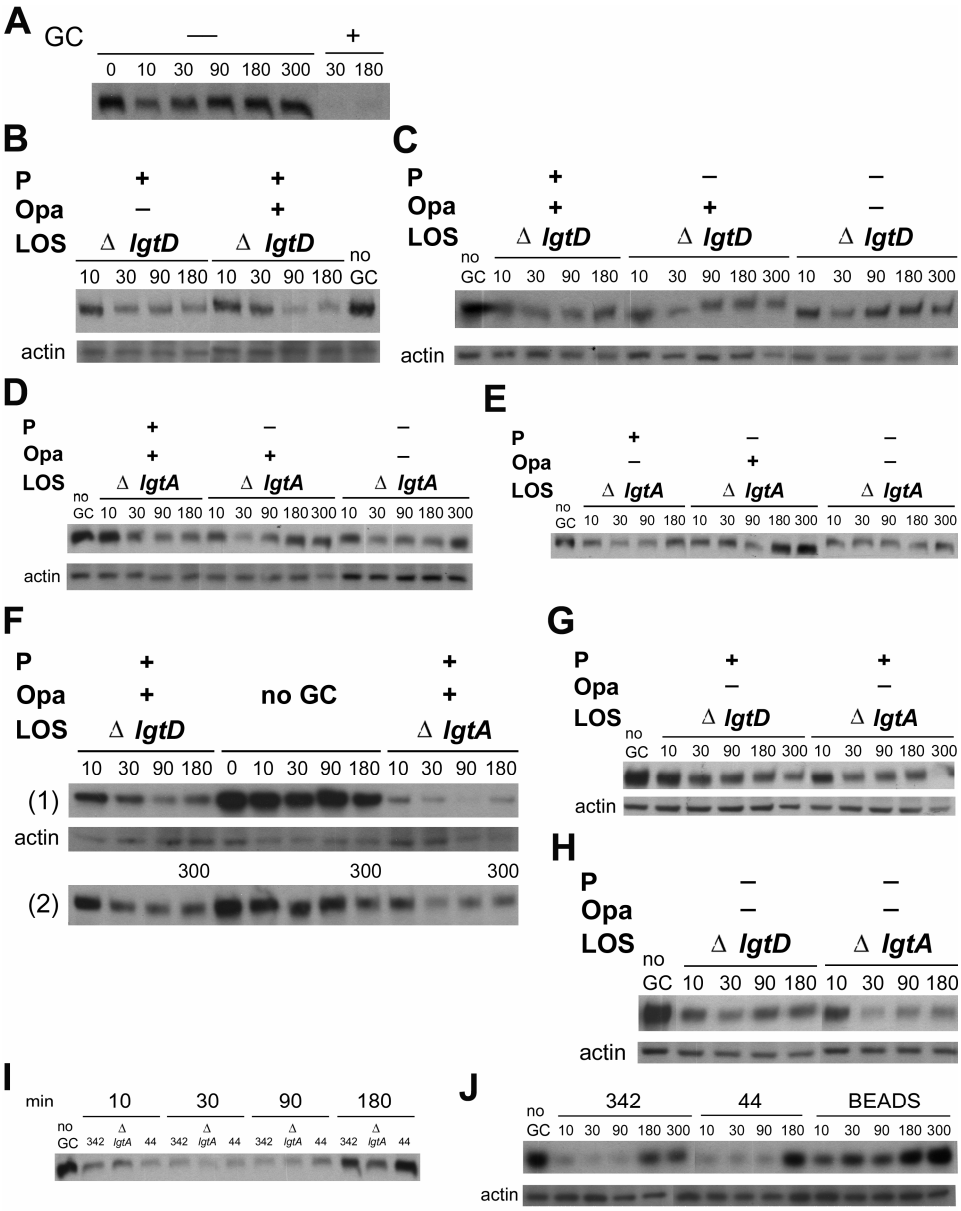

Figure 7—Extracellular stimuli decrease phosphorylation of ErbB1 at tyrosine 1173. Signaling assays were performed by incubating ME180 cells with (A) no GC (-) or P^+Opa^+ F62Δ*lgtA*, (B and C) F62Δ*lgtD*, (D-F) F62Δ*lgtD* or F62Δ*lgtA*, (G and H) F62Δ*lgtA*, (I) P^+Opa^+ F62Δ*lgtA* (Δ*lgtA*) or the commensal *Neisseria* strains *N. sicca* 342 (342) or *N. subflava* 44 (44), or (J) the commensal strains from panel I or bovine serum albumin-coated microspheres (BEADS); data in panels D and G representative of at least three independent experiments; panels A, H, and I representative of two independent experiments; panels B, C, E, F, and J = single experiment. In each panel, untreated ME180 cells incubated in media alone (labeled [no GC] or [-]) served as negative controls for ErbB1 activation and in selected panels, actin = loading control. ErbB1 phosphorylation was detected by probing lysates with an anti-phospho-ErbB1 polyclonal antibody; time periods = min. The image quality of each blot shown was optimized for presentation and equivalent adjustments were made for each lane within a given image.

dephosphorylation in epithelial cells is triggered by physical contact with extracellular stimuli rather than a specific interaction with GC. Even so, GC may utilize this signaling caveat to sustain prolonged ERK activation by continuous signaling through ErbB1 and thereby prevent ErbB1 autophosphorylation at Y^{1173}.

Identification of signaling molecules in ME180 cells whose phosphorylation levels are not altered by GC. Other proteins that exhibited changes in tyrosine phosphorylation in Figure 2 migrated in the 50-80 kDa range or below 30 kDa (data not shown) on SDS-PAGE. Therefore, I examined signaling molecules in this size range linked to regulation of the host cytoskeleton in order to identify other factors involved in GC invasion. I incubated ME180 cells with Opa^+ or Opa^- F62Δ*lgtD* displaying sialylated or nonsialylated LnNT LOS. LOS sialylation should block GC-induced signaling propagated by the LnNT moiety.

Lysates recovered from GC treated cells showed no differences in Akt, Bad, and PKC phosphorylation patterns compared to untreated cells regardless of LOS sialylation and showed no difference in Src phosphorylation regardless of Opa expression. Akt (~60 kDa) was not activated in untreated cells and no proteins in the Akt size range were activated by GC (Fig. 8A). The pro-apoptotic Bad protein (~23 kDa) was phosphorylated in both untreated and GC-treated cells (Fig. 8B), indicating GC did not induce apoptosis. Two proteins that may represent PKCα (~80 kDa) were also phosphorylated in untreated cells, but incubations with GC did not alter their activation state (Fig. 8C). Src phosphorylation was also constitutive in untreated cells and unaltered by GC infection (Fig. 8D). These results demonstrate that GC do not trigger global signaling changes in

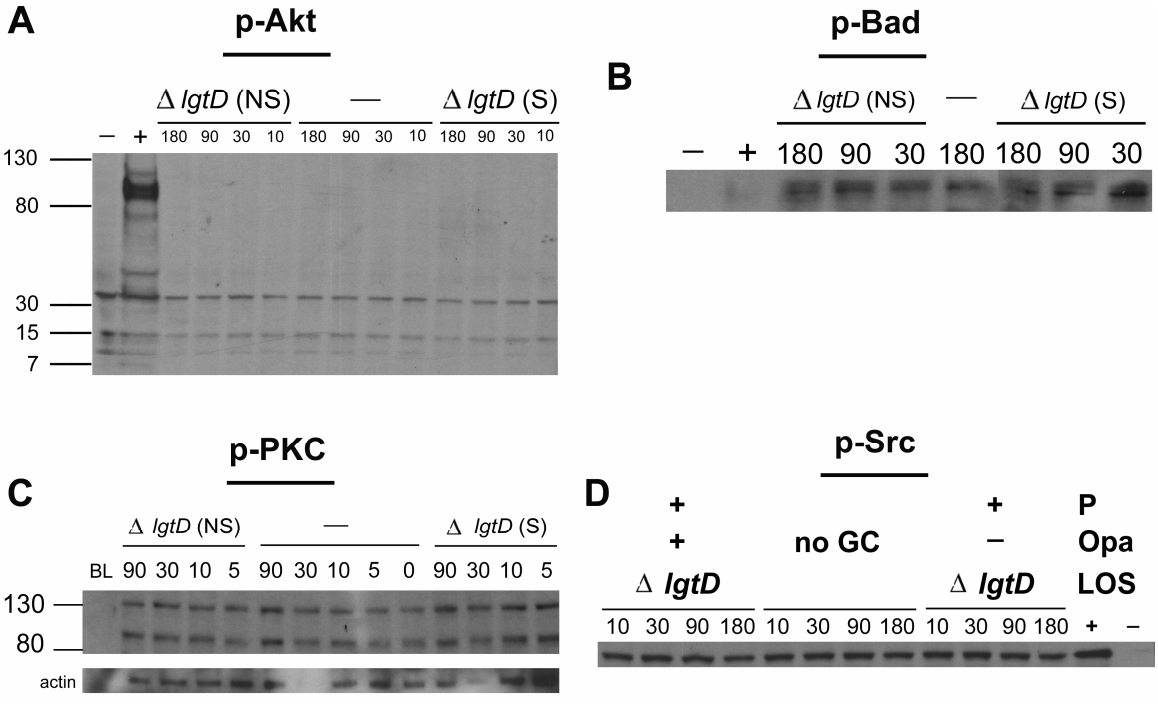

Figure 8—GC do not trigger universal changes in host cell signaling: central kinases not activated during GC infection. GC strain F62Δ*lgtD* was sialylated (S) by treatment with CMP-NANA or left untreated (NS). Signaling assays were performed by incubating ME180 cells with (A-C) sialylated or nonsialylated F62Δ*lgtD* or (D) Opa^{+} or Opa^{-} nonsialylated F62Δ*lgtD*; time periods = min. Activation of each protein was determined by immunoblot analysis by probing with an (A) anti-phospho-Akt (T^{308}); data representative of two independent experiments, (B) anti-phospho-Bad (S^{136}); data representative of two independent experiments, (C) anti-phospho-PKC (T^{638}); data representative of three independent experiments, or (D) anti-phospho-Src (Y^{418}); data representative of three independent experiments. In each panel, untreated ME180 cells incubated in media alone (labeled [no GC] or [-]) served as negative controls for protein phosphorylation and in selected panels, actin = loading control. In panels A, B, and D, positive (+) and negative (-) control lysates were analyzed as phosphorylation standards for each protein. In panel C, analysis of a F62Δ*lgtD* bacterial lysate (BL) treated with SDS, but not incubated with ME180 cells, ensured that the analyzed proteins were derived for the host cells (not from GC). The image quality of each blot shown was optimized for presentation and equivalent adjustments were made for each lane within a given image.

epithelial cells during infection. Instead, GC alter specific signaling targets, such as MAPKs, which may allow GC to mediate the inflammatory response and stimulate host cell entry.

Opa expression alters MAPK phosphorylation. To better understand the role of Opa in GC pathogenesis, I investigated the ability of GC that cannot express Opa to signal through the MAPK pathways. I incubated ME180 cells with variants of GC strain MS11 including: MS11 with an Opa^+ phenotype at the onset of the incubation; MS11 whose initial phenotype was Opa^-, but possess the genes to turn on Opa expression; and strain MS11Δ*opa* that cannot express Opa due to *opa* gene knockouts. ME180 cells incubated with phenotypic Opa^- or the genetic Opa^- (Δ*opa*) MS11 exhibited a general increase in p38 phosphorylation and similar p38 activation profiles (Fig. 9A). JNK activation in cells incubated with phenotypic Opa^- MS11 occurred at the 90 min and 3 h time points and was delayed compared to Opa^+ MS11 where JNK phosphorylation was observed at 30 min and 90 min. MS11Δ*opa*-infected ME180 cells showed a slight increase in JNK activation at 90 min in comparison to signaling by the phenotypic Opa^- variant (Fig. 9C). As for the ERK activation profile of these host cells, each MS11 variant triggered the characteristic prolonged ERK activation observed in host cells incubated with other GC strains (see Figure 3). However, MS11Δ*opa*-infected cells displayed a peak in ERK phosphorylation at 90 min that did not occur in the parent MS11 strain (Fig. 9B). During the infection with the phenotypic Opa^- strain, a mixed population of GC containing Opa^+ variants can arise due to Opa phase variation. Thus, the Opa^+ variants in both the Opa^+ starting inoculum and the phenotypic Opa^- starting inoculum may be responsible for the

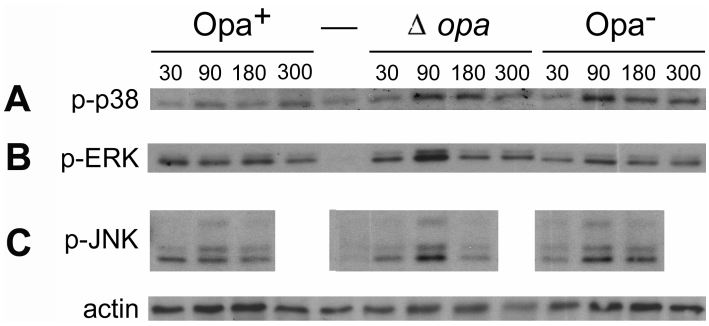

Figure 9—Effect of Opa expression on MAPK phosphorylation in ME180 cells. Signaling assays were performed by incubating ME180 cells with: P^+Opa^+, P^+Opa^-, or $P^+\Delta Opa$ MS11; time periods = min. Activation of each MAPK was determined by immunoblot analysis by probing with an (A) anti-phospho-p38 antibody, (B) anti-phospho ERK 1/2 antibody, or (C) anti-phospho JNK antibody; data in all panels = a single experiment and the same lysates were tested in each panel, but panel (C) was performed as a separate experiment. In each panel, untreated ME180 cells incubated in media alone (-) served as negative controls for MAPK activation and actin = loading control. The image quality of each blot shown was optimized for presentation and equivalent adjustments were made for each lane within a given image.

reduced ERK activation between the 30 min and 90 min time points. These data demonstrate that knocking out Opa expression affects GC-induced host cell signaling and further suggests signaling through ERK plays a role in GC pathogenesis.

Discussion

GC are well adapted to the female host and often infections are characterized by GC invasion into host tissues without eliciting symptoms. How GC achieve the balance of activating host cells for invasion without stimulating detrimental immune responses remains the subject of ongoing investigation. Nonphagocytic cells, such as cervical epithelial cells, are not designed to engulf bacteria, so GC must manipulate host cells to instigate invasion-promoting cellular processes. GC provoke these abnormal cellular events by binding to receptors and triggering alterations in host cell signaling pathways. One major reason GC hijack signaling pathways is to gain control over the actin cytoskeleton (117, 179, 187). In a normal state, host cells polymerize and rearrange actin for movement and to maintain cell integrity. GC-induced signaling amplifies and changes these actin-mediated processes to promote actin recruitment to sites of adherent bacteria and actin reorganization around invading GC. In this study, I identified signaling pathways in cervical epithelial cells that GC activate leading up to invasion. I discovered that, prior to invasion, GC activate each of the three MAPK (Fig. 10). Previous reports have demonstrated that MAPK signaling is linked to regulating actin reorganization and cytokine production—two major cell processes GC must regulate to ensure a successful infection (41, 126, 240).

MAPK activation within GC-infected epithelial cells may drive invasion-promoting actin dynamics. My data in Figures 3-5 show that each MAPK exhibited phosphorylation at 3 h when GC have established intimate adhesion to host cells. At this time, GC are positioned to elicit morphological changes in the host cell actin cytoskeleton to make them susceptible to invasion. GC could signal through MAPKs to manipulate

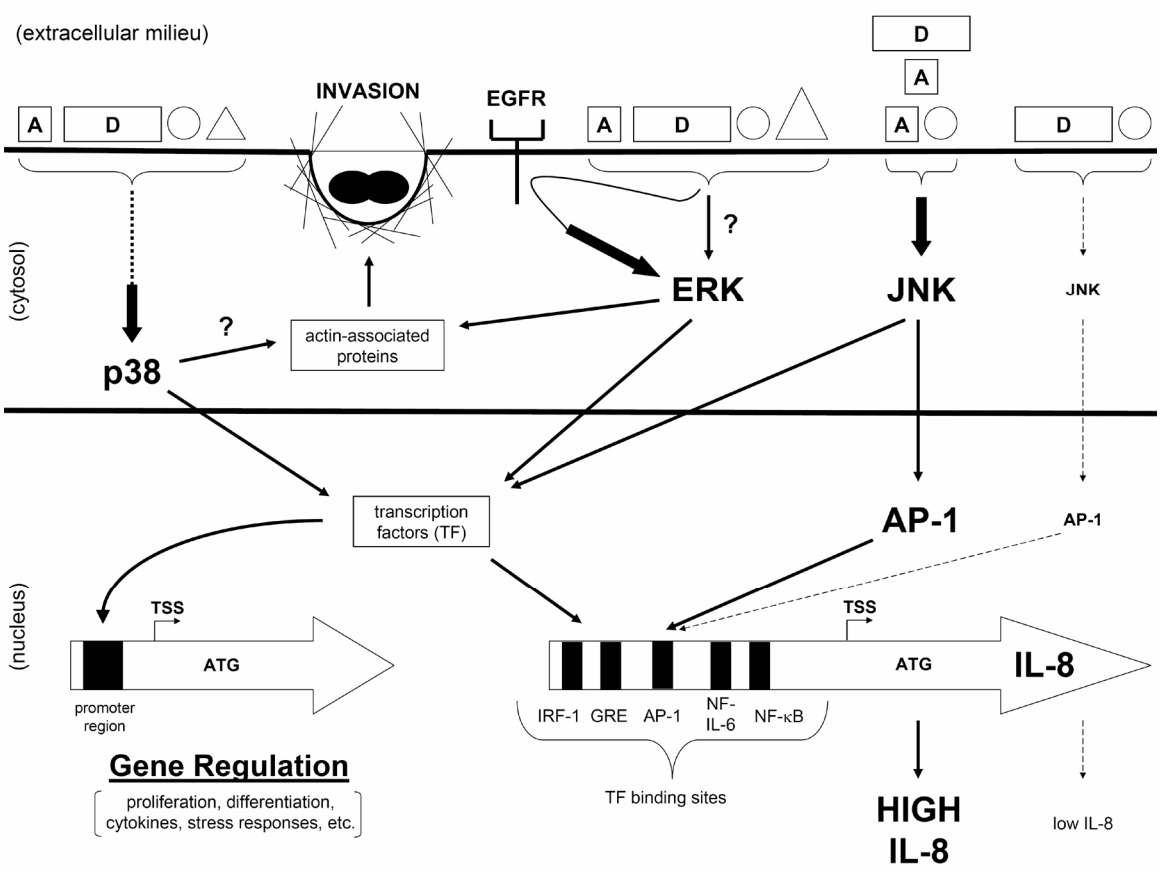

Figure 10—Working model for MAPK signaling by GC in cervical epithelial cells. GC expressing the different combinations of pili (triangle), Opa (circle), or LOS [LnNT (rectangle+D) or lactosyl (square+A)] each triggered a delayed activation of p38 and prolonged activation of ERK. Pili may play a greater role in ERK activation and ErbB1 transactivation appears to play a role in GC-induced ERK signaling. Activated p38 and ERK may signal to downstream actin-associated proteins or transcription factors to promote GC invasion and alter host cell gene expression. GC expressing LnNT LOS and Opa reduce JNK activation in host cells, but GC expressing other combinations of Opa and LOS exhibit stronger JNK activation. A portion of the IL-8 induced by GC is derived from the JNK signaling pathway. Decreased GC-induced JNK activation could diminish downstream signaling to transcription factors, such as AP-1, which may lower the IL-8 levels produced by epithelial cells.

actin-associated proteins. Activating actin-associated proteins could facilitate GC invasion by promoting actin polymerization and rearrangement at the plasma membrane. Therefore, even though I did not establish a direct link between MAPK signaling and GC invasion in this study, I propose that GC-induced MAPK activation contributes to host cell invasion based on the timing of signal activation, the links these pathways have to downstream cytoskeletal proteins, and their established role in the invasion pathways of other pathogens.

One of the most interesting findings in this study was the different time courses of MAPK activation by GC in cervical epithelial cells. Activation of p38 was delayed compared to ERK and JNK, and I also observation that GC induced prolonged ERK phosphorylation. Signaling through a specific MAPK could dictate a cellular response at a certain time point or signaling through a combination of MAPK could cooperate to manipulate the cell. For example, in the time course studied, activation of JNK and ERK is initiated earlier than p38, but only p38 and ERK sustain peak-level activation at the end of the time course. Extended ERK activation (i.e. sustained strong phosphorylation for greater than 2-3 h) is a rare occurrence. Most pathogens that trigger ERK signaling in various epithelial cells, including the commensals *N. sicca* and *N. subflava* tested in this study, only induce transient fluctuations in ERK phosphorylation (i.e. increased phosphorylation for usually less than 1 h) (30, 151, 198, 247, 296).

My results in Figure 3 demonstrated that no single surface structure analyzed was solely responsible for the GC-induced prolonged ERK activation. P^+ GC appeared to maintain a somewhat stronger ERK signal at the 3 h time point in Figure 3E and 3H, but P^- bacteria still exhibited a significant signal above the controls. These data suggest pilus-

mediated signaling may enhance prolonged ERK activation in infected cells. Howie, *et al*. presented the only previous report that revealed GC can induce sustained ERK activation. This group showed that mechanical forces on the host cell membrane generated by pilus retraction enhanced signaling by all three MAPK (123). Therefore, pilus retraction may be important in my proposed MAPK-directed regulation of actin that leads to GC invasion. The pilus receptor, CD46, has been shown to signal to ERK in PMA-treated T-cells (245).

Opa may also influence host cell ERK signaling and help prolong ERK mediated responses. In Figure 9B, I showed that GC incapable of expressing Opa (MS11Δ*opa*) elicited greater ERK activation in ME180 cells at a pre-invasion time point compared to host cells infected with the phenotypic MS11 Opa^+ and MS11 Opa^- strains. During incubations with the phenotypic Opa^- variants, Opa phase variation can occur to create a mixed population of Opa^+ and Opa^- GC that interact with host cells. Therefore, ME180 cells were most likely exposed to Opa^+ GC in these two scenarios, which may have contributed to their altered ERK signaling profile that differed from MS11Δ*opa*-infected cells. Overall, Opa expression may contribute to epithelial cell ERK activation during GC-host cell interactions.

GC also appear to signal to ERK through the well characterized ErbB1 pathway. I demonstrated that GC contact with host cells dephosphorylated ErbB1 at the Y^{1173} downregulation site throughout the 3 h time course. By blocking Y^{1173} phosphorylation over time, ErbB1 signaling can continue to downstream substrates, including ERK (149). The ErbB1 Y^{1173} dephosphorylation time course in Figure 7 correlated well with the time course for GC-induced ERK activation in Figure 3 indicating GC may signal to ERK

through ErbB1. Since ErbB1 is not known as a GC receptor, GC may trigger ERK activation through ErbB1 via transactivation after binding to one its primary receptors (Fig. 10). Whether pili-CD46 interactions or pilus retraction leads to ErbB1 transactivation has not been established. Clearly, there are several possible mechanisms for GC to maintain extended ERK activation, which could lead to greater GC control over actin dynamics to mediate invasion. Contributing to these results, a colleague in the lab has demonstrated that inhibiting ERK signaling blocks GC invasion into epithelial cells confirming a role for ERK activation in GC internalization (K.V. Swanson, unpublished observations).

Regulating JNK activation in host cells may contribute to the ability of GC to evade the innate immune response. Above, I also discussed the potential links between GC elicited JNK phosphorylation and regulating the actin cytoskeleton. However, my results in Figure 5 and 6 suggest that GC induction of JNK signaling may play a more prominent role in mediating proinflammatory cytokine production. In Figure 5E, I showed that the more virulent strain, Opa$^+$ F62Δ*lgtD* generated a lower JNK signal in infected ME180 cells relative to Opa$^+$ F62Δ*lgtA*. Furthermore, in Figure 6, the weaker JNK signal in Opa$^+$ F62Δ*lgtD*-infected cells corresponded to a decreased IL-8 response and, based on JNK inhibitor studies, the increased IL-8 production in Opa$^+$ F62Δ*lgtA*-infected cells was a result of greater JNK activation. Suppressing IL-8 production may help Opa$^+$ F62Δ*lgtD* better avoid provoking host immune responses, such as the recruitment of immune cells, which could help explain why GC expressing longer chain LOS structures are more infectious (142, 252, 266). Evidence exists that LOS modifications can influence cytokine production by GC since removal of an acyl chain

from the lipid A portion of LOS decreased IL-6 and IL-8 secretion by epithelial cells (108). Previous studies also indicate that GC expressing LnNT LOS (i.e. F62Δ*lgtD*) can bind to the asialoglycoprotein receptor (ASGP-R) and exhibit increased invasion of epithelial cells compared to GC expressing truncated LOS (i.e. F62Δ*lgtA*) (106, 266). The ASGP-R does possess a cytoplasmic domain that has been shown to signal to ERK after binding the IGF-1 growth (64, 161). However, no link between ASGP-R binding and JNK signaling has been demonstrated. So, whether LnNT LOS can serve as an inhibitor ligand for ASGP-R signaling to JNK or the truncated lactosyl LOS structure can activate greater JNK levels through an unidentified mechanism is unknown. Nevertheless, LnNT LOS expression appears to decrease the proinflammatory immune response in GC-infected epithelial cells by limiting JNK activation and this inhibition may contribute to the increased virulence of LnNT expressing GC (Fig. 10).

GC trigger unique MAPK activation profiles that differ from commensal *Neisseria*. The MAPK activation time course and the finding that changes in GC surface structures alter MAPK signaling provide clues that these pathways contribute to GC invasion and virulence. GC-induced MAPK signaling can also lead to the induction of cytokine expression and the development of immune responses against GC. How GC balance activating specific pathways to achieve their pathogenic goals without also stimulating defenses mechanisms that clear infection is undefined, but this study reveals that GC manipulate the MAPK pathways to help perform this balancing act in cervical epithelial cells.

CHAPTER 2—INVASION OF *NEISSERIA GONORRHOEAE* INTO HUMAN CERVICAL EPITHELIAL CELLS

Introduction

GC invasion requires both bacterial and host cell factors (186). Pili (P), in conjunction with one or more gonococcal invasins (Opa, LOS, and/or Por) or iC3b surface deposition, can induce changes in host cell signaling to drive host actin cytoskeleton polymerization beneath the site of GC adherence to trigger microvilli elongations that promote GC invasion (72, 84, 94, 98, 107, 182, 243, 274, 295). Pili retract to bring GC closer to host cells to permit more intimate adhesions through the binding of Opa and LOS to host cell surface receptors (123, 189, 229, 231). Opa proteins are thought to promote adherence and invasion by binding to CEACAM on host cells (40, 112, 162, 293). However, GC can invade cervical epithelial cells that do not express CEACAM (275), indicating that alternate ligand-receptor interactions can lead to invasion. A member of the Opa protein family can bind host cell HSPG to mediate invasion and alternative GC surface molecules can also serve as invasins (290, 292). LnNT LOS contributes to host cell invasion in an Opa^- background (266). In low phosphate environments, PorB IA mediates invasion in an Opa-independent manner that requires clathrin-coated pit formation, actin rearrangement, and Rho GTPases (160). Por, along with pili and iC3b deposition on the lipid A portion of LOS, can coordinate an interaction with CR3 on primary cervical epithelial cells to trigger invasion (71, 72).

One reason why Opa is believed to play a prominent role in GC invasion was from studies that investigated invasion into host cells transfected with CEACAM or HSPG as the sole GC receptor. Cells used in these studies did not permit GC invasion,

but following transfection with these Opa-specific receptors, Opa-expressing GC were internalized (2, 20, 26, 40, 95, 222). However, since these cells lack receptors for other proposed invasins, such as Por, LOS, and L12, the contributions of these factors in invasion were not analyzed. Clearly, GC possess alternate mechanisms to invade host cells that lack Opa receptors and can invade into host tissue in microenvironments where Opa expression is repressed. The redundancy of GC surface factors that promote invasion demonstrates the importance of this process in GC pathogenesis.

The hallmark of GC invasion into human epithelial cells is the recruitment and rearrangement of host cell F-actin at the site of colonization. F-actin polymerization occurs in host cells by adding globular (G)-actin monomers to the +end of a growing actin microfilament when G-actin exceeds a critical concentration in the cell (76). GC trigger actin polymerization in host cells to cause F-actin rich microvilli to elongate around GC and internalize them (84). Disrupting actin polymerization with inhibitors, such as cytochalasin D, reduced GC invasion into Chang epithelial cells (94). Cytochalasin D, a fungal toxin, and latrunculin B, a sponge toxin, inhibit actin polymerization (46, 248, 267). Phalloidin, another fungal toxin, prevents actin depolymerization by stabilizing F-actin filaments (46). Use of these agents has been useful in investigating the cellular processes that require actin, such as GC invasion.

GC invasion into host epithelial cells has been quantified through adaptations of an antibiotic protection assay first developed by Shaw and Falkow (261). GC are deemed invasive/intracellular based on their resistance to a membrane-impermeable antibiotic added to the host cells following infection (132, 261). Invasion data generated from the antibiotic protection assay possesses inherent limitations: it does not measure the number

of host cells invaded; it cannot measure the frequency by which bacteria invade and exit host cells; it cannot determine if nonviable bacteria are capable of entering into host cells; and the distinction between intracellular and extracellular bacteria is hindered by the protection of extracellular bacteria sequestered inside of a microcolony from antibiotics. Scanning electron micrographs comparing viable and chloramphenicol-treated FA1090 revealed that nonviable GC failed to induce microvilli elongation in Hec1B cervical epithelial cells, and visual internalization of nonviable GC by these cells was not seen (98). The cortical actin microfilament rearrangements normally observed during invasion by viable GC were not seen during the interaction of chloramphenicol and heat-killed GC with A431, Chang conjunctiva, Hec1B, or T84 epithelial cells (187). Heat-killed $MS11_{mk}$ GC do not downregulate the expression of the antimicrobial peptide LL-37 when they interact with ME180 cervical cells (17). While these studies suggest that bacterial viability is required for GC invasion into epithelial cells, methodological limitations prevent the direct quantification of invasion by nonviable GC.

I developed a reporter assay based on Bla expression to study GC-host cell interactions. Since Gram-negative bacteria localize Bla to the periplasm (163), I created a fusion protein that would express Bla on the outer membrane of GC. I took advantage of the fact that IgA protease is an enzyme consisting of an autotransporter domain (β-domain) and a passenger domain (protease domain) (225). (Autotransporter-mediated surface display, or autodisplay, is a protein expression strategy where heterologous passenger domains are express on the outer surface of bacteria when fused with an autotransporter protein (178)). In this study, I established a GC reporter strain, FA1090 Φ(*bla-iga'*), which expresses a Bla-IgA protease β-domain (IgAβ) fusion protein using

an autodisplay strategy. Using FA1090 Φ(*bla-iga'*) and the fluorescence-based, Bla reporter assay, I quantified the number of ME180 cervical epithelial cells invaded by GC variants expressing different surface molecules and compared the invasion levels of viable and nonviable GC. I found that despite their ability to adhere to almost all ME180 cells in an infected population, viable GC expressing pili invaded only a subpopulation of cells. Furthermore, FA1090 Φ(*bla-iga'*) that do not express Opa invaded a larger subpopulation of ME180 cells compared to Opa^+ GC. Nonviable GC adhered to, but did not invade into ME180 cells, regardless of their pili and Opa expression states. Nonviable GC adhered to, but did not invade into ME180 cells, regardless of their pili and Opa expression states, and failed to recruit F-actin to sites of adherent bacteria. Overall, I show that epithelial cell invasion is a dynamic process that requires viable GC that express pili, but not Opa, and I demonstrate the advantages of the Bla reporter system in quantifying bacterial invasion.

Results

FA1090 autodisplays β-lactamase as strain FA1090 Φ(*bla-iga'*). Autodisplay of a normally periplasmic protein onto the extracellular side of the bacterial outer membrane through fusion with an autotransporter domains is well documented (154, 163, 178). The GC IgA protease gene (*iga*) is composed of a Sec-dependent leader sequence, a protease domain, and a β-barrel autotransporter motif (β-domain). The β-lactamase-IgA protease β-domain (Bla-IgAβ) fusion protein expressed in GC strain FA1090 Φ(*bla-iga'*) was constructed using the cloning strategy outlined in Fig. 11A. The genetic constructs generated during the construction of FA1090 Φ(*bla-iga'*) are shown in Fig. 11B. In strain FA1090 Φ(*bla-iga'*), I replaced the protease domain of IgA protease with Bla and utilized the β-domain of IgA protease to localize Bla on the extracellular face of the GC outer membrane (Fig. 11C).

The expression of Bla can be quantified by measuring its enzymatic activity. Bla hydrolyzes nitrocefin to yield a red product detectable by spectrophotometry (Fig. 12A). To demonstrate that Bla is cell-associated in FA1090 Φ(*bla-iga'*), I compared FA1090 Φ(*bla-iga'*) nitrocefin hydrolysis activity to FA1090 and to FA1090(pFT180), which expresses soluble Bla from a multiple-copy number plasmid, pFT180. In general, FA1090(pFT180) displayed a higher level of Bla activity than FA1090 Φ(*bla-iga'*) (Fig. 12B). FA1090 showed no Bla activity. Most (~80%) of the enzymatic activity from FA1090 Φ(*bla-iga'*) was localized in the bacterial pellet (100 arbitrary units [AU] compared to <30 AU of Bla activity in the culture supernatant), whereas in FA1090(pFT180), most (~90%) of the Bla activity was detected in the culture supernatant (~7000 AU compared to ~700 AU in the bacterial pellet) (Fig. 12B). These

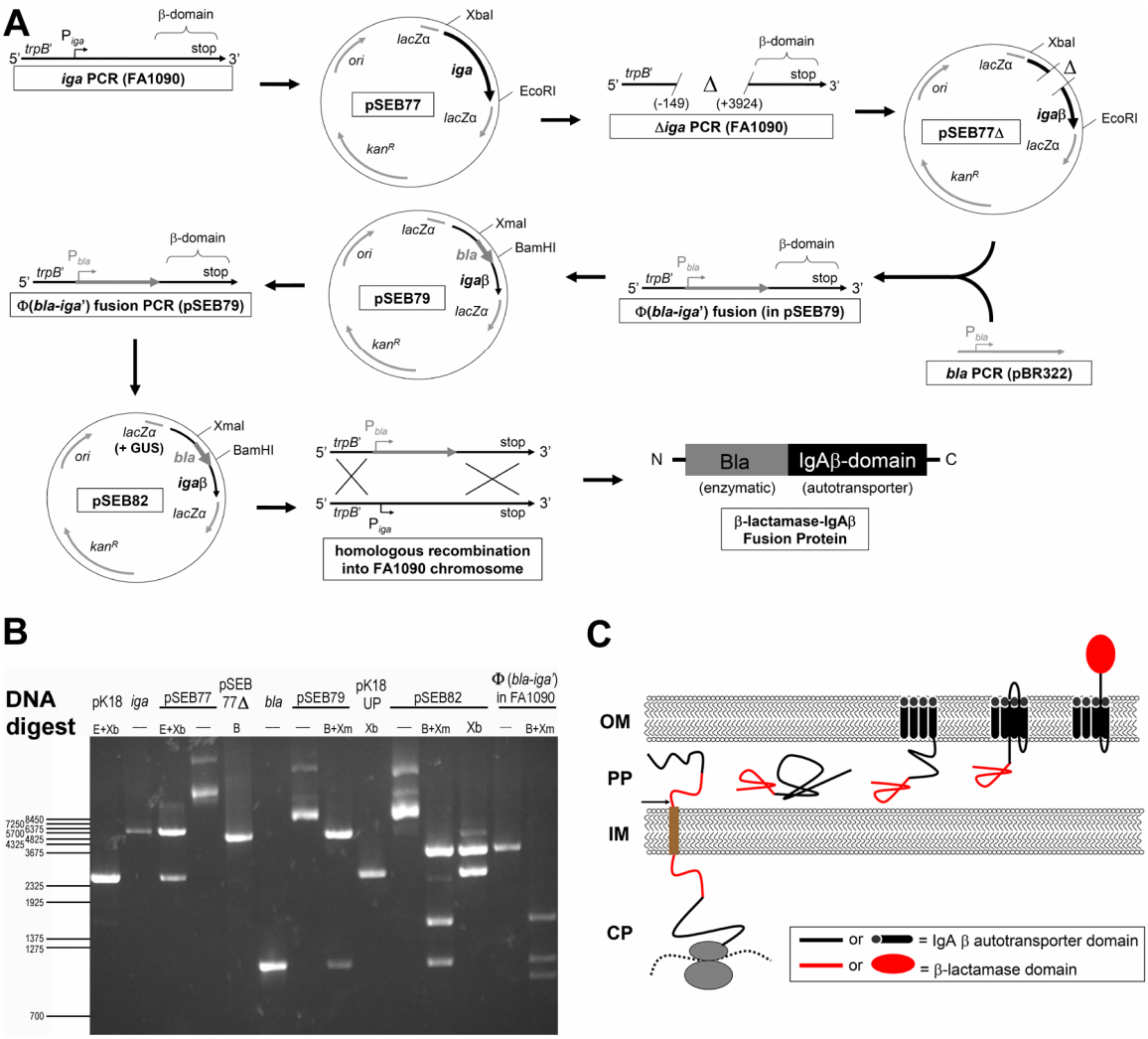

Figure 11—Construction of a GC strain that autodisplays the Bla-IgAβ fusion protein. (A) A schematic diagram showing the gene replacement strategy to construct Bla-IgAβ and establish FA1090 Φ(*bla-iga'*) (see Materials and Methods). (B) Agarose gel showing the DNA fragments generated during construction of FA1090 Φ(*bla-iga'*) to confirm the presence and proper orientation of each DNA of interest. Restriction enzymes used for digestions are as follows: E = EcoRI, Xb = XbaI, B = BamHI, and Xm = XmaI. DNA samples not treated with restriction enzymes represented PCR products [i.e. *iga*, *bla*, and Φ(*bla-iga'*) in FA1090] or uncut plasmids. (C) The predicted steps in the autodisplay of the Bla-Igaβ fusion protein in FA1090 Φ(*bla-iga'*). Passenger domains (red), such as Bla, fused to Igaβ (black), are translated in the bacterial cytoplasm (CP) and transported through the inner membrane (IM) into the periplasm (PP) in their unfolded state using the general Sec pathway (brown). In the PP, the fusion protein folds and the IgAβ domain inserts into the outer membrane (OM) forming a β-barrel motif. Bla is autotransported through the IgAβ domain to face the extracellular milieu. Image modified from (163).

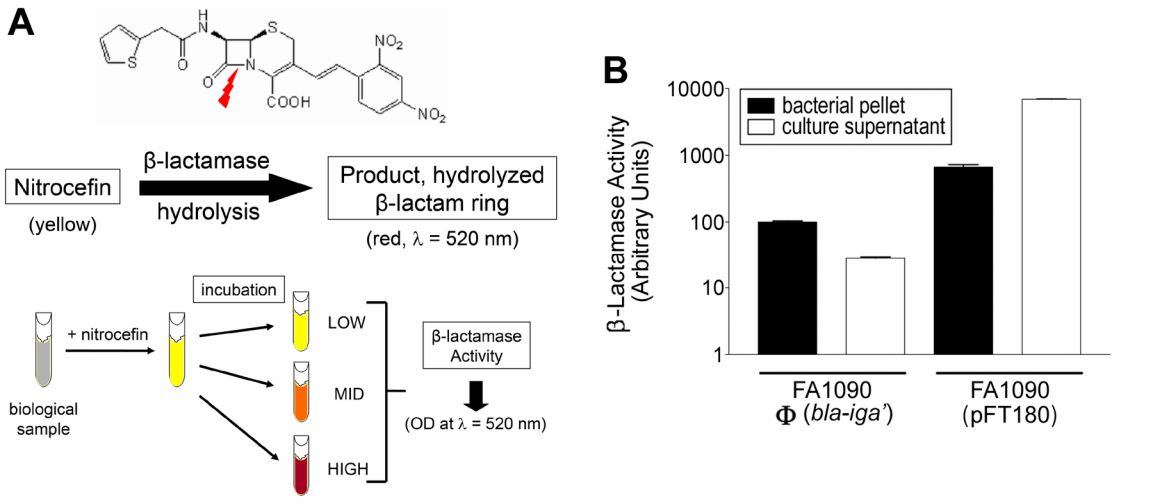

Figure 12—Quantification of Bla expression in GC strains. (A) The nitrocefin hydrolysis assay to measure Bla activity was modified from O'Callaghan, *et al*. (214). In the presence of Bla, the amide bond in the β-lactam ring of nitrocefin is cleaved (red bolt). The yellow substrate is converted into a reddish product detectable at λ = 520 nm over time. A sample with low, mid, or high Bla activity appear yellow, orange, or red, respectively, after incubation with nitrocefin. The molecular structure of nitrocefin was copied from www.nugi-zentrum.de/Bilder/Nitrocefin.gif. (B) Bla activity in FA1090 Φ(*bla-iga'*) is cell associated. Nitrocefin hydrolysis assays were performed on FA1090 Φ(*bla-iga'*) or FA1090(pFT180) pellets or culture supernatants. Bla activity for the FA1090 Φ(*bla-iga'*) pellet in a selected trial was defined as 100 AU and used as the standard to normalize the Bla activity of all other samples. Data are representative of three independent experiments performed in triplicate (± SD).

data indicate that Bla is anchored to the membrane in FA1090 Φ(*bla-iga'*) and secreted by FA1090(pFT180).

To determine if Bla autodisplay by FA1090 alters its ability to adhere to and/or invade into cervical epithelial cells, I performed a gentamicin protection assay. Gentamicin is a cell-impermeable aminoglycoside antibiotic that inhibits protein synthesis in prokaryotes, such as GC, but not eukaryotic cells (56). During a 6 h infection, a similar number of FA1090 and FA1090 Φ(*bla-iga'*) adhered (Fig. 13A, black bars) to and invaded (Fig. 13A, white bars) ME180 cells. Furthermore, laser scanning confocal microscopy (LSCM) analysis revealed that FA1090 Φ(*bla-iga'*) and FA1090 associated with ME180 cells in similar distribution patterns (Fig. 13B). FA1090 and FA1090 Φ(*bla-iga'*) are observed surrounding most ME180 cells (60-70%) to cover the cell surface, rather than appearing as a microcolony (20-30%) bound to a small surface area or dispersing randomly on the cell surface (<10%) (Fig. 13C). Bla expression by FA1090 does not alter the type of LOS structures expressed by GC, indicating Bla expression does not alter the GC surface that directly interacts with host cells (Fig. 13D). These data indicate that Bla expression by FA1090 does not interfere with GC-host cell interactions or GC surface molecule expression.

Quantification of cervical epithelial cells invaded by GC. I utilized the Bla-expressing reporter strain FA1090 Φ(*bla-iga'*) to quantify the number of cervical epithelial cells that were invaded by GC during a 6 h infection. Upon entering ME180 cells loaded with CCF2-AM, Bla^+ GC will cleave a portion of the green fluorescent dye to yield a blue, intracellular, fluorescent product. In noninvaded ME180 cells, CCF2-AM will remain

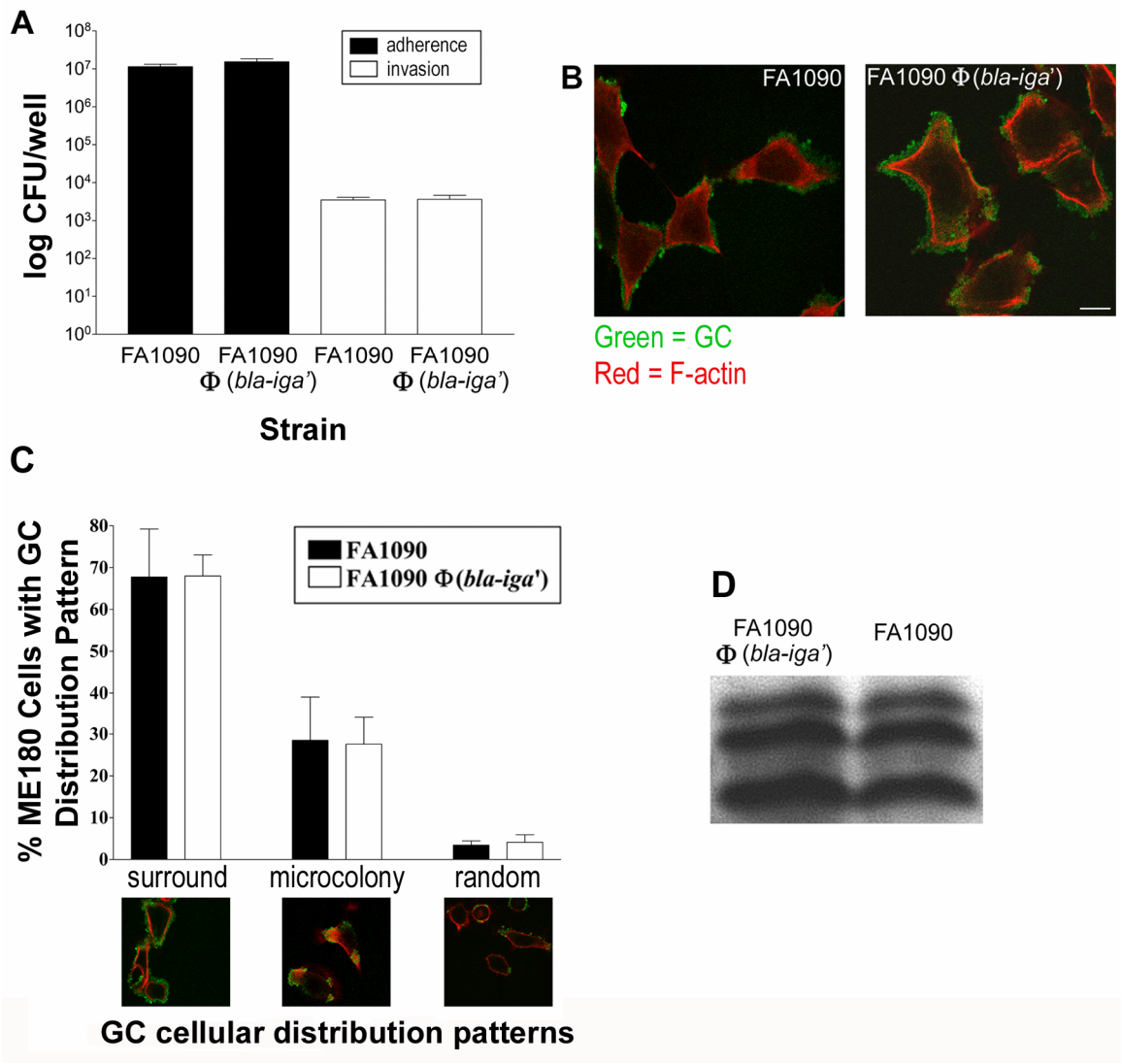

Figure 13—Analysis of FA1090 Φ(*bla-iga'*) and FA1090 interactions with ME180 cells and LOS expression. In panels A and B, ME180 cells were incubated with GC at an MOI of 10. (A) Gentamicin protection assays; data representative of three independent experiments performed in triplicate (± SD). Gentamicin = 200 µg/ml. (B and C) Immunofluorescence microscopy analysis: (B) Bar, 10 µm and (C) GC were scored on their cellular distribution patterns on approximately 300 randomly selected ME180 cells as layers of dispersed GC surrounding the cell (surround), microcolon(ies) on the cell (microcolony), or randomly distributed individual GC or small clusters (random). LSCM images are shown to provide a visual representation of each distribution category. Data = average (± SD) percentage of ME180 cells that display each distribution pattern from three independent experiments. (D) FA1090 Φ(*bla-iga'*) and FA1090 express identical LOS species. Crude LOS preparations from FA1090 and FA1090 Φ(*bla-iga'*) were resolved using Tris-Tricine SDS-PAGE and detected by silver stain. $P^{+}Opa^{+}$ GC were used in all experiments.

uncleaved and will not yield the blue fluorescent product (Fig. 14A). To examine the intracellular distribution of CCF2-AM, I analyzed uninfected CCF2-AM loaded ME180 cells under a fluorescent microscope. The data show that CCF2-AM was present in both cytosolic and nuclear compartments of ME180 cells and there were no detectable intracellular compartments where CCF2-AM was excluded (Fig. 14B).

To identify individual invaded host cells, I incubated ME180 cells with FA1090 Φ(*bla-iga'*) for 6 h at an MOI of 10, washed away non-adherent bacteria, and then loaded cells with CCF2-AM. Fluorescence microscopy showed that only ME180 cells inoculated with FA1090 Φ(*bla-iga'*) exhibited detectable blue fluorescence (Fig. 14C). I determined the percentage of ME180 cells that displayed blue fluorescence using flow cytometry to quantify the FA1090 Φ(*bla-iga'*)-invaded cells in the population. Less than 40% of ME180 cells show a fluorescence level of cleaved CCF2-AM higher than negative controls, indicating that only a subset of ME180 cells were invaded by FA1090 Φ(*bla-iga'*) (Fig. 14D, Fig. 21A, and Fig. 23A), (~36% invaded cells in the trial shown). Uninfected ME180 cells and cells inoculated with FA1090 that did not express the reporter construct were analyzed as negative controls (Fig. 14D, Fig. 21A, and Fig. 23A).

The conditions utilized to quantify invaded ME180 cells in Figure 14C and Figure 14D represent the optimal conditions for the β-lactamase reporter assay as determined experimentally. I found that a minimum of 0.25 μM CCF2-AM and 45-60 min dye loading time were needed for optimal detection of GC-invaded ME180 cells (Fig. 14E, Fig. 14F, Fig. 22A, Fig. 22B, Fig. 23E, and Fig. 23F). I noted that invasion appeared to be more efficient when lower starting MOI were used to initiate the assay (Fig. 14G, Fig. 22C, and Fig. 23G). I also observed that the number of invaded ME180 cells increased

Figure 14—Analyses of FA1090 Φ(*bla-iga'*) invasion into ME180 cells utilizing the fluorescence-based Bla reporter assay. (A) The Bla reporter system. The Bla reporter assay can detect invaded host cells loaded with CCF2-AM based on their fluorescent properties. CCF2-AM is a cell permeable molecule that remains colorless until it crosses a host cell membrane and is converted into CCF2 by cytosolic esterases. CCF2 is a charged Bla substrate that emits green fluorescence when excited at λ = 405 nm. When Bla is present in the host cell, CCF2 is cleaved to release a coumarin product that emits blue fluorescence when excited at λ = 405 nm. Image modified from (312). (B) CCF2-AM cellular distribution assay in ME180 cells; CCF2-AM (1 μM, green) and Hoechst 33342 (100 ng/ml, blue). (C-I) Fluorescence-based Bla reporter assays were performed by incubating ME180 cells with FA1090 or FA1090 Φ(*bla-iga'*). After invasion, cells were loaded: (C) with or without 1 μM CCF2-AM for 90 min; bars, 20 μm. Image quality was optimized using the AxioVision 4.6 software release from Carl Zeiss North America, (D) 0.25 μM CCF2-AM for 45-60 min, (E) different concentrations of CCF2-AM for 45-60 min, (F) 0.25 μM CCF2-AM for different lengths of time, (G) 0.25 μM CCF2-AM after being incubated with GC at different MOI during the invasion, (H) 0.25 μM CCF2-AM after being incubated with GC for different invasion time periods, (I) 0.25 μM CCF2-AM after being incubated with filtered supernatants (with varied levels of Bla activity) derived from overnight broth cultures of wild-type FA1090 (<1 AU), FA1090 Φ(*bla-iga'*) (<3 AU), or FA1090(pFT180) (~700 AU). ME180 cells were incubated with FA1090 Φ(*bla-iga'*) at an MOI 10 (10 AU) as a positive control for CCF2-AM cleavage in part H. In (D-I), Bla reporter assays were analyzed by flow cytometry and FA1090 or a FA1090 culture supernatant served as gating controls. All flow cytometry dot plots shown are representative data of two to five independent experiments. All GC used in these experiments were P^+Opa^+.

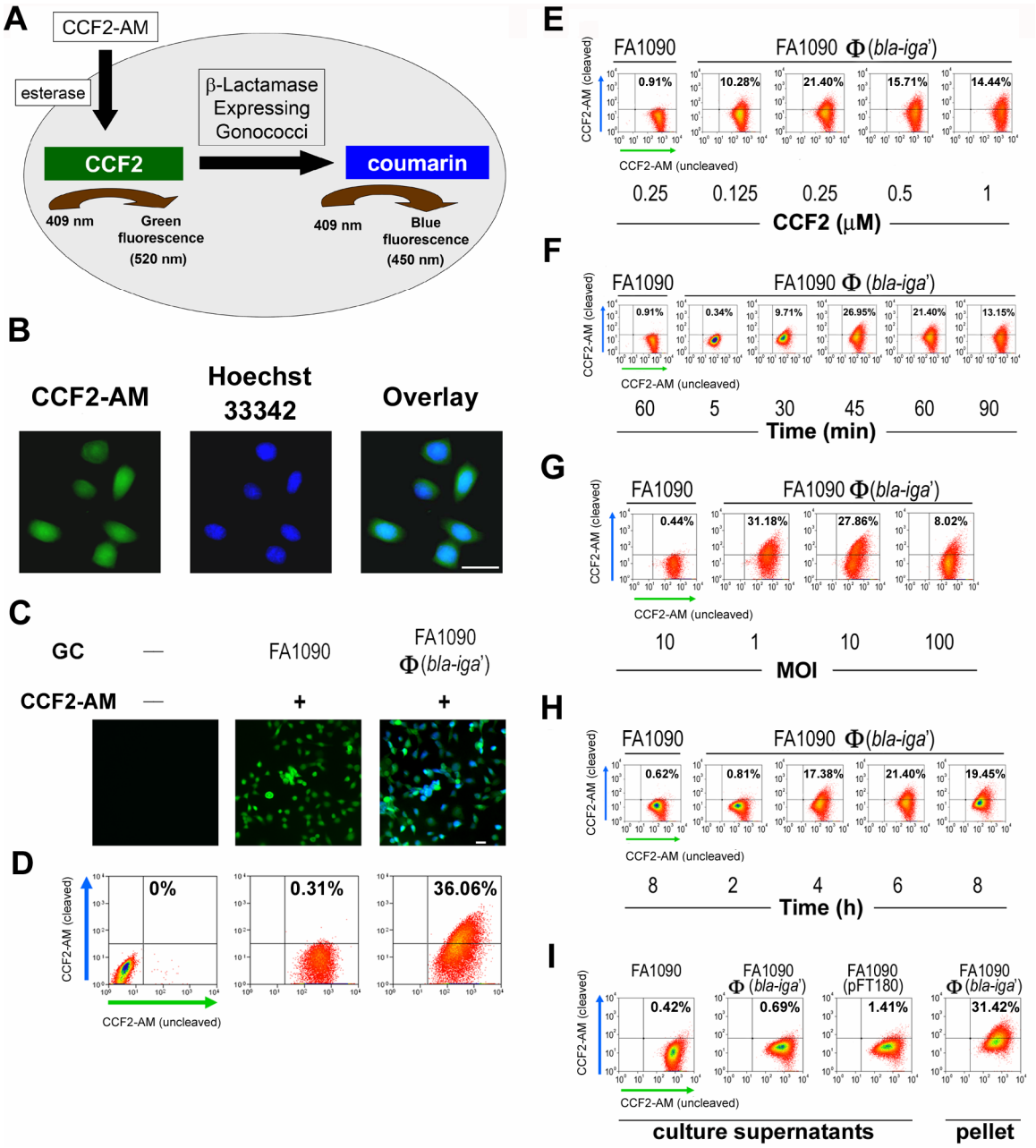
A
CCF2-AM
esterase
β-Lactamase Expressing Gonococci
CCF2
coumarin
409 nm
Green fluorescence (520 nm)
409 nm
Blue fluorescence (450 nm)
B
CCF2-AM
Hoechst 33342
Overlay
C
GC — FA1090 FA1090 Φ(bla-iga')
CCF2-AM — + +
D
CCF2-AM (cleaved)
0%
0.31%
36.06%
CCF2-AM (uncleaved)
E
FA1090
FA1090 Φ(bla-iga')
0.91%
10.28%
21.40%
15.71%
14.44%
CCF2-AM (uncleaved)
0.25 0.125 0.25 0.5 1
CCF2 (μM)
F
FA1090
FA1090 Φ(bla-iga')
0.91%
0.34%
9.71%
26.95%
21.40%
13.15%
CCF2-AM (uncleaved)
60 5 30 45 60 90
Time (min)
G
FA1090
FA1090 Φ(bla-iga')
0.44%
31.18%
27.86%
8.02%
CCF2-AM (uncleaved)
10 1 10 100
MOI
H
FA1090
FA1090 Φ(bla-iga')
0.62%
0.81%
17.38%
21.40%
19.45%
CCF2-AM (uncleaved)
8 2 4 6 8
Time (h)
I
FA1090
FA1090 Φ(bla-iga')
FA1090 (pFT180)
FA1090 Φ(bla-iga')
0.42%
0.69%
1.41%
31.42%
CCF2-AM (uncleaved)
culture supernatants
pellet

from 0-6 hr reaching their maximal level by 4-6 h. Few invaded ME180 cells were recovered at the early 2 h time point (< 1% invaded), and the number of invaded cells did not increase with continued incubation after 6 h. Invasion with control Bla^- GC yielded < 1% invaded cells (Fig. 14H, Fig. 22D, and Fig. 23H). To demonstrate that CCF2-AM cleavage was the result of FA1090 Φ(*bla-iga'*) uptake and not soluble secreted Bla pinocytosed by ME180 cells from the culture supernatant, I incubated ME180 cells with culture supernatants of FA1090(pFT180) for 6 h. The FA1090(pFT180) supernatants contained approximately 700 times more arbitrary units of Bla activity than was present in incubations of ME180 cells with intact FA1090 Φ(*bla-iga'*) at an MOI 10 (Fig. 12B). The cleavage of CCF2-AM loaded into ME180 cells occurred in less than 1.5% of the population after incubation with FA1090(pFT180) supernatants, which is much lower than the ~31% of ME180 cells that exhibited internalized FA1090 Φ(*bla-iga'*) at an MOI 10 in the same experiment (Fig. 14I, Fig. 21B, and Fig. 23B). Taken together, these data show that I have identified the optimal conditions to detect and quantify GC-invaded host cells using the Bla reporter system. The results also show the assay is highly specific for invasion events since no CCF2-AM cleavage is detected in host cells in the absence of Bla or in the presence of extracellular Bla. The Bla reporter assay shows that only a subpopulation of ME180 cells with cell-associated GC are invaded during infection. The Bla cell reporter assay provides a strong method to quantify the number of host cells invaded by GC.

Expression of pili, but not Opa, is required for GC invasion into cervical epithelial cells. I examined the contributions of pili and Opa, two major GC surface structures, to

host cell invasion using the Bla reporter assay. I selected phenotypic P^+Opa^-, P^-Opa^+, and P^-Opa^- variants spontaneously arising during passage of P^+Opa^+ FA1090 Φ(*bla-iga'*). I compared the invasive capabilities of each FA1090 Φ(*bla-iga'*) variant to the P^+Opa^+ strain. A higher percentage of ME180 cells were invaded by P^+Opa^- GC (24.41%) than P^+Opa^+ GC (14.69%). GC lacking pili displayed almost no invasion (<0.75%) into ME180 cells compared to P^+Opa^+ GC. Invasion with control $Bla^-P^+Opa^+$ GC yielded <1% invaded cells (Fig. 15A, Fig. 21C, and Fig. 23C). These data indicate that GC lacking pili do not efficiently invade ME180 cells and the lack of invasion by P^-Opa^- GC serves to validate the capability of the Bla reporter assay to distinguish between invaded and noninvaded strains of GC. Furthermore, GC that express pili, but not Opa, were more efficient at invading ME180 cells than GC expressing both pili and Opa.

I compared the invasion data generated by the Bla reporter assay with the gentamicin protection assay. Each of the four variants (P^+Opa^+, P^+Opa^-,P^-Opa^+, P^-Opa^-) displayed an ability to adhere to and invade into ME180 cells, but the P^-Opa^- strain exhibited reduced adherence and invasion compared to the other variants (Fig. 15B). Significant numbers of gentamicin resistant GC for P^+Opa^+ and P^+Opa^- strains were recovered (Fig. 15B). These data were consistent with data from the Bla reporter assay in Figure 15A indicating that P^+ GC invade into ME180 cells. In contrast, incubation of ME180 cells with P^- Opa^+ and P^-Opa^- GC did not yield detectable numbers of invaded host cells in the Bla reporter assay, yet gentamicin resistant GC were recovered for each of these stains in the gentamicin protection assay (Fig. 15B). These data suggest that, compared to the Bla reporter assay, the gentamicin protection assay may overestimate the number of P^- GC variants that invade ME180 cells.

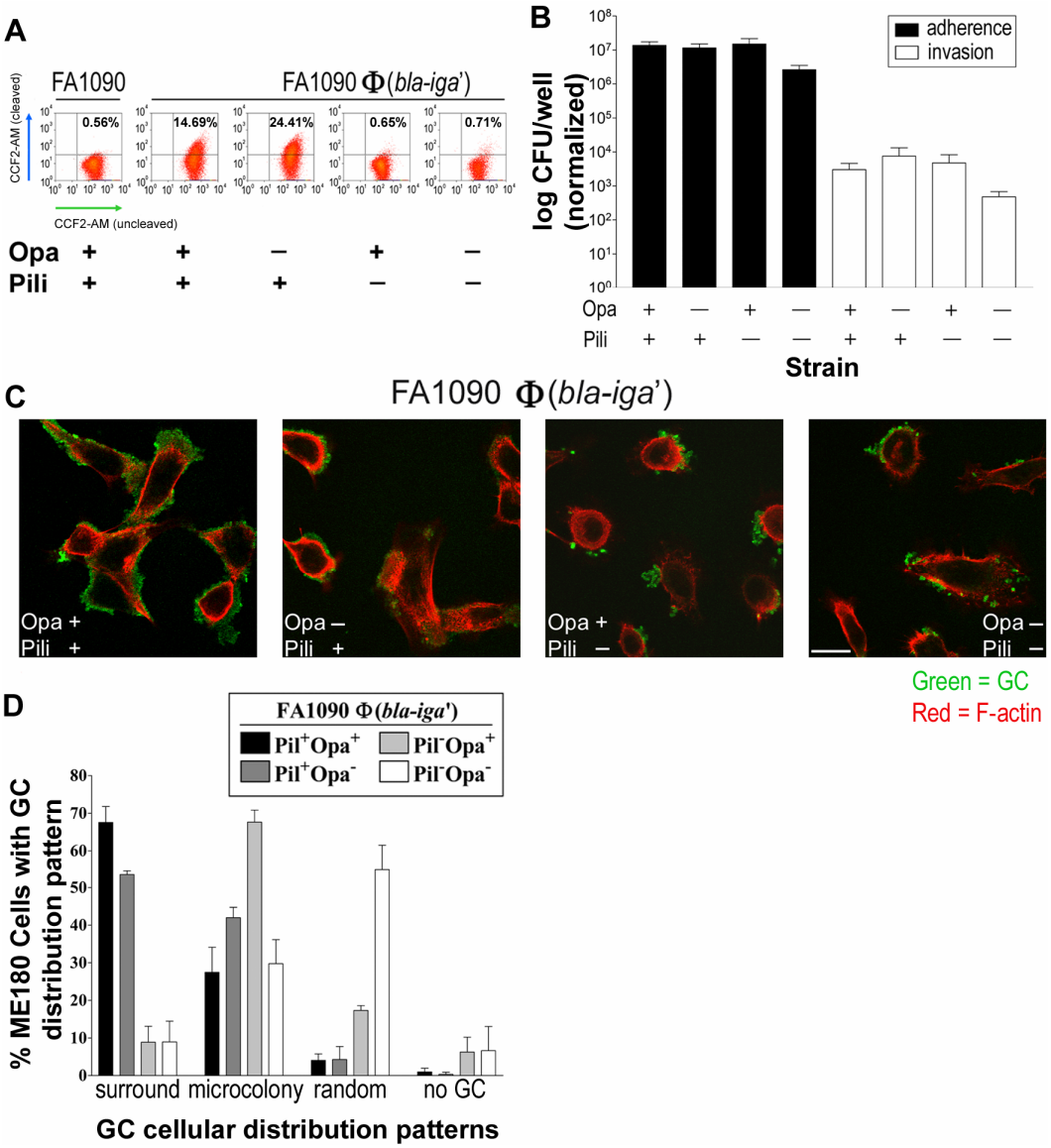

Figure 15—GC invasion requires the expression of pili, but not Opa. Bla reporter assays (panel A), gentamicin protection assays (panel B), and immunofluorescence microscopy analysis (panels C and D) were performed by incubating ME180 cells with FA1090 or FA1090 Φ(*bla-iga'*) expressing different combinations of Opa and pili at an MOI 10. (A) Cells were loaded with 0.25 μM CCF2-AM for 45-60 min and P^+Opa^+ FA1090 served as a gating control; data are representative of three independent experiments [p value = 0.0225 for the statistical comparison between P^+Opa^+ P^+Opa^- FA1090 Φ(*bla-iga'*)]. (B) Gentamicin = 200 μg/ml; data = average (± SD) of two independent experiments each performed in triplicate; data normalized to CFU/well at t = 0. (C and D) Bar, 15 μm; FA1090 Φ(*bla-iga'*) expressing different combinations of pili and Opa were scored on their cellular distribution patterns on approximately 200 randomly selected ME180 cells as described in Fig. 13C; data = average (± SD) percentage of ME180 cells that display each distribution pattern from three independent experiments.

To understand the discrepancy in the data generated from these two different assays, I used LSCM analysis to examine the distribution pattern of different variants of FA1090 Φ(*bla-iga'*) that associate with ME180 cells during infection. After being incubated with P^+ FA1090 Φ(*bla-iga'*), the majority of ME180 cells were surrounded by GC in a uniform distribution, regardless of their Opa phenotype. In contrast, P^-Opa^+ FA1090 Φ(*bla-iga'*) formed visible microcolonies on the majority of ME180 cells. P^-Opa^- FA1090 Φ(*bla-iga'*) did not form microcolonies or surround ME180 cells, but were randomly dispersed as individual diplococci or small clusters (Fig. 15C and Fig. 15D). These data suggest that the expression of pili allows GC to adhere better and spread out along the cell surface of ME180 cells, which could allow more GC to be internalized during infection. Formation of microcolonies on host cells by P^-Opa^+ GC may create "false positives" for invasion in the gentamicin protection assay due to the protection of GC sequestered within microcolonies from gentamicin despite their extracellular location. Thus, Opa appears to facilitate microcolony formation on host cells more than it promotes invasion.

Failure to recruit F-actin prevents nonviable GC from invading cervical epithelial cells. The Bla reporter assay allowed me to determine if GC viability was required for GC invasion. I generated a culture of nonviable P^+Opa^+ FA1090 Φ(*bla-iga'*) though gentamicin treatment and storage at 4^oC overnight. Killing GC with gentamicin leaves GC intact and does not denature surface molecules that interact with host cells (218). Data from the nitrocefin hydrolysis assay showed that gentamicin-killed FA1090 Φ(*bla-iga'*) maintained a Bla activity level similar to live FA1090 Φ(*bla-iga'*) (Fig. 16A). I

Figure 16—GC viability is required for F-actin recruitment and invasion into ME180 cells. ME180 cells were incubated with viable or gentamicin-killed (nonviable) FA1090 Φ(*bla-iga'*). (A) A nitrocefin hydrolysis assay; data representative of three independent experiments performed in triplicate (± SD). (B) Bla reporter assay; cells loaded with 0.25 μM CCF2-AM for 45-60 min after incubation with nonviable FA1090 Φ(*bla-iga'*) at different MOI; data representative of five independent experiments. Cells incubated with viable FA1090 Φ(*bla-iga'*) at an MOI 10 served as a positive control for invasion/CCF2-AM cleavage. (C and D) Immunofluorescence microscopy analyses. (C) Images of cells after incubation with nonviable FA1090 Φ(*bla-iga'*) at different MOI. (D) Quantification of the GC cellular distribution patterns on approximately 200 randomly selected ME180 cells scored as described in Fig. 13C; data = average (± SD) percentage of ME180 cells that display each distribution pattern from three independent experiments. (E) Higher magnification images of ME180 cells incubated with viable FA1090 Φ(*bla-iga'*) at an MOI 10 or nonviable FA1090 Φ(*bla-iga'*) at an MOI 100. (F) Highly magnified regions of ME180 cells associated with individual viable FA1090 Φ(*bla-iga'*) or nonviable FA1090 Φ(*bla-iga'*). (G) Quantification of the actin recruitment by viable and nonviable FA1090 Φ(*bla-iga'*) on approximately 100 randomly selected ME180 cells from the LSCM images in panel E. Actin recruitment was scored as specific actin recruitment to sites of adherent GC (+GC, + actin), accumulation of actin in regions where no GC were bound (-GC, +actin), and no actin recruitment at sites of adherent GC (+GC, -actin). Some cells were scored into two or more categories. P^+Opa^+ FA1090 Φ(*bla-iga'*) were used in all trials. Bars, 5 μm.

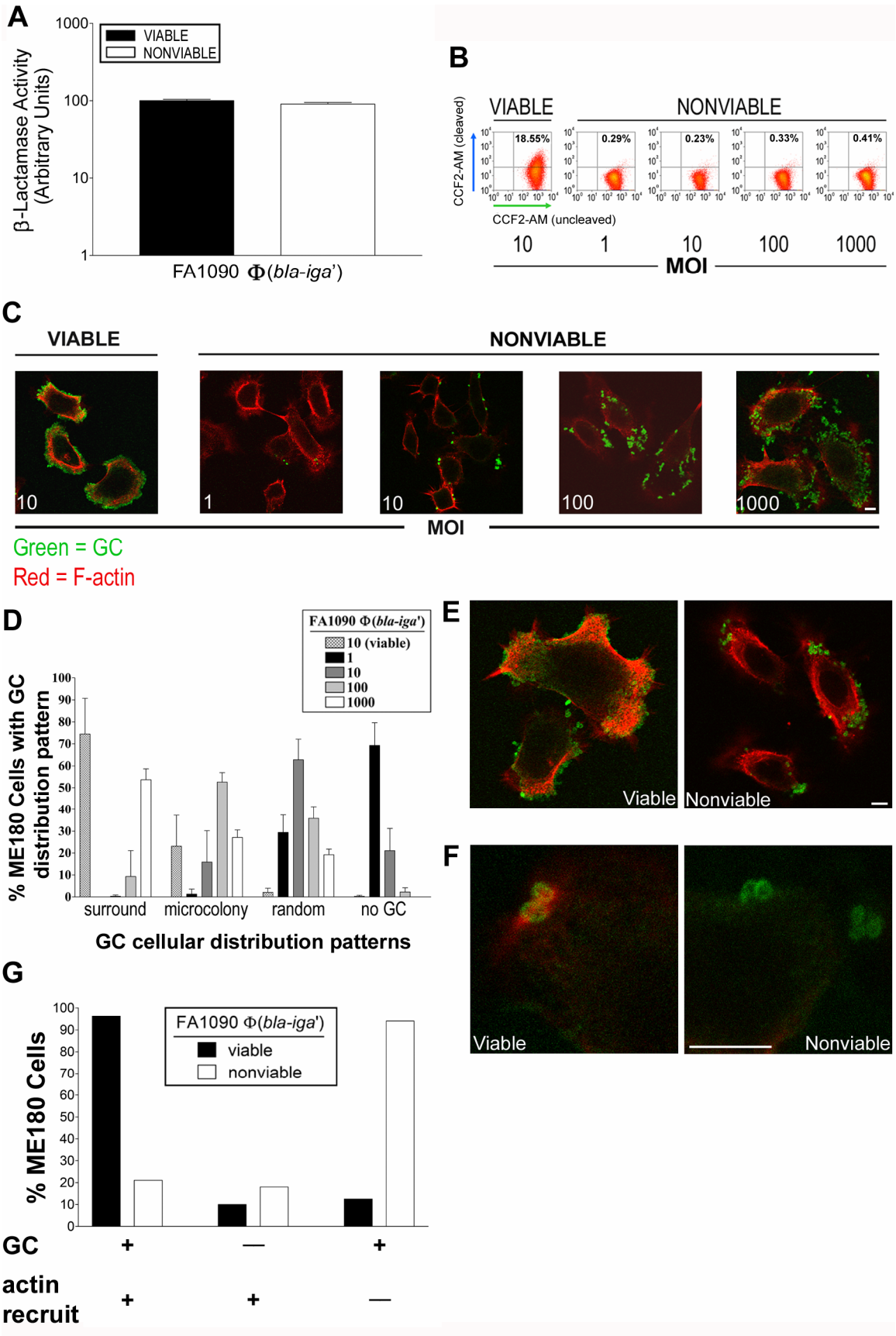
A
β-Lactamase Activity (Arbitrary Units)
1000
100
10
1
VIABLE
NONVIABLE
FA1090 Φ(bla-iga')
B
VIABLE
NONVIABLE
CCF2-AM (cleaved)
CCF2-AM (uncleaved)
18.55%
0.29%
0.23%
0.33%
0.41%
10
1
10
100
1000
MOI
C
VIABLE
NONVIABLE
10
1
10
100
1000
MOI
Green = GC
Red = F-actin
D
FA1090 Φ(bla-iga')
10 (viable)
1
10
100
1000
% ME180 Cells with GC distribution pattern
surround
microcolony
random
no GC
GC cellular distribution patterns
E
Viable
Nonviable
F
Viable
Nonviable
G
% ME180 Cells
FA1090 Φ(bla-iga')
viable
nonviable
GC
actin recruit
+
—
+
+
+
—

tested to see if the physical interaction of GC surface molecules with the host cell is sufficient to induce GC uptake by ME180 cells when GC are nonviable. Internalization of gentamicin-killed GC was monitored by the Bla reporter assay. At all MOI tested, no significant percentage of ME180 cells fluoresced blue, indicating that cervical epithelial cells were not invaded by nonviable FA1090 Φ(*bla-iga'*) (Fig. 16B, Fig. 21D, and Fig. 23D). These data show that, in addition to expressing the required surface molecules to trigger internalization, GC must also be viable to invade host cells.

To determine why nonviable GC that possess the same repertoire of virulence factors as their viable counterparts failed to invade into cervical epithelial cells (see Fig. 24), I examined the interaction of viable or gentamicin-killed P^+Opa^+ FA1090 Φ(*bla-iga'*) with ME180 cells at various MOI by LSCM. If I assume a generation time for FA1090 Φ(*bla-iga'*) during incubation with ME180 cells to be ~45 min a starting inoculum of live GC at an MOI 10 would yield ~1000 GC/cell after 6 h incubation. Since no GC replication will occur for gentamicin-killed FA1090 Φ(*bla-iga'*) during the assay, I assumed that the starting MOI and MOI after the 6 h incubation will be similar. I quantified the FA1090 Φ(*bla-iga'*) distribution patterns on 200^+ randomly chosen ME180 cells over three independent experiments in each case using LSCM. When inoculated with viable bacteria, GC surrounded the majority of ME180 cells in a uniform distribution (Fig. 16C and Fig. 16D). ME180 cells incubated with gentamicin-killed GC at lower MOI had either no associated GC (MOI 1), were in contact with randomly dispersed mono- and diplococci (MOI 1 or 10), or were associated with GC patterns that resembled small microcolonies (MOI 10 or 100). At the higher MOI of nonviable bacteria (MOI 100 and 1000), some microcolony-like clusters of gentamicin-killed GC

start to form association patterns on ME180 cells that appeared similar to viable GC inoculated at a starting MOI of 10 (Fig. 16C and 16D). These data indicate that nonviable GC can adhere to ME180 cells. To understand why adherent nonviable GC fail to invade into ME180 cells, I examined the intracellular distribution of filamentous (F)-actin relative to adhered GC. I found that the intracellular distribution of F-actin in the majority of ME180 cells (> 90%) interacting with nonviable GC appeared evenly distributed beneath the plasma membrane. In contrast, the majority of ME180 cells (> 90%) interacting with live GC revealed F-actin accumulations beneath sites of GC adherence (Fig. 16E and 16G). At small locations on ME180 cells where individual GC were attached, the recruitment of F-actin was only observed under the adherence sites of individual live GC, but such recruitment was not observed with single nonviable GC (Fig. 16F). These data indicate that nonviable GC, possessing the same surface molecules as invasive viable GC, do not efficiently recruit F-actin and do not invade host cells.

Analysis of host cell F-actin dynamics and GC invasion in the presence of potential inhibitors. I wanted to further determine if the inhibition of host cell actin dynamics altered the invasion of FA1090 into ME180 cells. I pretreated ME180 cells with various concentrations of cytochalasin D, a fungal toxin that binds to the + end of growing actin microfilaments to prevent further F-actin polymerization (248), and stained these cells with phalloidin to observe F-actin distribution. ME180 cells treated with 3 μM, 15 μM, and 30 μM cytochalasin D all showed punctate F-actin staining, indicating disruption of F-actin assembly (Fig. 17A). However, gentamicin protection assays demonstrated that FA1090 invaded into ME180 cells treated with cytochalasin D at similar levels to

Figure 17—Analysis of GC invasion in the presence of invasion inhibitors. ME180 cells were incubated with: (A) no GC, (B) FA1090, (C-D) FA1090 or FA1090 Φ(*bla-iga'*), or (E) FA1090. (A-D) Disrupting host cell actin polymerization increases non-specific bacterial invasion into ME180 cells. (A) Immunofluorescence microscopy analyses of cells treated with different concentrations of cytochalasin D (0, 3, 15, and 30 μM); bar, 5 μm. (B) Gentamicin protection assay; cells pretreated with or without cytochalasin D (3 μM, 45 min and throughout invasion); gentamicin = 200 μg/ml; data = average (± SD) of two trials from a single experiment. (C and D) Bla reporter assays, cells loaded with 0.25 μM CCF2-AM following invasion; cells pretreated with or without: (C) cytochalasin D (100 μM, 60 min and throughout invasion) or (D) latrunculin B (5 μM, 45 min and throughout invasion). FA1090 served as a CCF2-AM loading control and the data panels C and D are each single experiments. (E) Inhibition of actin dynamics in TA treated cells blocks GC invasion. Gentamicin protection assays; cells pretreated and post-treated with gentamicin (200 μg/ml, 2 h) or TA (0.2% for 90 min + 1% for 30 min); data = average (± SD) of a single experiment performed in triplicate. GC used in panels D and E were $P^{+}Opa^{+}$.

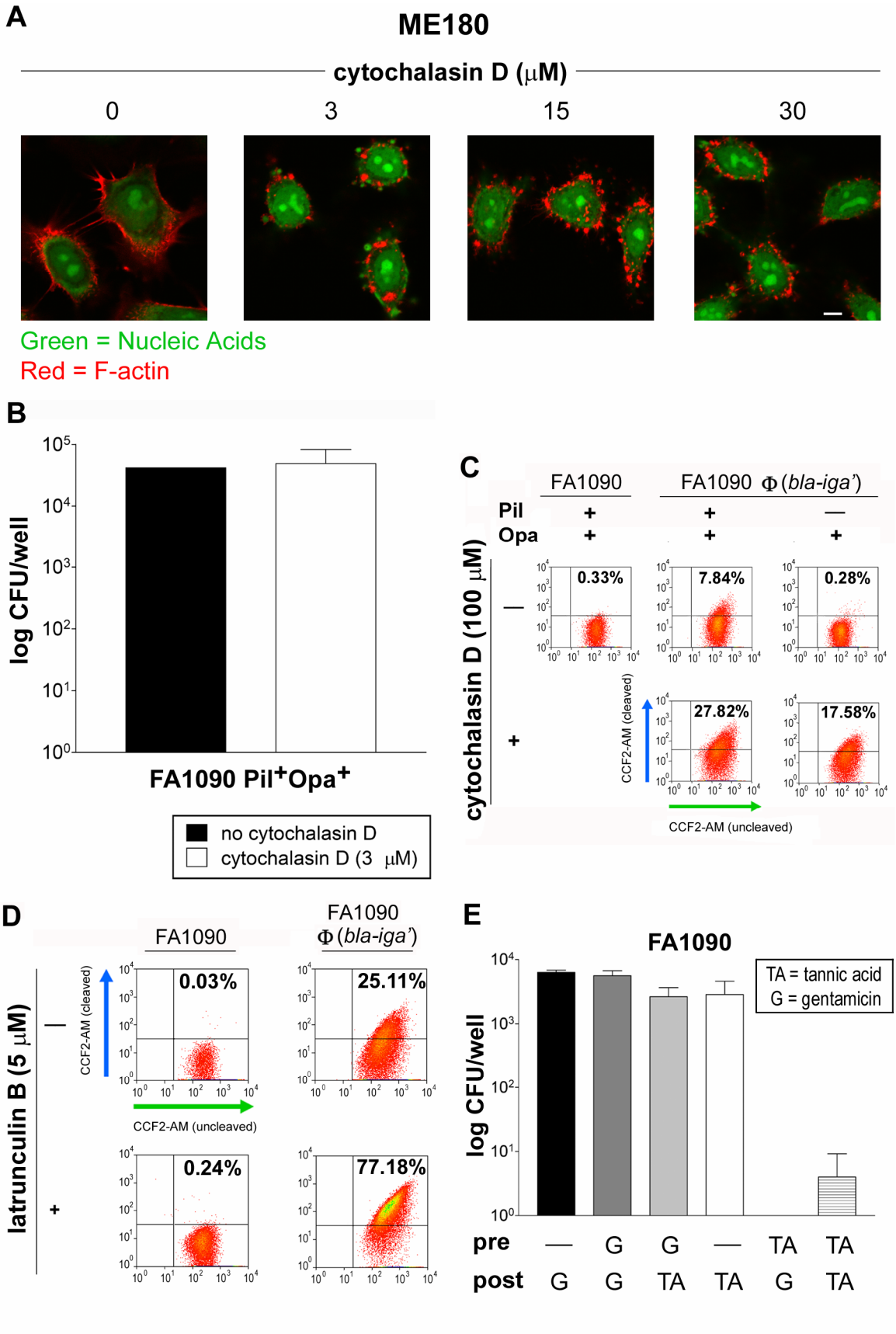
A
ME180
cytochalasin D (μM)
0
3
15
30
Green = Nucleic Acids
Red = F-actin
B
log CFU/well
FA1090 Pil+Opa+
no cytochalasin D
cytochalasin D (3 μM)
C
FA1090
FA1090 Φ(bla-iga')
Pil
Opa
cytochalasin D (100 μM)
0.33%
7.84%
0.28%
27.82%
17.58%
CCF2-AM (cleaved)
CCF2-AM (uncleaved)
D
FA1090
FA1090 Φ(bla-iga')
latrunculin B (5 μM)
0.03%
25.11%
0.24%
77.18%
CCF2-AM (cleaved)
CCF2-AM (uncleaved)
E
FA1090
log CFU/well
TA = tannic acid
G = gentamicin
pre
post

untreated cells, suggesting actin polymerization is not required for invasion (Fig. 17B). In contrast, the Bla reporter assay revealed that, compared to untreated ME180 cells, a higher percentage of cytochalasin D-treated cells are invaded by P^+Opa^+ FA1090 Φ(*bla-iga'*) (~28% vs. ~8%) and P^-Opa^+ FA1090 Φ(*bla-iga'*) (~18% vs. <1%), which do not invade into untreated ME180 cells (Fig. 17C). To confirm these results, I treated ME180 cells with latrunculin B, a different actin polymerization inhibitor, and observed that a higher percentage of latrunculin B-treated cells are invaded by P^+Opa^+ FA1090 Φ(*bla-iga'*) compared to untreated cells in the Bla reporter assay (Fig. 17D). Together these data suggest that disrupting actin polymerization causes host cells to weaken their barrier function for invasion, which allows even noninvasive GC to enter into host cells in an actin-independent manner at a relatively high frequency.

To further investigate the role of F-actin in invasion, I treated ME180 cells with the cell impermeable fixative TA prior to invasion. TA inhibits endocytosis and exocytosis by restricting membrane fluidity and blocking vesicle-membrane fusion without interfering with intracellular processes (207, 226) (see pgs. 123-124). The gentamicin protection assay showed that the invasion of FA1090 into ME180 cells was blocked in TA treated cells (Fig. 17E). These data suggest that host cell F-actin cannot rearrange to internalize GC in TA treated cells since intracellular F-actin recruitment should occur as normal. Overall, these data confirm that GC invasion into host cells is a specific process. Viable GC must recruit F-actin and induce the proper F-actin rearrangements in host cells to direct their own internalization. When actin dynamics are disrupted, GC entry becomes inhibited or non-specific.

Various GC strains, but not *E. coli*, interact with a broad range of cervical epithelial cells. To better understand the host cell range and specificity of GC invasion into epithelial cells, I employed the gentamicin protection assay. I incubated cervical epithelial cell lines with GC or *E. coli* DH5α for 6 h, washed away nonadherent bacteria, and quantified adherence and invasion of host cells after 2 additional h with or without gentamicin treatment. GC strain FA1090 adhered to and invaded ME180 cells, but *E. coli* DH5α displayed limited adherence and no detectable invasion into these cells (Fig. 18A). MS11 mKC, a clinical GC isolate recovered from a male challenge study at the onset of dysuria (253), adhered to and invaded ME180 cells at similar levels compared to FA1090 (Fig. 18B). Furthermore, FA1090 adherence and invasion were analogous in ME180 cells and Hec1B endometrial-like cells (Fig. 18C). These data suggest invasion into ME180 cervical epithelial cells is GC-specific, but not specific to strain FA1090. These data suggest a broad range of GC strains can invade into a variety of host cells.

TA eliminates background resistant GC to provide "cleaner" quantification of GC invasion. One consistent issue encountered with the gentamicin protection assay was the recovery of viable GC in the extracellular supernatants of wells treated with gentamicin. They represent extracellular GC that survived gentamicin treatment by means other than internalization into host cells. The number of recovered GC seemed to vary between experiments and the Opa, pili, and LOS expression states of GC appeared to contribute to the varying degree of gentamicin resistance (data not shown). These resistant GC indicate the level of background GC that were quantified in a particular invasion lysate as "false positives" for invasion. I tested whether the background gentamicin resistance was

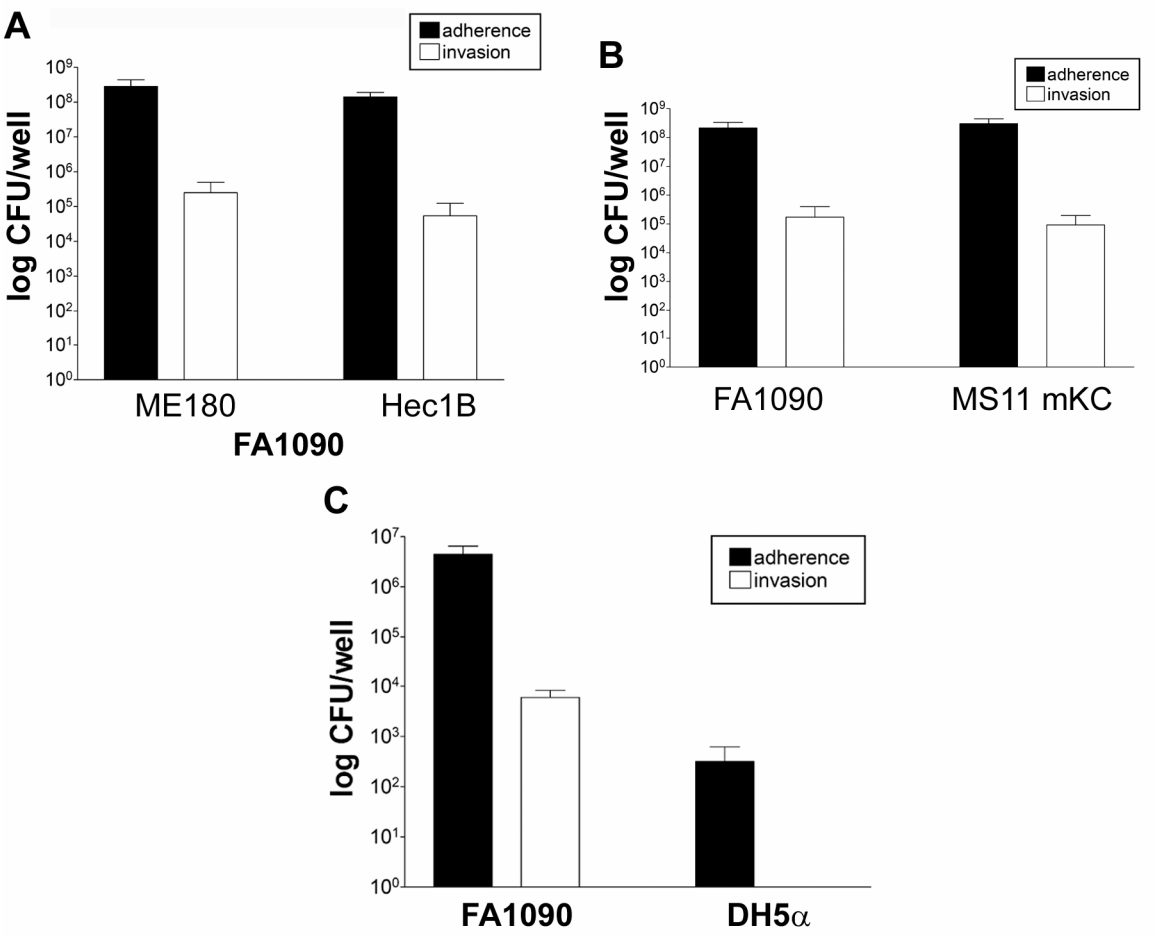

<u>Figure 18</u>—Invasion into cervical epithelial cells is GC-specific. Gentamicin protection assays were performed by incubating host cells with: (A) FA1090, (B) FA1090 or MS11 mKC, or (C) FA1090 or DH5α. Data in panel A = average (± SD) of a single experiment performed in triplicate; panel B = average (± SD) of four trials performed as four independent experiments for the adherence data and the invasion data is an average (± SD) of six (FA1090) or seven (MS11 mKC) trials performed over four independent experiments; panel C = average (± SD) of two trials performed as two independent experiments for the adherence data and the invasion data is an average (± SD) of four trials performed over three independent experiments. ME180 cells were utilized in all trials (and Hec1B in panel A). GC were P^+Opa^- in panels A and B; gentamicin = 500 μg/ml and GC in panel C were P^+Opa^+; gentamicin = 200 μg/ml.

limited to experiments where FA1090 interact with host cells. I incubated a culture of FA1090 with different concentrations of gentamicin for 2 h in the absence of ME180 cells and plated GC for viable plate count every 20 min. Incubations in the presence of 200 μg/ml gentamicin killed an entire culture (over 4 x 10^7 GC/well) in 60-80 min. Even the lowest concentration of gentamicin tested (100 μg/ml) killed the entire population of GC by 2 h (Fig. 19A). These data indicate that the background gentamicin resistant GC is due to the interaction of GC with host cells.

In order to address the background gentamicin resistance issue, I replaced gentamicin with TA in the gentamicin protection assay. TA is a plant-derived, cell-impermeable fixative with anti-GC activity (207, 226). I tested the survival of FA1090 in the presence of different concentrations of TA similar to the gentamicin survival tests in Figure 19A. Only the highest concentration of TA tested (0.5%) killed an entire culture (over 1 x 10^8 GC/well) in fewer than 2 h (Fig. 19B). To confirm these results, I stained FA1090 to detect viable and nonviable GC after incubation in the absence or presence of TA. In this staining method, viable GC with intact membranes only incorporate the cell permeable SYTO dye to fluoresce green and nonviable GC with compromised membranes incorporate SYTO dye and the normally cell-impermeable propidium iodide to fluoresce yellow. FA1090 treated with IM and then stained for viability fluoresced green indicating that they remained viable, but FA1090 treated with TA concentrations as low as 0.1% for 1 h stained yellow and were nonviable (Fig. 19C). In addition, I performed a disc diffusion assay with FA1090 in the presence of filter paper discs containing different concentration of TA. Both the high (0.5%) and moderate (0.05%) concentrations of TA generated zones of FA1090 growth inhibition, but the lowest

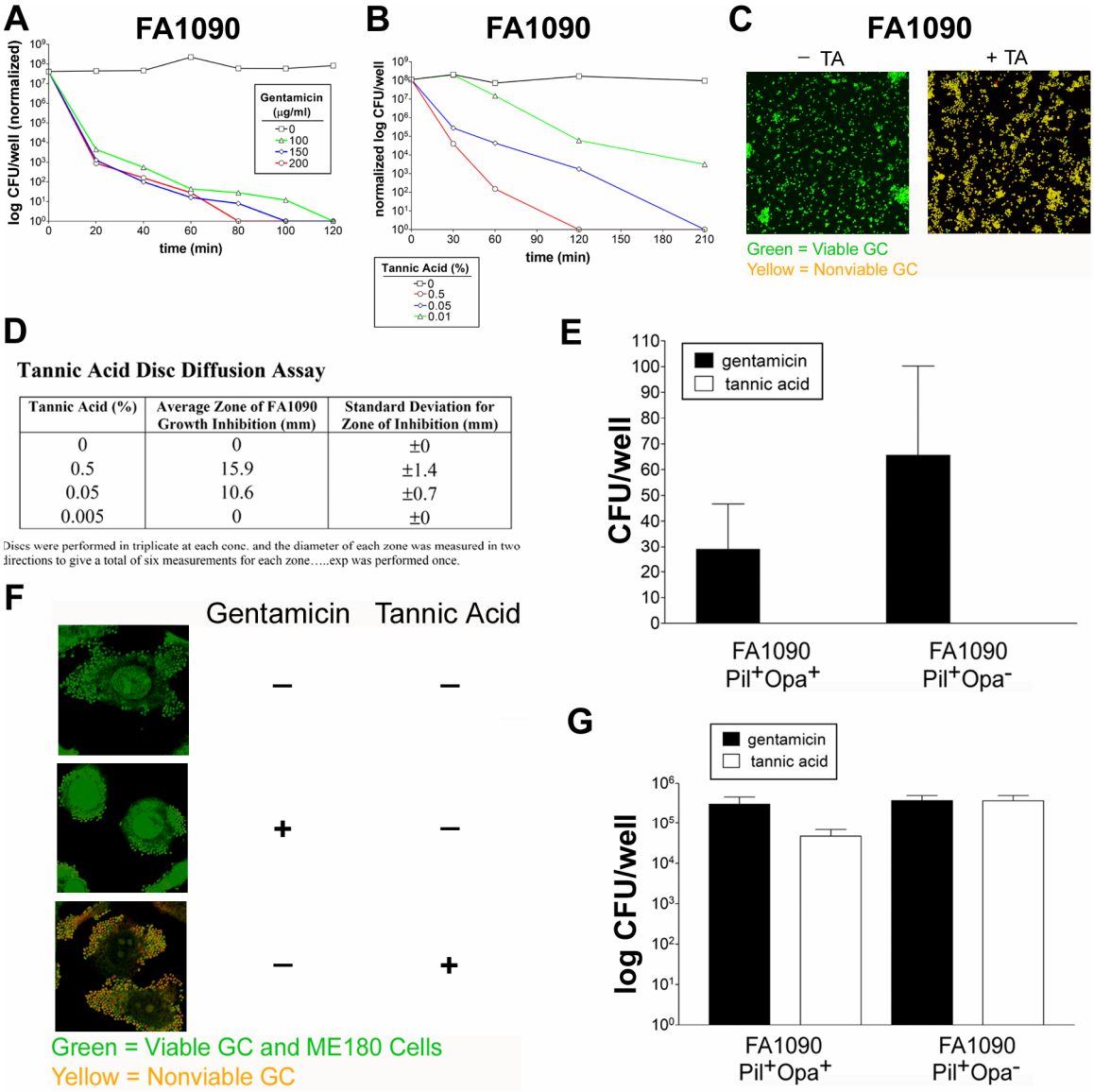

Figure 19—Analysis of the ability of TA and gentamicin to kill background GC in the presence of host cells. (A-B) FA1090 kill curve assays in the presence of (A) gentamicin or (B) tannic acid; each data point is a single trial. Data were normalized to the concentration of FA1090 at t = 0 min. (C) Viability staining of FA1090 treated with or without TA (0.1%, 60 min); samples analyzed by LSCM, bar = 10 µm. (D) TA disc diffusion assay for FA1090; data = average (± SD) of six measurements taken from three separate discs. Discs immersed in PBS served as negative controls for FA1090 growth inhibition. (E) Gentamicin protection assay performed by incubating ME180 cells with FA1090 and quantifying the number of background (not intracellular) GC resistant to gentamicin (500 µg/ml) or TA (0.5%). (F) Viability staining of FA1090 associated with ME180 cells and treated with or without TA (0.1%). Samples were analyzed using LSCM, bar = 5 µm. (G) Gentamicin protection assay to quantify invasive GC from the experiment in panel E; Data in panels E and G = averages (± SD) of at least eight trials over five independent experiments. GC used in panels A-D, P^+Opa^-; in panel F, P^+Opa^+.

concentration tested (0.005%) yielded no zone of inhibition (Fig. 19D). These data demonstrate that concentrations of TA between 0.5%-0.05% are bactericidal to FA1090.

I performed parallel gentamicin protection assays with gentamicin or TA as the antimicrobial agent and collected supernatants and saponin-treated lysates from each well to compare background resistance GC and invasive GC levels. The assays performed with TA revealed no background GC in the supernatants compared to the gentamicin treated assays (Fig. 19E). Viability staining assays of ME180 cells incubated with FA1090 and treated with TA revealed that most GC stained yellow indicating TA treatment killed the majority of GC adherent to host cells (Fig. 19F). (Few GC stained yellow in wells treated with gentamicin suggesting gentamicin did not kill FA1090 interacting with ME180 cells. However, gentamicin renders GC nonviable by inhibiting protein synthesis and does not compromise membrane integrity as needed for incorporation of propidium iodide during viability staining.) Despite the enhanced anti-GC activity of TA compared to gentamicin, similar numbers of invasive GC were recovered from lysates of TA treated cells compared to lysates from gentamicin treated cells (Fig. 19G). Overall, these data show that TA better eliminates background extracellular GC in the gentamicin protection assay to yield a more accurate representation of the total number of GC that invade into a population of host cells.

Analysis of CCF2-AM loading at different time points in the Bla reporter assay. In the Bla reporter assay protocol, CCF2-AM is added after ME180 cells are incubated with GC. I performed a Bla reporter assay where CCF2-AM was loaded into ME180 cells at the beginning of the incubation with FA1090 Φ(*bla-iga'*) and maintained in the growth

media throughout the experiment. Treatment of ME180 cells with CCF2-AM throughout incubation with FA1090 Φ(*bla-iga'*) does not yield an increase in the subpopulation of cells invaded by GC. A similar percentage of ME180 cells showed an increase in blue fluorescence when incubated with FA1090 Φ(*bla-iga'*) regardless of whether CCF2-AM was loaded into cells at the beginning or after the 6 h incubations (Fig. 20). These data suggest that CCF2-AM is degraded by host cells during prolonged incubation. FA1090 Φ(*bla-iga'*) that invade into host cells, but are killed by or escape from host cells prior to flow cytometry analysis could cleave CCF2-AM. However, since CCF2-AM appeared to degrade over time, these "early invasion" events may not be detected in the Bla assay. An alternative explanation is that only the subpopulation of invaded host cells recovered at the conclusion of the Bla reporter assay are the only cells susceptible to invasion throughout the assay. The majority of host cells may be insensitive to GC invasion regardless of whether GC are viable and express an invasion-promoting surface profile.

The relative mean fluorescence of CCF2-AM loaded ME180 cells parallels the percentage of invaded cells. I graphed the relative mean fluorescence due to uncleaved and cleaved CCF2-AM from all trials represented in Figure 14D-I, Figure 15A, and Figure 16B (Fig. 21 and Fig. 22). In all trials where a significant percentage of ME180 cells displayed an increase in relative blue fluorescence due to CCF2-AM cleavage, there was parallel trend of increased relative mean fluorescence over controls with no CCF2-AM cleavage (not statistically significant). Among trials where CCF2-AM cleavage was observed, populations with a higher percentage of invaded ME180 cells also showed a higher relative mean blue fluorescence (not statistically significant). The only exception

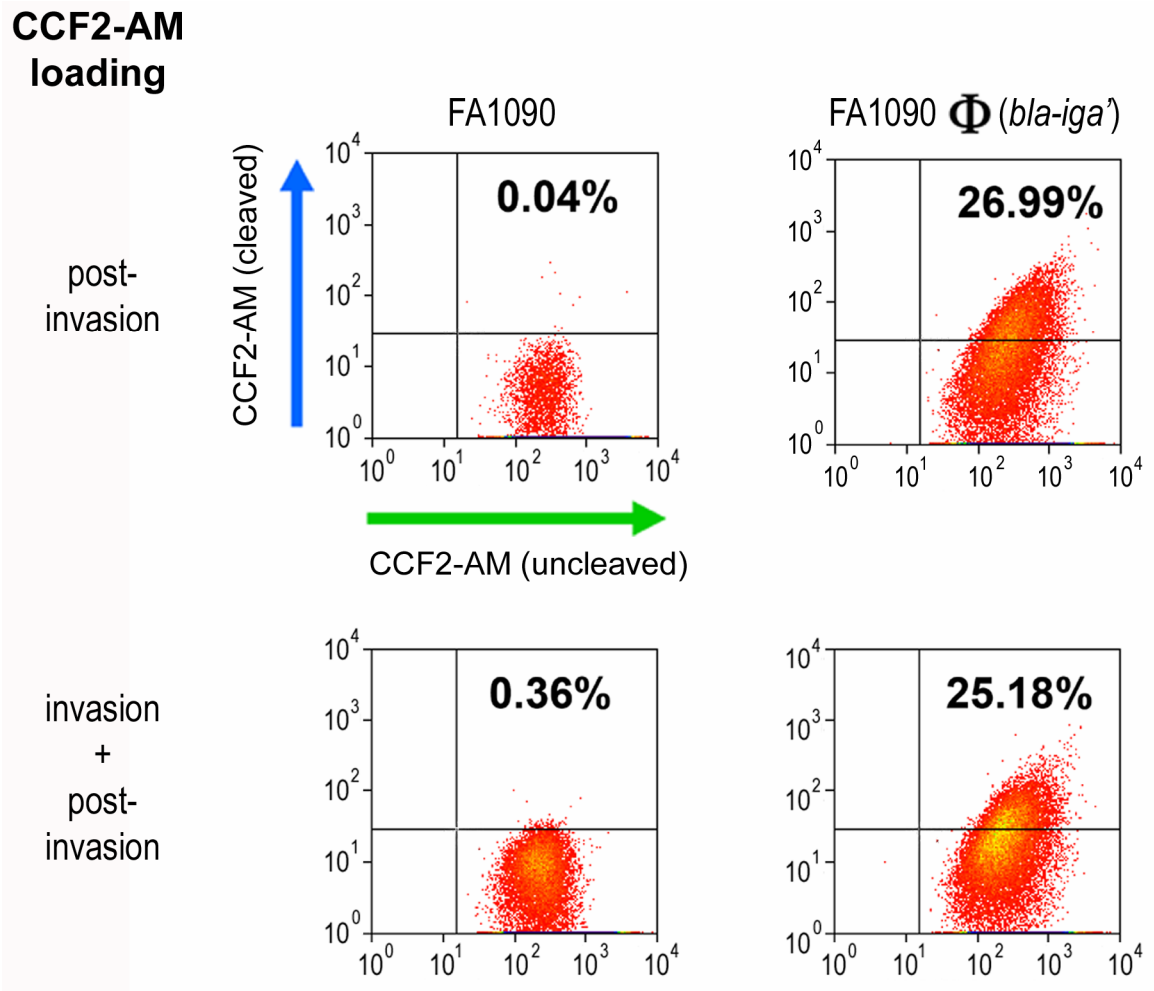

Figure 20—Analysis of CCF2-AM: pre-invasion loading vs. post-invasion loading. Bla reporter assays showing the subpopulation of ME180 cells invaded by FA1090 Φ(*bla-iga'*) does not change when CCF2-AM is loaded into cells at the beginning of the assay; data = a single experiment. In the CCF2-AM pre-loading assay, cells were loaded with 0.25 µM CCF2-AM at the time of GC addition, incubated for 6 h, and then also loaded with 0.25 µM CCF2-AM post-invasion as in a standard Bla reporter assay. Assays were analyzed via flow cytometry; cells incubated with FA1090 served as a gating control; GC used were P^+Opa^+.

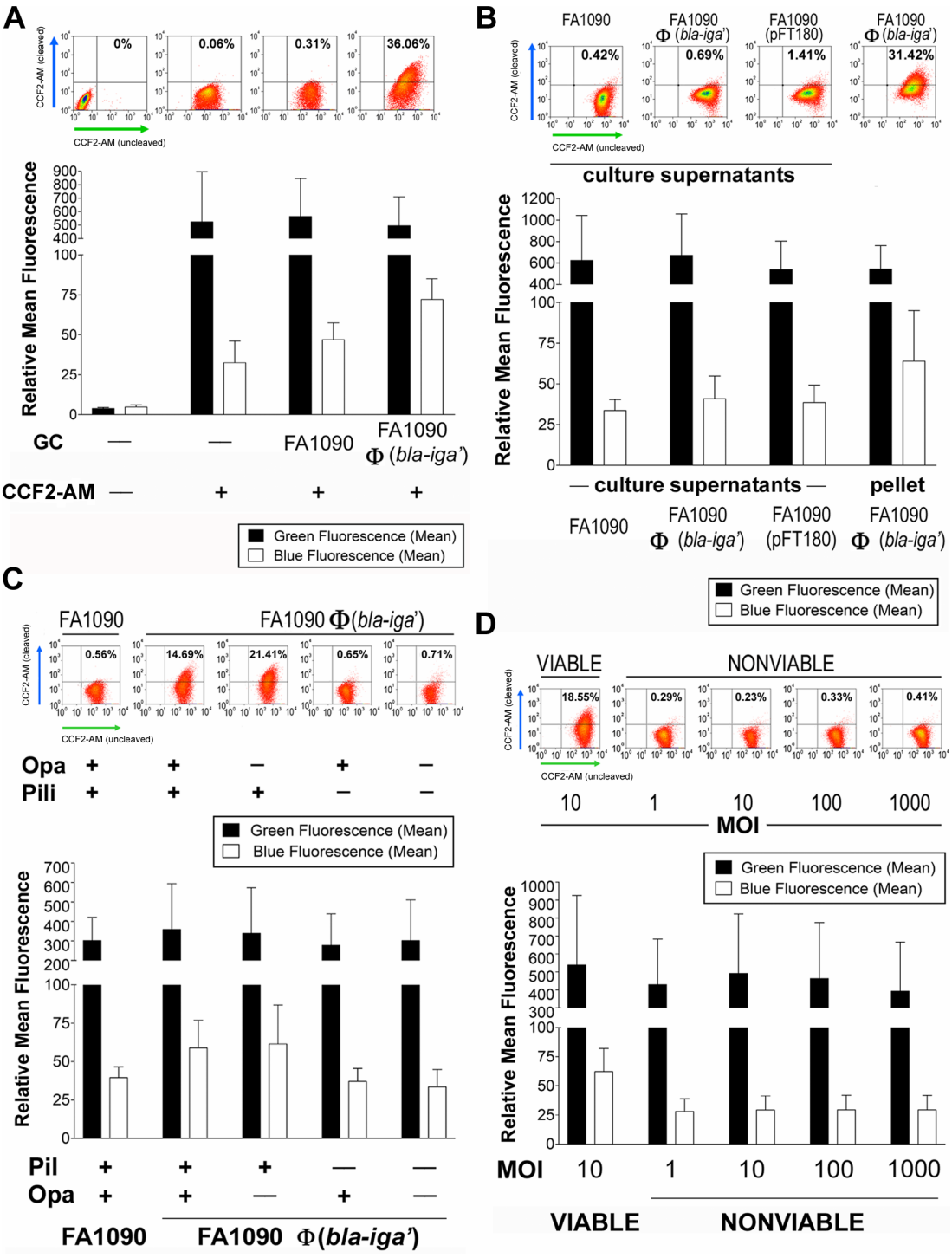

Figure 21—Quantification of the relative mean fluorescence. Bla reporter assay data from (A) Fig. 14D, (B) Fig. 14I, (C) Fig. 15A, and (D) Fig. 16B and graphical representations of the relative mean fluorescence of each sample; data representative of two to five independent experiments and the mean fluorescence plots are averages (± SD) from those experiments. Green fluorescence = mean fluorescence due to uncleaved CCF2-AM; blue fluorescence = mean fluorescence due to cleaved CCF2-AM.

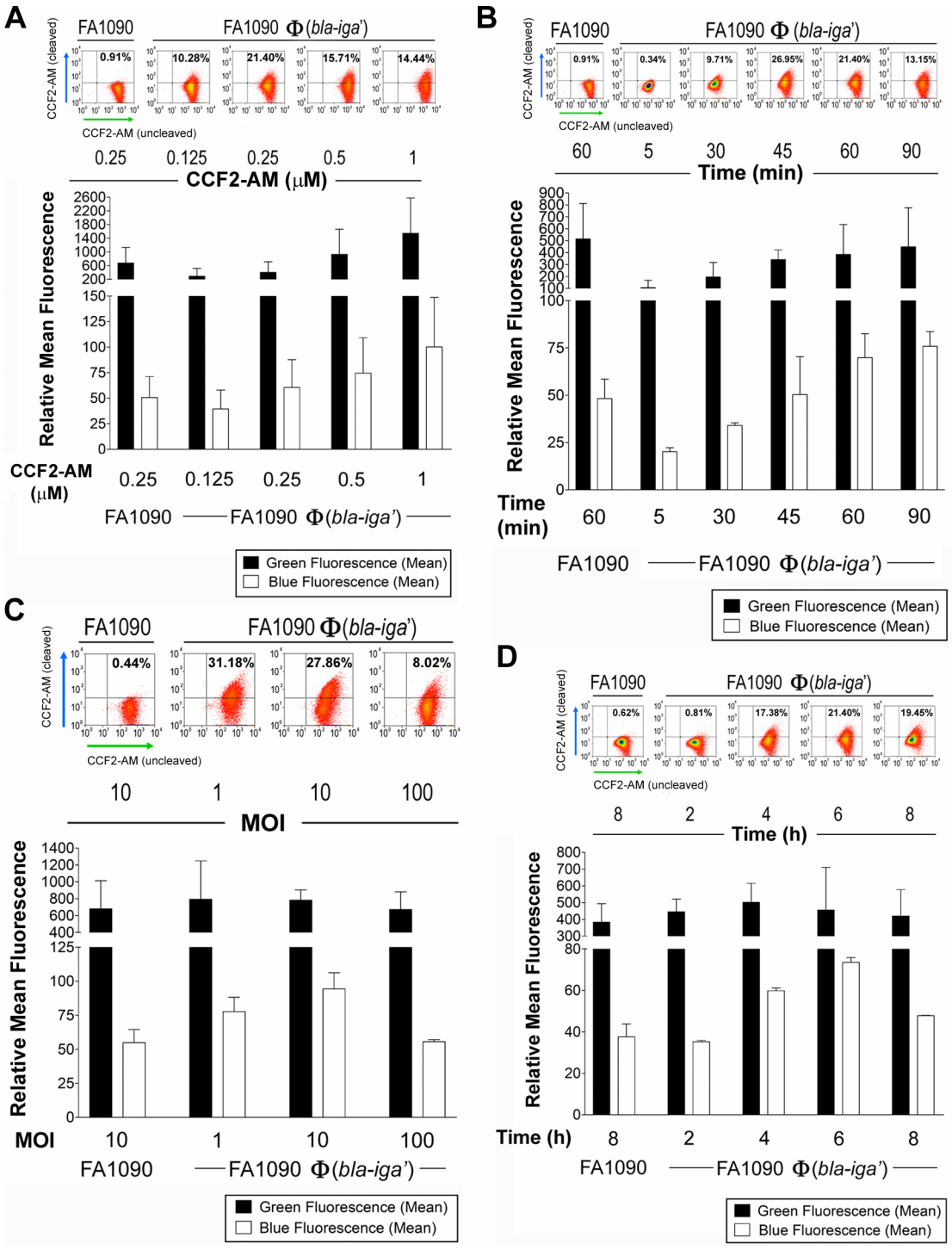

<u>Figure 22</u>—Quantification of the relative mean fluorescence. Bla reporter assay data from (A) Fig. 14E, (B) Fig. 14F, (C) Fig. 14G, and (D) Fig. 14H and graphical representations of the relative mean fluorescence of each sample; data representative of two to four independent experiments and the mean fluorescence plots are averages (± SD) from those experiments. Green fluorescence = mean fluorescence due to uncleaved CCF2-AM; blue fluorescence = mean fluorescence due to cleaved CCF2-AM.

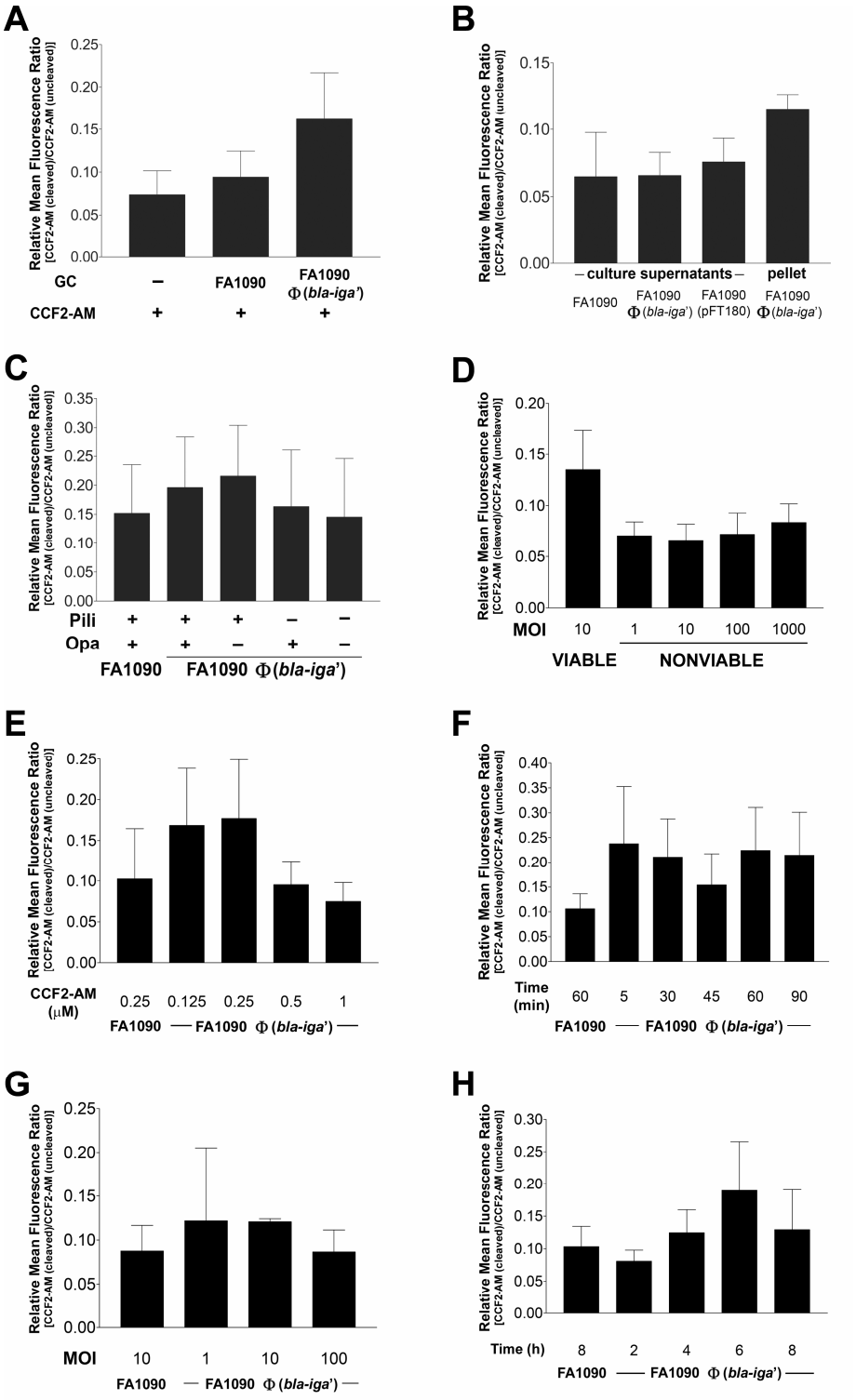

Figure 23—Quantification of the relative mean fluorescence ratios. Graphical representations of the relative mean fluorescence ratios for the data in Fig. 21 and Fig. 22. The ratio of the relative mean blue fluorescence (cleaved CCF2-AM) to the mean green fluorescence (uncleaved CCF2-AM) was calculated for each trial; data represents the average (±SD) of the individual ratios from each trial.

occurred in Figure 14G and Figure 22C where FA1090 Φ(*bla-iga'*) invaded a slightly smaller subpopulation of ME180 cells at a starting MOI 10 (~28%), yet had a slightly higher relative mean blue fluorescence, compared to trials with a starting MOI 1 (~31% of cells invaded) (not statistically significant). This observation suggests that fewer ME180 cells are invaded at an MOI 10, but these invaded cells contain more FA1090 Φ(*bla-iga'*), which cleave more CCF2-AM to yield a higher relative mean fluorescence (Fig. 22C). In all other trials, the data suggest that when a higher subpopulation of ME180 cells are invaded, a greater number of FA1090 Φ(*bla- iga'*) are internalized within those cells compared to the number of GC internalized by a smaller subpopulation of invaded cells.

FA1090 maintain their pili and Opa expression states following gentamicin-killing. To confirm that the gentamicin treatment and 4^{o}C storage processes utilized to render GC nonviable in Figure 16A and Figure 16B did not alter the $P^{+}Opa^{+}$ phenotype of the FA1090 Φ(*bla-iga'*) strain used in these studies. I tested the ability of the gentamicin-killed $P^{+}Opa^{+}$ variant to interact with ME180 cells at MOI 100 using LSCM and compared this interaction with the gentamicin-killed $P^{+}Opa^{-}$, $P^{-}Opa^{+}$, and $P^{-}Opa^{-}$ variants. The nonviable $P^{+}Opa^{+}$ strain was able to adhere to greater than 95% of the ME180 cells in the population. On the majority of host cells, this variant formed small microcolony-like patterns (46%) and some cells displayed a random distribution (30%) of GC. The nonviable $P^{-}Opa^{+}$ FA1090 Φ(*bla-iga'*) variant adhered to greater than 90% of the ME180 cells, but on the majority of cells, GC were randomly dispersed (53%). For ME180 cells incubated with gentamicin-killed $P^{+}Opa^{-}$ and P^{-} Opa^{-} variants, the cells either displayed

randomly dispersed GC (62% and 47%, respectively) or no adherent GC (27% and 42%, respectively) (Fig. 24A and Fig. 24B). These data suggest that the nonviable P^+Opa^+ FA1090 Φ(*bla-iga'*) strain utilized in Figure 16A and Figure 16B does not lose pili or Opa surface expression when killed by gentamicin since these GC still interact with host cells. Therefore, the lack of F-actin recruitment by the nonviable P^+Opa^+ strain in Figure 16E and Figure 16F is not due to altered surface expression profile of pili or Opa.

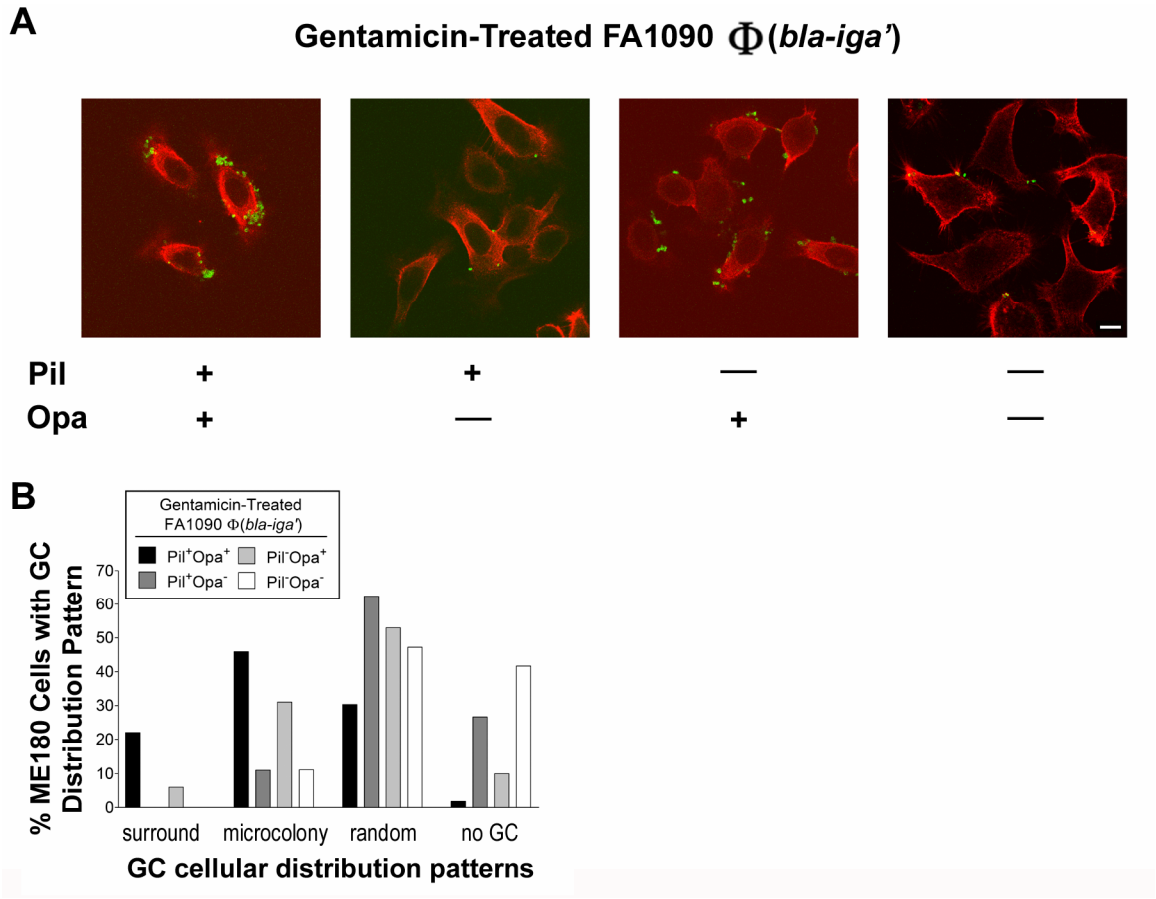

Figure 24—Analysis of the interaction of nonviable GC expression different combinations of pili and Opa. (A and B) Immunofluorescence microscopy analysis of ME180 cells incubated with gentamicin-killed FA1090 Φ(*bla-iga'*) expressing different combinations of pili and Opa. (A) bar = 5 μm; MOI of 100 and (B) scoring of the cellular distribution patterns on approximately 100 randomly selected ME180 cells from a single experiment.

Discussion

Considerable effort has been devoted to understanding how GC invade into human mucosal tissues. Invasion provides GC with a mechanism to avoid the extracellular, innate immune defenses, including neutrophils and macrophages, as well as antimicrobial peptides, defensins, and mucin (60, 190, 232). Invasion through epithelial barriers into underlying tissues can result in PID. Serum resistant GC can migrate through the subepithelium to secondary sites to cause DGI (182).

Invasion is a multi-stage process where GC can utilize multiple adhesins and invasins to initiate cross-talk with host cells by activating signaling pathways and altering gene expression. Bacteria that present an acceptable combination of surface adhesins and invasins to surface receptors on the host cells can initiate colonization and invasion. I show in Figure 18A that *E. coli* DH5α did not trigger invasion into cervical epithelial cells indicating they do not possess the specific surface molecules required for invasion into this cell type. When an appropriate combination of ligand-receptor interactions are engaged between GC and cervical epithelial cells, host cell factors are recruited to induce cell signaling patterns that lead to GC invasion (185). Pilus retraction allows pathogenic *Neisseria* to achieve a more intimate adhesion to host cells (231). The level of GC-host cell cross-talk progresses as more GC surface molecules, such as Opa, LOS, Por, and/or iC3b, bind to the host cell (72, 192). Ultimately, GC orchestrate F-actin-rich rearrangements in host cells at sites of adherence to internalize GC (73, 94, 187). If these receptor-ligand interactions were sufficient to trigger the GC-host cell responses necessary for invasion, gentamicin-killed GC that possess the same ligands as viable GC should invade into host cells. However, using a novel Bla reporter assay, I showed in

Figure 16B that nonviable GC do not enter into human cervical epithelial cells. This finding indicates that the molecular cross-talk between GC and host cells that leads to invasion requires GC viability in addition to the appropriate surface ligand-receptor interactions.

There are many stages of the invasion process where GC viability may be required to establish GC-host cell cross-talk to promote GC internalization. During each stage of pathogenesis, GC undergo changes in gene expression to adapt to new microenvironments in the host (195). Nonviable GC would be metabolically and physically inactive and, thus, fail to modulate their response to the host. The lack of cross-talk by nonviable GC after contact with host cells could be one explanation for their lack of invasion. Several microarray studies have revealed extensive alterations in gene expression by viable pathogenic *Neisseria* in the presence of host cells (83, 96, 97). Several neisserial genes that possess the contact regulatory element of *Neisseria* (CREN) in their promoter regions are activated during contact with host cells (57, 58, 200). Only viable GC are capable of proper gene regulation; therefore, nonviable GC may not invade host cells due to a lack of invasion-promoting gene regulations.

Data from the Bla reporter assay in Figure 15A show that viable FA1090 Φ(*bla-iga'*) must express pili to invade ME180 cells. Gentamicin-killed P^+ FA1090 Φ(*bla-iga'*) can adhere to, but not invade into ME180 cells, suggesting adhesion defects do not account for the inability of nonviable GC to invade into ME180 cells. These results indicate that loss of pilus functions (other than mediating attachment) by nonviable GC could also explain why they do not invade host cells. After adhering to host cells, GC retract pili powered by the ATPase motor protein, PilT (189). PilT-mediated pilus

retraction triggers the PI3K/Akt signaling pathway in epithelial cells and blocking this retraction-induced signaling inhibits invasion (167). Gentamicin-killed GC are metabolically inactive and cannot generate adenosine triphosphate (ATP) to drive pilus retraction. Without pilus retraction, nonviable GC would not trigger retraction-induced signaling in host cells or form more intimate adhesions with host cells to establish subsequent cross-talk essential for GC entry.

I and others (187) have shown that the interaction of nonviable GC with host cells does not culminate in F-actin recruitment and rearrangement at sites of adherent GC (see Fig. 16E-G), which prevents nonviable GC from completing the invasion process. I show in Figure 17C and Figure 17D that host cells treated with F-actin inhibitors resulted in the opposite outcome by triggering an increase in the non-specific entry of GC into host cells. These results suggest that nonviable GC fail to stimulate F-actin recruitment and reorganization, rather than disrupt the polymerization of recruited F-actin, and further indicate that F-actin-dependent GC invasion is a bacteria-directed process that requires GC viability. In this study, I showed that viable P^+ GC, but not nonviable P^+ GC, can induce cortical actin rearrangements and invade host cells. These data support the notion that pilus retraction is important in the induction of F-actin rearrangements and invasion.

Most methodologies employed to investigate GC invasion into host cells fail to quantify GC-host interactions at the single cell level. The gentamicin resistance assay represents the standard method to quantify bacterial invasion into host cells by estimating the total number of viable, intracellular GC recovered from the entire population of infected cells (261). This assay has helped reveal many important aspects of GC invasion, yet it is restricted in measuring the cellular details of the invasion process. The

gentamicin protection assay does not provide direct information about the infected host cells, including the number of host cells in a population invaded by GC or how many GC are present in each infected cell. Since the assay only makes quantitative measurements on the total number of GC recovered before and after gentamicin treatment, formulating an assumption on the number of invasive GC per host cell overextends the data. To better quantify invasion into host cells, Pils, *et al*. developed a method where they fluorescently pre-labeled GC prior to invasion and detected GC fluorescence inside host cells using flow cytometry (222). Host cells are infected and quenched with trypan blue prior to flow cytometry analysis to remove background fluorescence from adherent GC. Invasion is quantified by measuring the fluorescent intensity of labeled GC inside host cells. However, this approach is limited to investigating invasion during short time course invasions (1-2 h) because the fluorescent signal in pre-labeled bacteria dissipates as GC replicate over time. After only a few rounds of replication, the fluorescent label becomes undetectable in the population (data not shown). Data from the Bla reporter assay in Figure 14H and previous investigations show that GC invasion into most host cell types requires 4-6 h. The Pils, *et al*. approach cannot quantify GC invasion at these extended time points.

I utilized the Bla reporter assay in combination with flow cytometry throughout this study to quantify the number of host cells in the population invaded by GC during any time course. Our data reveal that even though nearly 100% of ME180 cells displayed viable adherent P^+ FA1090 Φ(*bla-iga'*) by 4-6 h, the percentage of invaded cells in the population never exceeded 40% without the aid of cytoskeletal disrupting agents. In addition, within the invaded subpopulation of cells, the flow cytometry analyses revealed

a wide range of relative blue fluorescence. Together, these data indicate that GC only trigger invasion into a subset of cervical epithelial cells and some invaded cells may contain more internalized Bla-expressing GC compared to other invaded cells. These findings also imply that GC-host cell interactions on the majority of cells do not produce the proper sequence of cross-talk responses to yield invasion.

The gentamicin protection assay also has the propensity to recover extracellular, non-invaded GC sequestered within microcolonies that represent "false-positives" for invasion. During gentamicin treatment, a fraction of adherent extracellular GC localized within the cores of microcolonies may be protected from gentamicin by layer(s) of surrounding GC and misinterpreted as invaded, intracellular GC. Different GC variants can cluster together into microcolonies to varying degrees depending on their surface composition, which leads to varying degrees of GC invasion overestimations. For example, Opa^+ GC aggregate more than Opa^- GC due to Opa-LOS interactions between neighboring GC (24), which may create an overestimation of the number of invaded Opa^+ GC in this assay. Due to this variable clumping phenotype by GC, the gentamicin protection assay may not accurately compare the invasion of different variants with different GC-GC interaction abilities.

The Bla reporter assay does not rely on antibiotic resistance, and GC microcolony formation has no significant effect on its readout for invasion. Therefore, this assay permits a more accurate comparison of invasion between GC variants with different surface properties. Data in Figure 15B suggest that the gentamicin resistance assay may have mischaracterized the role of Opa in the invasion process. The Bla reporter assay in Figure 15A showed that P^+ Opa^- FA1090 Φ(*bla-iga'*) invade a higher percentage of

ME180 cells compared to P^+ Opa^+ FA1090 Φ(*bla-iga'*), which suggests Opa interferes with the invasion process and indicates the existence of Opa-independent invasion pathways. These data agree with our previous findings that Opa expression is not required for GC invasion into ME180 cells (266). I propose Opa acts predominately as a host cell adhesin and a "clumping" factor that promotes GC microcolony formation on host cells. Our findings argue that GC possess a redundancy of surface invasins that contribute to the overall invasion potential of the organism. When Opa expression is phase "off" (Opa^-) other surface factors, such as Por, LOS, and/or L12 can compensate in GC invasion.

The Bla reporter system provides a powerful tool to measure bacterial invasion into host cells and host cell responses to invasion at the single cell level. The assay can be used to isolate invaded host cells from noninvaded cells and examine their gene expression patterns and signaling pathways. The gene expression in bacteria recovered from invaded host cells in the assay can be compared to bacteria not exposed to host cells to identify novel genes essential for invasion. The Bla reporter assay also provides a new way to assess the virulence potential of clinical isolates, uncharacterized strains, or mutant libraries within a single population of host cells or over a range of cell types. To our knowledge, this represents the first study where the Bla reporter assay has been used to investigate the invasion of bacteria, rather than the secretion of effector proteins, into host cells and the first time the invasion potential of nonviable bacteria has been directly quantified. This assay should be expandable to quantify invasion into any cell type, by any bacteria, and on any time scale providing a new approach to resolve the cellular and molecular details of host cell invasion.

CHAPTER 3—*NEISSERIA GONORRHOEAE* INTRACELLULAR SURVIVAL AND ESCAPE FROM CERVICAL EPITHELIAL CELLS

Introduction

The ability of GC to be continually transmitted and adapt to new host environments allows the organism to establish long-term persistence in the human population. GC are internalized by host cells during infections and, thus, contend with intracellular environments. Their survival and persistence during infection of epithelial cells helps determine whether GC will establish disease and is likely to contribute to the severity of the disease outcome (191, 192, 272). GC appear to be well adapted for immune evasion and ICS in the female reproductive tract, since female hosts remain asymptomatic during the initial stages of infection and develop features of PID after prolonged survival of GC (69, 270). As described in Chapter 2, GC invade into cervical epithelial cells via multiple pathways. However, the fate of intracellular GC after invasion, including the GC-host cell interactions that regulate ICS, the intracellular compartments where GC reside, and how GC maintain their survival and control inflammation in order to continue efficient host to host transmission, is not clear.

The notion that GC can survive and/or replicate inside human epithelial cells remains controversial due to limitations and variations in ICS quantification methods. Most GC ICS studies involve the gentamicin protection assay followed by a chase period to quantify the surviving population of intracellular organisms. How host cells are incubated during these chase periods varies and can involve continuously exposing cells to gentamicin throughout the chase, treating cells with gentamicin both before and after the chase, or administering a single gentamicin treatment prior to the chase period.

Researchers have utilized these various strategies to attempt to devise the most accurate method to measure GC ICS. Overall, it is generally accepted that GC can persist within host tissue since GC survive for long durations in the female reproductive tract and migrate to secondary sites.

Epithelial cells possess killing mechanisms directed at limiting the ICS of invading pathogens, but GC have developed strategies to overcome these defenses. GC can induce the expression of pro-inflammatory cytokines, such as TNFα, IL-6, and IL-8, from host cells to trigger phagocytes to migrate to the site of infection and to phagocytize both extracellular GC and GC-infected host cells (78, 211, 234, 235). Epithelial cells also possess lysosomal compartments similar to phagocytes for pathogen degradation. Images of intracellular GC show both disintegrated and morphologically intact GC both inside vacuoles or free in the cytoplasm of epithelial cells (5, 98, 107, 203, 281, 293, 297, 298, 303). GC can disrupt LAMP function to prevent phagolysosome maturation in epithelial cells and GC exhibit enhanced ICS in cells derived from LAMP knockout mice (10-12, 16, 21, 111, 173, 206, 224, 225, 298). These data indicate that epithelial cells can clear internalized bacteria within phagolysosome-like compartments, but also show GC possess mechanisms to avoid phagolysosomal killing. Epithelial cells can kill intracellular bacteria using oxygen and nitrogen radicals (14, 219). Some epithelial cells produce nitric oxide (NO) radicals that combat intracellular pathogens (129, 170). GC possess enzymes to deal with bactericidal agents inside host cells. GC could utilize at least three nitrogen reductases including, nitrite reductase (AniA), nitroreductase (NfsB), and nitric oxide reductase (NorB), for anaerobic respiration or to inactivate reactive nitrogen intermediates (RNI) if cytoplasmic granules fuse with GC-containing vacuoles

(122, 156). GC also produce high levels of peroxidase (CcpA) and catalase (KatA), enzymes suggested to protect GC against reactive oxygen intermediates (ROI) and hydrogen peroxide (7, 285, 308).

GC must acquire iron from host cells for ICS (104, 284). Hagen and Cornelissen demonstrated that FA1090 survival in ME180 cells declined initially for 8 h post-invasion, but then GC replicated over the final 16 h of the chase period in iron supplemented media. However, in iron-depleted media, GC survival continued to decline throughout the chase (104). Epithelial cells can sequester iron to starve internalized bacteria to prevent their growth and proliferation (279).

GC that survive inside epithelial cells can further progress to other cellular niches. GC can transcytose through host cells and exit through the basolateral surface into subepithelial tissues without disrupting cell tight junctions (186, 293). GC could also persist by escaping back into the extracellular environment. The re-emergence of pathogens from host cells after invasion has been demonstrated for *Trypanosoma cruzi* and group A *Streptococci* and was speculated to occur for GC (4, 36, 179, 203). Criss and Seifert showed that FA1090 exited from T84 cells into both apical and basolateral compartments (51), which suggests GC do cycle out of epithelial cells after invasion.

During the experiments presented in this chapter, I utilized TA to investigate GC intracellular survival and escape. TA is a complex polyphenolic polymer primarily composed of gallic acid and glucose that is produced in the cell wall and vacuoles of many plant species (101, 201). TA acts as a cell-impermeable mordant/fixative when added to cell membranes by cross-linking the amino or carboxyl groups of extracellular proteins (201). Thus, TA treatment prevents endocytosis and exocytosis from host cells

without interfering with intracellular functions by fixing secretory and endocytic vesicles as they fuse with cell membrane (201, 226). Through these cellular effects, TA can inhibit the re-emergence of bacteria from host cells. Treating mouse embryonic fibroblasts with tannic acid prevented the escape of internalized *Streptococcus pyogenes* without compromising bacterial intracellular survival (207). TA can also trigger the redistribution of tight junction proteins in polarized cells to disrupt polarization (216). Furthermore, the pytochemicals found in *Terminalia macroptera* leaves, including TA derivatives and precursors, are bactericidal to GC (262).

In this chapter, I demonstrate that subsets of intracellular GC can persist in the host by surviving inside cervical epithelial cells or by cycling in and out of host cells via an escape pathway. I developed a TA survival assay to demonstrate that GC trapped inside host cells maintain a relative intracellular stasis when bactericidal agents are not left in the extracellular media for long time periods. Therefore, I utilized TA to disconnect GC ICS from escape so that these two processes could be analyzed apart from each other. I generated a catalase deficient mutant and acquired a nitrogen reductase (*nfsB*) mutant and determined that neither enzyme contributed to GC ICS in cervical epithelial cells. My data also indicate that a subpopulation of internalized GC escape intracellular killing by utilizing host cell exocytosis machinery to exit host cells. I propose GC cycle in and out of host cells as a mechanism to avoid both extracellular immune defenses and intracellular killing as a means of persisting at a low-level in the female reproductive tract.

Results

GC do not survive inside cervical epithelial cells after invasion when subjected to continuous exposure to bactericidal agents. Using a modified gentamicin protection assay as a method to recover viable intracellular GC, I determined if GC internalized by the invasion susceptible subpopulation of cervical epithelial cells can survive inside these host cells. ME180 cells were infected with GC expressing different cell surface molecules to allow for invasion. Cells were treated with gentamicin or TA to kill extracellular GC. These killing agents were also maintained in the extracellular media during an ICS chase period to prevent the proliferation of any GC in the extracellular environment and to force GC to persist inside host cells as the only option for survival. The data show that GC ICS decreased in ME180 cells during 4 h chase periods after invasion (Fig. 25A). FA1090 exhibited a similar negative slope for ICS in Hec1B cervical endometrial cells when compared to ME180 cells over the same 4 h time span (Fig. 25B). FA1090 showed an even more rapid decline in ICS when incubated in the constant presence of TA (Fig. 25C). Furthermore, altering Opa or LOS phenotypes did not alter GC ICS. Opa-expressing FA1090 did not exhibit increased survival over an Opa^- strain (Fig. 25C). In strain F62, LnNT LOS-expressing variants did not display any change in survival compared to lactosyl LOS-expressing variants in Opa^+ or Opa^- backgrounds (Fig. 25D). Taken together, these data suggest that GC die over time inside cervical epithelial cells, regardless of their LOS and Opa phenotypes.

Expression of the enzymes catalase (KatA) and the nitrogen reductase NfsB do not influence GC intracellular survival. Bacteria are known to encounter oxidative stresses

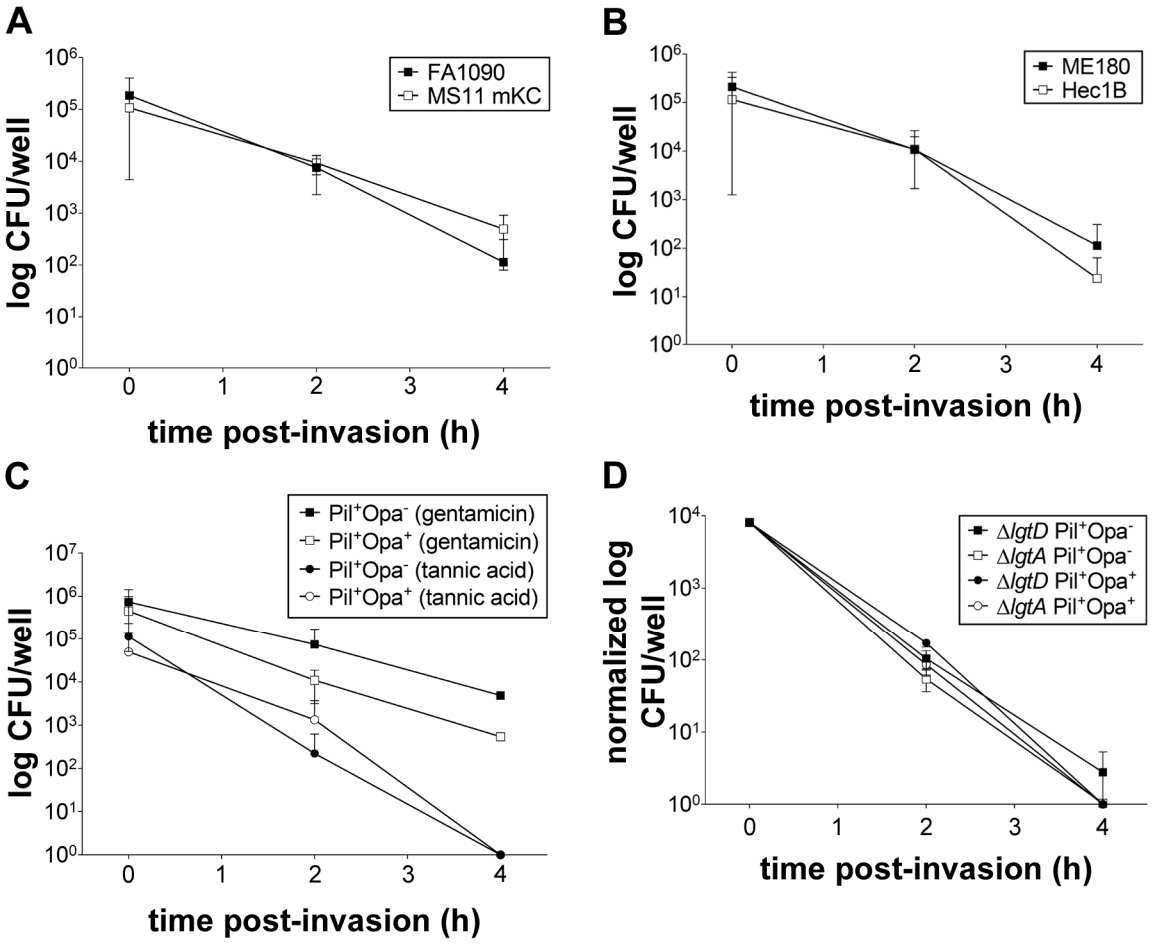

Figure 25—Analysis of GC intracellular survival when subjected to prolonged exposure to bactericidal agents. GC intracellular survival assays were performed in the presence of prolonged gentamicin or TA treatment. Host cells were incubated with: (A) FA1090 or MS11 mKC; data = average (± SD) of six (FA1090) or seven (MS11 mKC) trials from four independent experiments. (GC were P^+Opa^-) (B) FA1090; data = average (± SD) of seven trials from five independent experiments. (GC were P^+Opa^-) (C) FA1090; data = average (± SD) of five (gentamicin trials) or seven (TA trials) trials from three independent experiments. (D) F62Δ*lgtD* or F62Δ*lgtA*; initial invasion (t = 0) were normalized to 8 x 10^3 CFU/well and data = average (± SD) of three trials from a single experiment. ME180 cells were utilized in all trials (and Hec1B in panel B). GC were added to cells at an MOI of 1000 in panels A-C and at a MOI of 10 in panel D. Gentamicin = 500 μg/ml in panels A-C and 200 μg/ml in panel D. TA = 0.5% in panel C.

in the intracellular environment of host cells, including superoxide radicals, peroxide derivatives, and nitrogen radicals (130). To better understand how host cells kill GC, I analyzed mutants lacking genes that may be required for ICS. GC express high levels of catalase—an enzyme that contributes to bacterial survival by combating oxidative stresses within host cells, such as hydrogen peroxide and peroxide radicals (7, 309, 310). I deleted the catalase gene (*katA*) from FA1090 to yield the catalase deficient mutant FA1090Δ*katA* (see Fig. 26). FA1090Δ*katA* did not react with hydrogen peroxide to form water and O_2 gas bubbles confirming that catalase enzymatic activity was eliminated in this strain (Fig. 26C). I tested whether FA1090Δ*katA* displayed altered adherence, invasion or ICS. FA1090Δ*katA* was less efficient at adhering to ME180 cells compared to FA1090, but the strains displayed similar invasion frequencies among the adherent GC (Fig. 27A). FA1090Δ*katA* exhibited a similar negative slope for ICS compared to FA1090 suggesting that the parent and mutant have similar ICS properties (Fig. 27B).

In order to better understand the interactions of FA1090Δ*katA* with cervical epithelial cells, I performed competitive survival assays between FA1090 and FA1090Δ*katA*. I isolated spontaneous rifampicin (Rif^R) and naladixic acid (Nal^R) resistant FA1090 and FA1090Δ*katA* mutants and tested the adherence, invasion, and ICS of these mutants using the gentamicin protection and survival assays. I incubated ME180 cells the corresponding Rif^R and Nal^R FA1090 and catalase mutant strain in the same well (i.e. FA1090 Rif^R vs. FA1090Δ*katA* Nal^R or FA1090 Nal^R vs. FA1090Δ*katA* Rif^R). As observed in the noncompetitive assays, FA1090Δ*katA* adhered to ME180 cells at lower levels compared to FA1090 in the same well, but showed a similar percentage of invaded GC (Fig. 27C). The ICS of FA1090Δ*katA* also decrease over time in accordance with

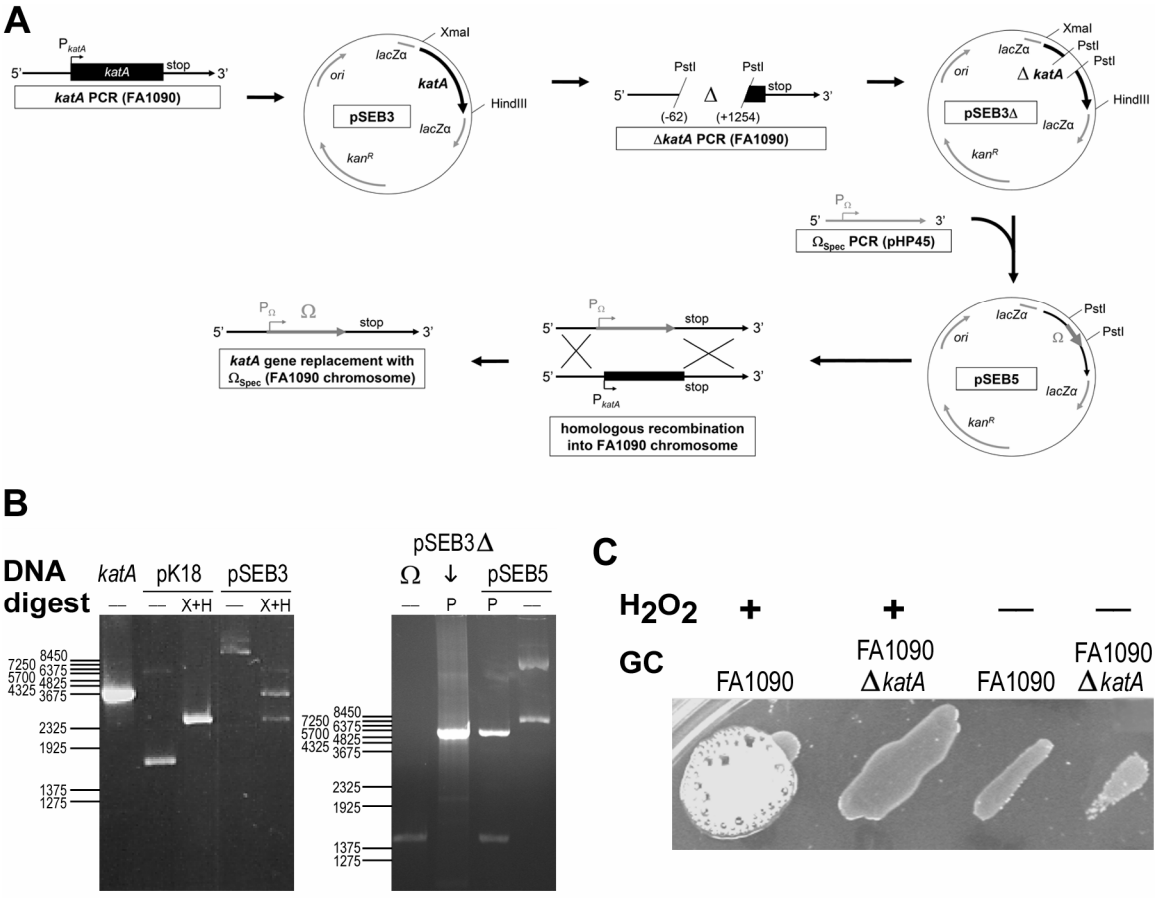

Figure 26—Construction of FA1090Δ*katA*, a GC strain deficient for the catalase enzyme. (A) Gene replacement strategy to establish the *katA* deletion strain (see Materials and Methods). (B) Agarose gel showing the DNA fragments generated during construction of FA1090Δ*katA* to confirm the presence and proper orientation of each DNA of interest. Restriction enzymes used for digestions are as follows: X = XmaI, H = HindIII, and P = PstI. DNA samples not treated with restriction enzymes represented PCR products [i.e. *katA* and Ω_{Spec} in FA1090] or uncut plasmids. (C) FA1090 and FA1090Δ*katA* were patched onto GCK agar overnight and treated (+) or not treated (-) with hydrogen peroxide (10%).

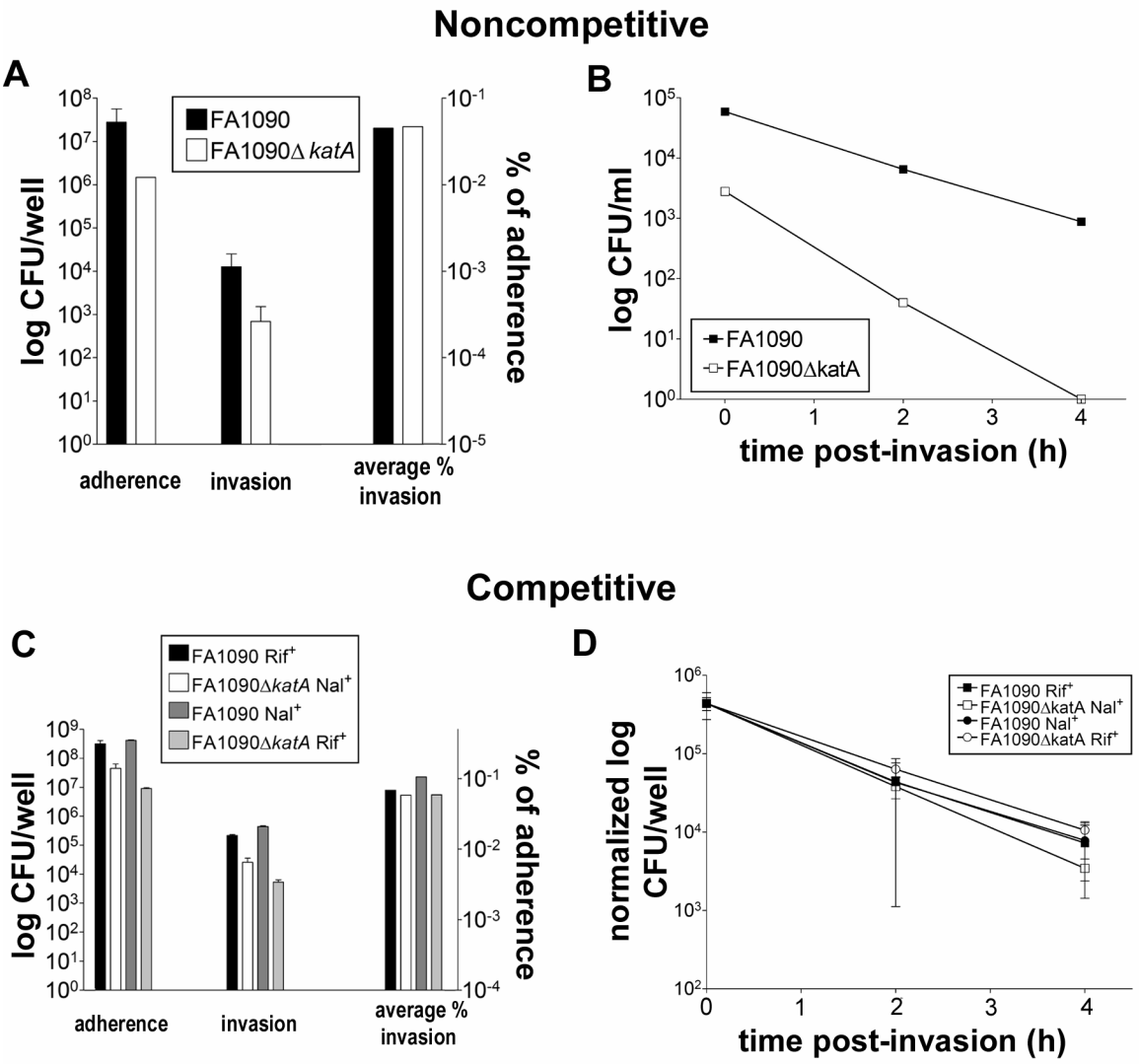

Figure 27—Deletion of the catalase gene does not alter GC intracellular survival. Gentamicin protection assays (panels A and C) or intracellular survival assays (panels B and D) performed in the presence of prolonged gentamicin treatment. ME180 cells were incubated with (A and B) FA1090 or FA1090Δ*katA* in noncompetitive assays and (C and D) FA1090 Rif^R + FA1090Δ*katA* Nal^R or FA1090 Nal^R + FA1090Δ*katA* Rif^R in competitive assays. Data in panel A = average (± SD where possible) of one, two, or three trials from two independent experiments; panel B = average of two trials from two independent experiments; panels C and D = average (± SD) of three trials from a single experiment. GC (P^+Opa^-) were added at a MOI of 10 (gentamicin = 200 μg/ml) in panels A and B and at a MOI of 1000 (gentamicin = 500 μg/ml) in panels C and D; Rif^+ = rifampicin resistant and Nal^+ = naladixic acid resistant.

FA1090 (Fig. 27D). These data demonstrate that catalase expression does not play a role in protecting the gonococcus from dying inside cervical epithelial cells.

NfsB is an oxygen insensitive nitrogen reductase shown to be important in bacterial resistance to nitroaromatic compounds (301). A colleague in the laboratory created a mutation in *nfsB* in an FA1090 background (FA1090 M1, Esteban Carrizosa, unpublished data). FA1090 M1 adhered to and invaded ME180 cells at similar levels compared to FA1090 (Fig. 28A). FA1090 M1 was also killed at a similar rate to FA1090 inside ME180 cells (Fig. 28B). These data indicate that *nfsB* does not play a role in GC ICS and suggests GC do not encounter nitroaromatic compounds inside cervical epithelial cells. Overall, these data show that neither catalase expression nor NfsB expression altered the rate of GC intracellular killing.

Analysis of GC intracellular survival and potential escape during intermittent bactericidal agent exposure. To determine if the observed decrease in FA1090 ICS within cervical epithelial cells was due to intracellular killing by host cells or penetration of the bactericidal agent into the cells, I incubated ME180 cells with FA1090 for 6 h and, after washing away nonadherent GC, treated the cells with TA for 1 h. In the samples incubated in TA-containing media for the duration of the chase period (continuous treatment), FA1090 ICS decreased over time (Fig. 29A). In the samples incubated in growth media during the chase period except for the final h (intermittent treatment) when samples were treated again with TA, FA1090 ICS decreased during the first 2 h, but then recovered over the remainder of the chase period (Fig. 29A). These data indicate that subjecting infected host cells to prolonged treatments with TA decreases GC ICS.

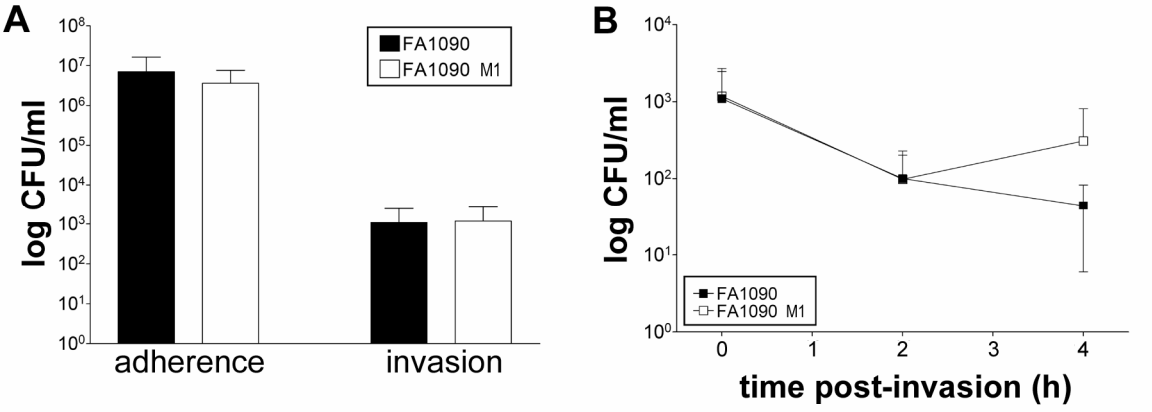

<u>Figure 28</u>—Inactivation of the nitrogen reductase gene, *nfsB*, does not alter GC intracellular survival. Gentamicin protection assays (panel A) or intracellular survival assays (panel B) performed in the presence of prolonged gentamicin treatment. ME180 cells were incubated with FA1090 or FA1090 M1 in noncompetitive assays (A) ME180 cells were incubated with FA1090 (black bars) or FA1090 M1; data = average (± SD) of two independent experiments each performed in triplicate. GC were $P^{+}Opa^{-}$.

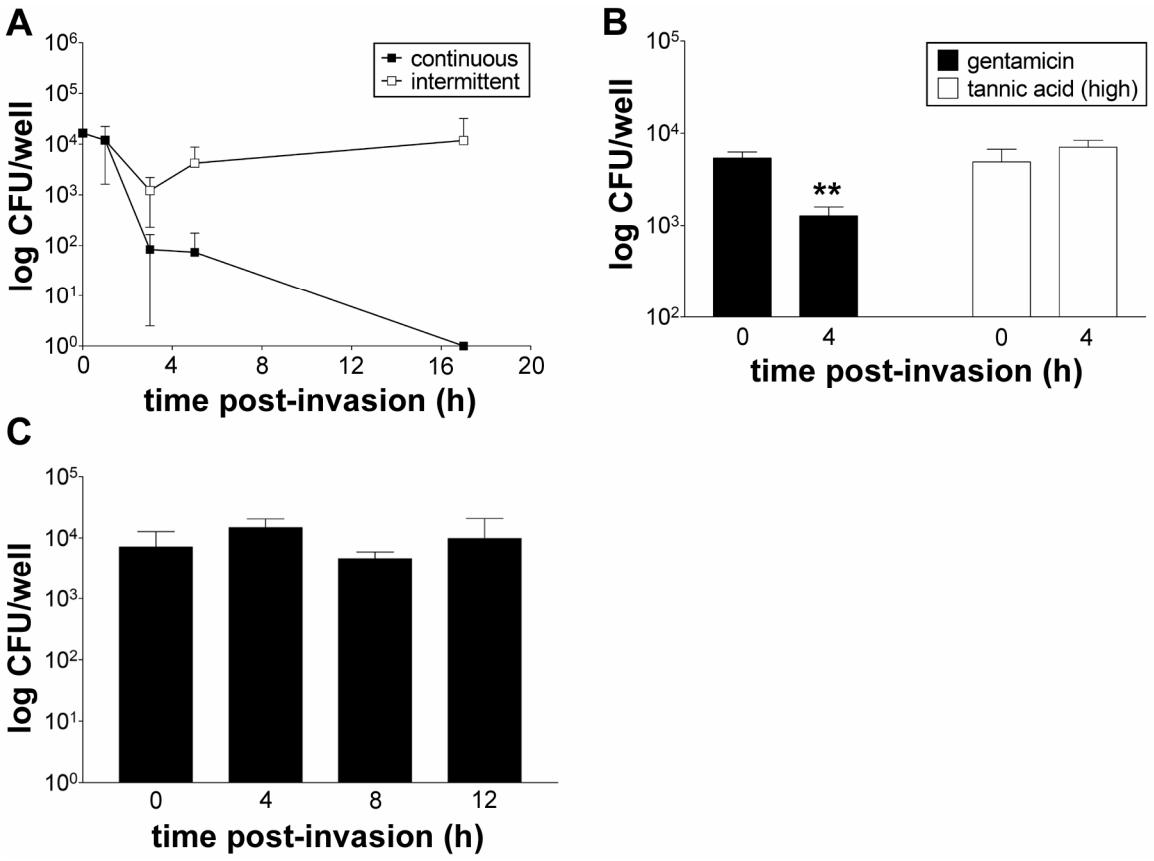

Figure 29—Analysis of GC intracellular survival and potential escape. GC intracellular survival assays performed by incubating ME180 cells with P^+Opa^- FA1090 in panel A and P^+Opa^+ FA1090 in panels B and C. (A) Comparison of GC intracellular survival when subjected to prolonged or intermittent exposure to 0.1% TA; data are representative (± SD) of two independent experiments each performed in triplicate. (B) GC may escape from inside host cells when not trapped by TA. Comparison of GC intracellular survival after an initial gentamicin (200 μg/ml) or TA (0.2% [90 min] + 1% [30 min]) treatment and no additional bactericidal agent treatment; data = average (± SEM) of three independent experiments each performed in triplicate, p-value = 0.0004 for gentamicin-treated samples. (C) GC intracellular survival maintains a steady state when GC are forced to remain intracellular by TA (0.2% [90 min] + 1% [30 min]) treatment; data = average (± SD) of three trials from a single experiment. GC were added at a MOI of 100 in panel A and at a MOI of 10 in panels B and C.

However, when the selective pressure of bactericidal agents is removed from invaded host cells, GC survive inside host cells. These data suggest that TA can penetrate into host cells to contribute to GC intracellular death when the agent is maintained in the extracellular media.

As observed in Figure 17E, pretreatment of host cells with TA prior to incubation with GC blocks invasion. Therefore, treatment of host cells with TA post-invasion should trap invaded GC inside cervical epithelial cells and prevent additional GC from entering into the cells. I incubated ME180 cells with FA1090 for 6 h and treated the cells with either gentamicin or TA for 2 h. Extracellular adherent GC were efficiently killed by both treatments as little or no viable GC were recovered from cell culture supernatants following treatment (data not shown). In accordance with the intermittent survival assay, I removed the bactericidal agents after an initial 2 h treatment, incubated the cells in growth media until various time points, and quantified the levels of intracellular GC from cell lysates. In the TA treated samples, the number of intracellular GC remained relatively constant post-invasion (~10^4 GC/well) (Fig. 29B and Fig. 29C) indicating that GC were indeed surviving inside cervical epithelial cells even over an extended time course. Surprisingly, in the gentamicin treated samples, I observed a significant decrease in the number of intracellular GC over time despite GC being incubated in favorable growth media (Fig. 29B, p-value = 0.0004). These data suggest GC are escaping from host cells after invasion when not trapped within these cells by TA. Overall, these data demonstrate GC survive within cervical epithelial cells in a relative stationary state where intracellular GC are either in stasis or are replicating and dying at similar rates.

GC escape from cervical epithelial cells to persist after invasion. To test if intracellular GC could escape back the extracellular milieu, I incubated ME180 cells with GC to allow for invasion, treated cells with gentamicin to kill extracellular GC, and added growth media during the 2 h and 4 h chase periods. Culture supernatants were collected at each time point to quantify the number of GC contained in the culture media. During the initial 2 h chase period, the number of FA1090 in the supernatants increased by about 10-fold above the background levels of bacteria present in the supernatant after gentamicin treatment (Fig. 30A). These data suggest that a portion of the invasive population of GC cycle back out of host cells to escape into the extracellular environment. The ability to escape from host cells is not strain-specific, since MS11 mKC also appeared to escape from ME180 cells (Fig. 30A). Gentamicin was less efficient at killing extracellular GC associated with the Hec1B cell line during the 2 h treatment. Therefore, I was unable to determine if GC escaped from Hec1B cells since the high initial background level of GC in the supernatant prevented distinguishing escaping GC from extracellular GC replicating in the growth media (Fig. 30B). Since the data show that most GC escaped during the initial 2 h chase period, I wanted to determine the rate of GC escape from host cells. I collected supernatants at shorter intervals during the initial 2 h chase and found that the most rapid increase in GC escape occurred in the first 30 min of detection (Fig. 30C). Furthermore, the expression of Opa had little effect on GC escape during the initial chase period (Fig. 30C). I also ensured that washing the cells in growth media (following gentamicin treatment and prior to the beginning of the escape chase period) did not contribute to the background levels of extracellular GC after gentamicin killing (Fig. 30D).

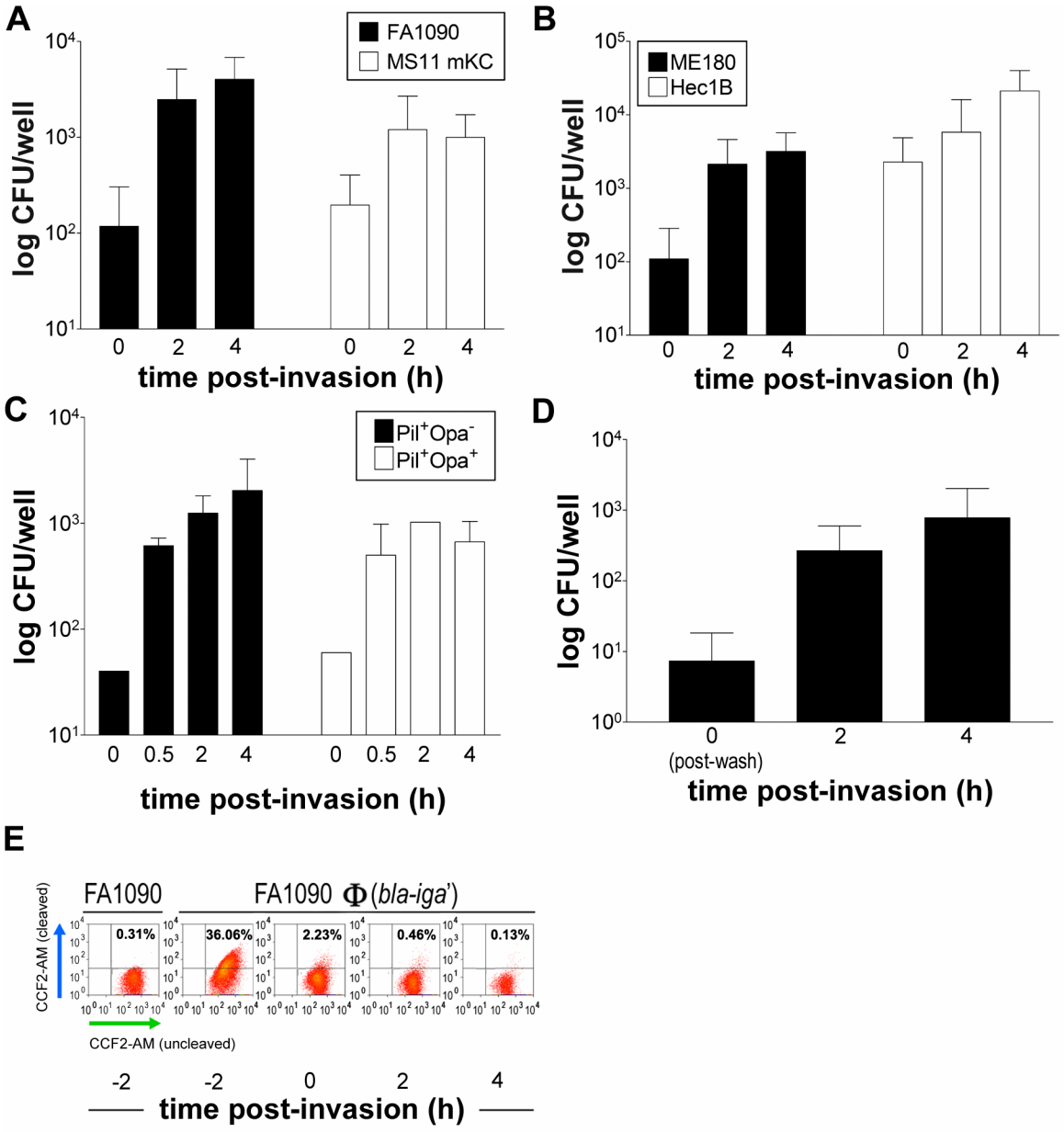

Figure 30—Investigation of GC escape from the host cell intracellular environment after invasion. GC escape assays (panels A-D) and Bla reporter escape assays (panel E) were performed by incubating cells with:(A) FA1090 or MS11 mKC, (B-D) FA1090, or (E) FA1090 or FA1090 Φ(*bla-iga'*). Data in panel A = average (± SD) of 10 or 11 trials from six independent experiments; panel B = average (± SD) of 12 trials from seven independent experiments; panel C = one to three trials from a single experiment; panel D = average (± SD) of three trials from a single experiment and the t = 8 h supernatant is the final wash before adding IM for the chase period, panel E = single experiment and incubations with FA1090 served as gating control. ME180 cells were utilized in all trials (and Hec1B in panel B). GC were added to cells at a MOI of 1000 (panels A-C) and MOI of 10 (panels D and E). GC in panels A-B were P^+Opa^- and in panels D-E were P^+Opa^+. Gentamicin = 500 µg/ml in panels A-C and 200 µg/ml in panel D-E.

I utilized the Bla reporter assay to further determine if GC were exiting host cells. Host cells loaded with CCF2-AM that contain intracellular Bla^+ GC should cleave the dye and fluoresce blue and cells that do not internalize Bla^+ GC should not cleave the dye and fluoresce green. Invaded cells in the population that yield blue fluorescence at one time point would exhibit green fluorescence at a later time point if their internalized Bla^+ GC escape. I incubated ME180 cells with FA1090 Φ(*bla-iga'*) for 6 h, treated cells for 2 h with gentamicin to kill extracellular GC and prevent escaping GC from re-entering host cells, and incubated cells in growth media for an additional 2 h and 4 h chase period. Our data show a large decline in the number of invaded ME180 cells at 6 h (~36%) compared to the number of cells with intracellular GC after gentamicin treatment at t = 8 h (~2%) (Fig. 30E), which supports the data in Figure 30C that escape is rapid. Taken together, these data indicate that GC can escape from within cervical epithelial cells and suggest that invaded GC may only reside in an intracellular location for a short time span before escaping into the extracellular milieu.

GC escape by utilizing a host cell exocytosis pathway that can be inhibited by TA.

In order to understand the cellular processes that contribute to GC escape, ME180 cells were treated with various cellular inhibitors after invasion. The actin polymerization inhibitors cytochalasin D and latrunculin B did not inhibit FA1090 escape during the initial 2 h chase period (Fig. 31A and Fig. 31B), indicating the actin microfilaments do not play a role in FA1090 exiting host cells. Disrupting microtubules with microtubule depolymerizing agent nocodazole also did not inhibit FA1090 escape (Fig. 31C).

I modified the escape assay by treating cells with TA after the 6 h incubation instead of gentamicin. In Figure 17E, TA was shown to inhibit GC invasion. Thus, I reasoned that since TA inhibits vesicular fusions with the plasma membrane it may block escape. In cells treated with low or moderate concentrations of TA, FA1090 escape was not inhibited, but the moderate concentration did eliminate the background GC sometimes observed in the supernatants after gentamicin treatment (Fig. 31D and Fig. 31E). The highest concentration of TA tested eliminated background FA1090 and blocked escape during the initial 2 h chase (Fig. 31E). Even after a 4 h chase period, only background levels of GC escaped into the supernatants from cells treated with high levels of TA (Fig. 31F). The high TA concentration also inhibited the escape of F62Δ*lgtD* and F62Δ*lgtA* (Fig. 31G), which demonstrated this inhibitory effect is not specific to FA1090. Alternatively, TA may not be blocking escape, but instead could be killing GC as they escape from host cells to prevent their recovery in the supernatants. To test this possibility, I incubated ME180 cells in high levels of TA for 2 h and then added back to the cells the number of FA1090 that appear to escape during a 2 h chase period from gentamicin- treated cells. During the 2 h chase period, the number of FA1090 in the supernatant increased indicating TA did not kill the added GC. TA inhibited escape rather than kill GC as they escape (Fig. 31H). TA fixes host cells without inhibiting intracellular functions and blocks vesicular fusion with the host cell membrane. Therefore, our data suggest GC escape from host cells by utilizing host cell exocytosis mechanism and TA blocks the escape by preventing GC-containing vacuoles or vesicles from fusing the cell membrane.

Figure 31—Analysis of the GC escape mechanism. GC escape assays (panels A-G) and a GC escape control assay (panel H) were performed by incubating ME180 cells with: (A-F and H) FA1090 or (G) F62Δ*lgtD* or F62Δ*lgtA*. (A-C) The GC escape pathway cannot be blocked by cytoskeletal inhibitors (15 min pre-escape treatment and maintained throughout the chase period): (A) cytochalasin D (3 μM); data = average (± SD) of four to seven trials from three independent experiments, (B) latrunculin B (1 μM); data = one to three trials from a single experiment, (C) nocodazole (35 μM); data = an average of two trials from a single experiment. (D-H) GC escape from cervical epithelial cells via a host exocytosis mechanism that can be blocked by TA. Data in panel D = average (± SD) of four to eight trials from three independent experiments; panel E is representative of three independent experiments performed in triplicate; panel F = average (± SEM) of three independent experiments each performed in triplicate; panel G = average (± SD) of two independent experiments each performed in triplicate; panel H = average (± SD) of three trials from a single experiment. GC were added at a MOI of 1000 in panels A-D and at a MOI of 10 in E-H; GC in panels A-C were P^+Opa^- and in panels D-H were P^+Opa^+. Gentamicin = 200 μg/ml in panels A-G; TA = 0.5% in panels D, 0.2% or 0.2 % (90 min) + 1% (30 min) in panels E, 0.2 % (90 min) + 1% (30 min) in panels F and G, 0.2% TA (90 min) + 1% (30 min) prior to adding FA1090 for 2 h.

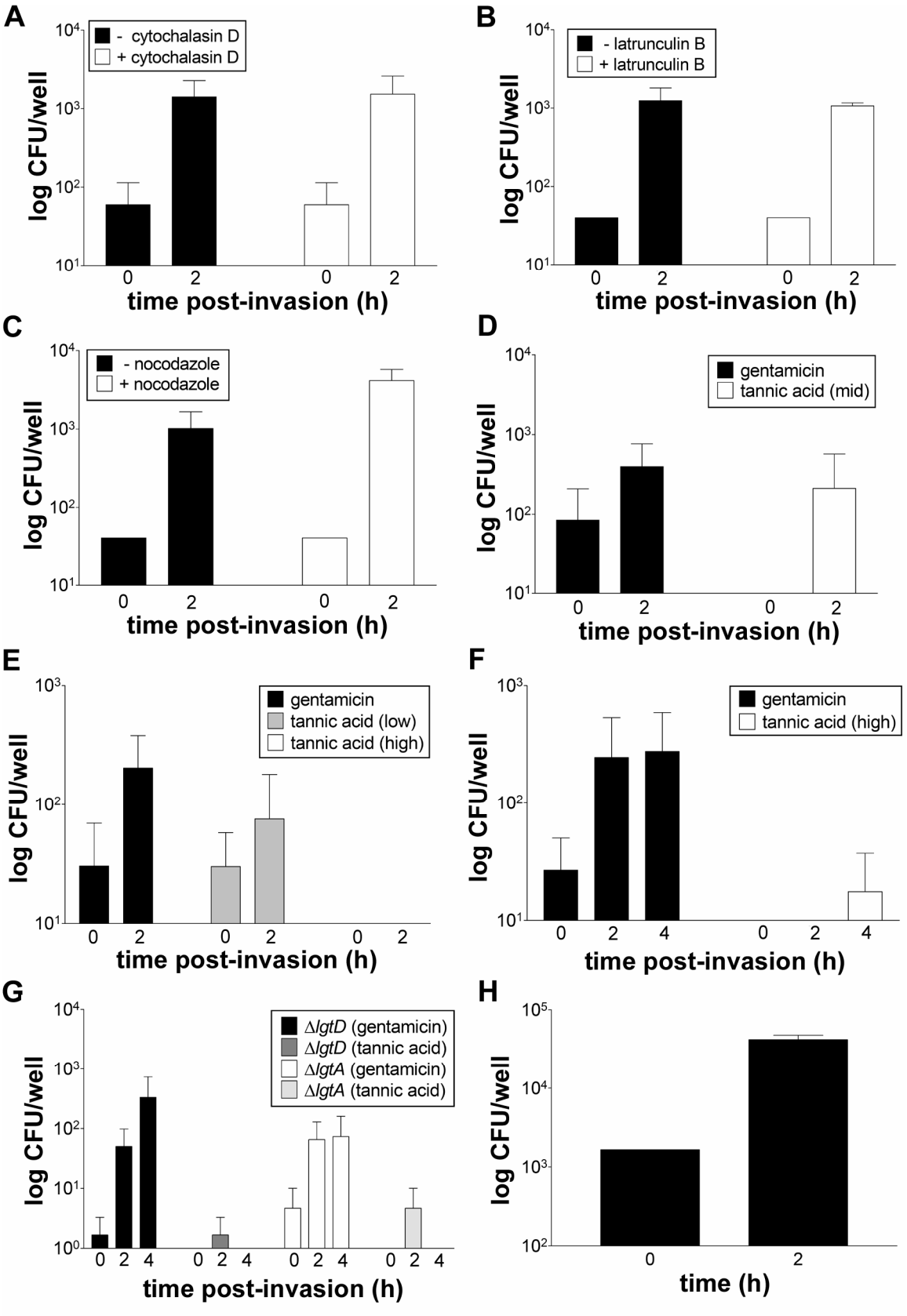
A
- cytochalasin D
+ cytochalasin D
log CFU/well
time post-invasion (h)
B
- latrunculin B
+ latrunculin B
log CFU/well
time post-invasion (h)
C
- nocodazole
+ nocodazole
log CFU/well
time post-invasion (h)
D
gentamicin
tannic acid (mid)
log CFU/well
time post-invasion (h)
E
gentamicin
tannic acid (low)
tannic acid (high)
log CFU/well
time post-invasion (h)
F
gentamicin
tannic acid (high)
log CFU/well
time post-invasion (h)
G
ΔlgtD (gentamicin)
ΔlgtD (tannic acid)
ΔlgtA (gentamicin)
ΔlgtA (tannic acid)
log CFU/well
time post-invasion (h)
H
log CFU/well
time (h)

Discussion

Pathogens can utilize host processes to support their survival and transmission without eliciting a bactericidal immune response. The extent of GC ICS and persistence in a particular host may be contingent on a variety of factors, including the cell type invaded, the mechanism of invasion, the signaling pathways activated, and the specific innate defenses generated. It is thought that GC survive inside epithelial cells until they spread to other host tissues or are transmitted to a new host. GC ICS may contribute to the severity of tissue damage that occurs during disease (181, 261). The cellular interactions and factors that mediate the GC intracellular life cycle represents one of the least studied aspects of GC pathogenesis.

My data indicate that GC invasion of cervical epithelial cells yields three possible outcomes. GC are killed when bactericidal agents are present in the extracellular milieu. Under more favorable conditions, some GC survive within host cells and may avoid cellular killing strategies. Another subpopulation escapes from cells via an exocytotic pathway and may reinvade nearby cells, be transmitted to a new host, or interact with PMN's to elicit pro-inflammatory responses.

Throughout this study, I used different modifications of the survival assay to monitor GC ICS and escape. My data show that continuous exposure of cells to cell-impermeable bactericidal agents accelerated GC intracellular death compared to performing the assay with intermittent gentamicin or TA treatments. Data from the continuous treatment assays suggest the supposed "cell-impermeable" gentamicin and TA penetrate into cervical epithelial cells after prolonged exposure. Gray-Owen and colleagues also observed a decline in GC survival in CEACAM 3-expressing epithelial

cells and fibroblasts using the continuous treatment approach and gentamicin uptake into epithelial cells has been observed in other systems (21, 179). For example, researchers discovered that intestinal epithelial cells infected with *Campylobacter jejuni* (CJ) took up gentamicin at low levels during a continuous treatment assay and was responsible for killing a portion of the intracellular CJ (158). Overall, the intracellular killing attributed to gentamicin or TA permeability masks GC ICS in the continuous treatment survival assay and, thus, does not provide the most accurate measurement of GC ICS.

I wanted to determine which genes were needed for GC survival inside epithelial cells. To investigate the role of catalase in GC ICS, I deleted the GC catalase (*katA*) gene, a highly expressed cytoplasmic enzyme speculated to contribute to GC ICS (7, 310). I utilized the continuous treatment assay where cells were exposed to gentamicin throughout the survival chase period. The continuous treatment assay was employed in these analyses because I had not yet developed the intermittent survival assay at the time of this study. The potential penetration of gentamicin into host cells during the continuous treatment assay was expected to have a similar killing effect on both strains; therefore, any additional changes in ICS between them can be attributed to the affect of the catalase mutation. However, my results showed a similar rate of intracellular killing between FA1090 and FA1090Δ*katA*, suggesting that catalase is not important for ICS. This is consistent with other published findings where a catalase mutant showed similar survival compared to wild-type GC in the estradiol-treated mouse model (265). These data indicate that catalase does not play a role in GC ICS in epithelial cells. Recent studies show factors other than catalase, such as the MntABC transporter, CcpA, and

Laz, play prominent roles in fighting oxidative stress (258, 285, 307), which further indicates that catalase is not essential for GC ICS.

In the intermittent survival assays, the GC-restrictive chase incubations were lifted by removal of the bactericidal agent after the initial treatment. My data show that GC can persist within cervical epithelial cells under these conditions or escape from host cells when treated with gentamicin or a low relative concentration of TA (i.e. escape-permissive conditions). GC ICS appeared to decline at the beginning of the chase period under escape-permissive conditions. Other groups have also observed an initial lag or decline in FA1090 ICS after invasion into ME180 or T84 epithelial cells (51, 104). After the initial decline in GC ICS, my data show GC survival recovers over time in the intermittent assay in Figure 29A and Figure 29C suggesting GC may proliferate and/or escaping GC may re-enter into cells.

Treatment of cells with a high relative concentration of TA in Figure 29C (i.e. escape-restrictive conditions) blocked GC escape and restricted GC to intracellular locations where they appeared to survive at a stasis level. These data suggest the capability of epithelial cells to kill intracellular GC does not increase when a greater number are forced to remain inside host cells. In any case, it appears that GC can maintain a static or stationary level of ICS within epithelial cells over time.

The specific defense mechanisms that may kill some intracellular GC were not identified. Many invaded GC could die of starvation if unable to obtain an intracellular iron source since infected host cells could sequester this nutrient from the bacteria. Expression of the TonB-dependent iron transporter TdfF has been shown to be required for FA1090 survival in ME180 cells (104), suggesting GC that acquire iron could

represent the population that overcomes host intracellular defense and survive over time. Alternatively, GC subpopulations that signal and invade host cells via different mechanisms may enter into different subcellular compartments and realize different survival fates. As mentioned above, GC have been visualized in vacuoles or free in the cytoplasm in different cell types and entering into these different cellular locations may alter GC ICS. Timmerman, *et al*. display evidence of GC replication inside vacuoles and Weel, *et al*. show GC are destroyed inside some intracellular compartments (281, 297). These findings indicate that some, but not all, GC-infected cells develop vacuoles that mature into phagolysosomes and it appears some host cells may be more equipped to kill invaded GC than other cells.

GC re-emergence from host cells also represents a strategy for GC to persist in the host. My data from the gentamicin-based and Bla reporter-based escape assays showed that GC escape was rapid (30 min—2 h) suggesting GC cycled out of host cells soon after invasion. Therefore, the gentamicin-based escape assay may not be ideal for quantifying escape since many GC seem to emerge during the initial 2 h gentamicin treatment. The most rapid escaping GC would be killed prior to the chase period by gentamicin and would not be quantified in the escape pool. In addition, the late emerging GC during this gentamicin treatment period could represent the background extracellular GC sometimes observed in this assay. This subset of escaping GC would be extracellular prior to the chase period, but not exposed to the bactericidal agent long enough to be rendered nonviable.

I demonstrated that GC escape via a host exocytosis pathway blockable by TA. Since exocytosis occurs when intracellular vacuoles or vesicles fuse with the plasma

membrane, GC localized within intracellular compartments, not free in the cytoplasm, appear to be more probable escape candidates. Recently, Criss and Seifert demonstrated GC that invaded polarized T84 epithelial cells from the apical side could also exit through the apical membrane (51), but they did not identify the mechanism of GC re-emergence. One potential mechanism for GC escape is the recycling endosome pathway, a route utilized by host cells to recycle receptors and cargo back to the cell surface (100). GC that remain bound to particular cell receptors after invasion or divert endosomes into the recycling track could be targeted for escape. Transferrin receptors and the ASGP-R undergo recycling. GC express transferrin binding proteins, TbpA and TbpB and bind to the ASGP-R via LnNT LOS (43, 48, 55, 165, 229, 255). GC that remain bound to the ASGP-R after invasion could recycle back to the plasma membrane. In theory, one could envision intracellular GC and cellular transferrin receptors both binding to transferrin molecules to compete for the iron source. Upon recycling, transferrin receptors, apotransferrin, and bound GC would cycle back to the plasma membrane to release both the apotransferrin and the bound GC to escape (55). GC could use many different receptors to carry out this recycling/escape strategy.

Escape, i.e. intracellular-extracellular cycling, may represent an important mechanism for GC persistence in the female reproductive tract. A subset of invaded GC could evade extracellular and intracellular host defenses by continual transitioning in and out of host cells. This subdued level of survival may contribute to the asymptomatic nature of GC disease in women and prevent GC from eliciting a strong innate immune response. Epithelial cells could provide GC with a location to sustain a small pool of protected organisms that persist in the host. These intracellular organisms are well

positioned to either transcytose into subepithelial tissues to propagate disease progression or escape into the extracellular milieu where they are localized for transmission to a new host or positioned to reinvade neighboring cells. In this study, I showed that some invaded GC can evade host cell killing mechanisms to maintain a surviving intracellular pool. Other GC escape back into the extracellular milieu using host cell exocytosis machinery. I found that the utilization of TA to block GC re-emergence in the escape and survival assays helped to uncover some details of the escape mechanism and uncouple the ICS and escape processes to better quantify GC ICS. The long-term fates of viable intracellular GC and re-emerging GC will require further study, but each subpopulation may contribute to the outcome of disease by affecting the magnitude of host cell activation and the extent of GC dissemination from the initial site of colonization.

CHAPTER 4—CONCLUSIONS

As a leading communicable disease and one of the most common STDs, gonorrhea continues to be a global public health issue known for its high morbidity. The disease is characterized by an intense neutrophil-mediated proinflammatory response in symptomatic individuals, yet many infected persons (especially women) do not produce recognizable symptoms and fail to seek treatment until the disease reaches greater severity. Infected hosts can generate innate immune responses to GC, but fail to mount a substantial adaptive immune response. Since GC do not create a protective antibody response, a cell-mediated response, or immunological memory, repeat infections of increasing severity are common. Furthermore, the rise in antibiotic-resistant GC along with the lack of a successful GC vaccine provides motivation for further GC research to discover new therapeutics and prevention methods.

To establish infection, GC must overcome mucosal epithelial cells and innate immune defenses. GC have been shown to adhere to, invade into, and survive within both phagocytic and nonphagocytic cells. However, correlating the impact of these events in GC pathogenesis with disease outcomes remains difficult. My work has focused on determining how pili, Opa, LOS, bacterial viability, etc. contribute to GC invasion and ICS by identifying host cell factors and processes (signaling molecules, actin dynamics, exocytosis, etc.) that GC target to accomplish these pathogenic events.

In order to identify potential host cell signaling molecules GC activate to initiate invasion, I incubated human cervical epidermal carcinoma cells (ME180 cells) with different GC variants expressing different combinations of pili, Opa, and/or LOS. I probed infected cell lysates for the phosphorylated forms of different kinases to

determine their activation status. The data produced in this study combined with findings in previous reports indicate that GC can activate a variety of signaling pathways prior to invasion [see (188, 209, 227) for reviews]. The combination of surface structures GC express, the type of host receptors bound, and the order of receptor binding can all influence the level of host cell activation and help determine if a cell will internalize GC. Since the GC surface undergoes high frequency PV and AV, most GC infections will involve a mixed population of GC expressing varied cell surfaces. Thus, GC possess the ability to induce different cellular responses leading to varied disease severity in women based on the specific GC-host cell interactions that occur within a population of cervical epithelial cells. For example, data from this work and previous reports indicate changes in LOS can impact host cell interactions and disease progression. If the majority of the infecting GC express the lacto-*N*-neotetraose LOS glycoform, then host cell JNK activation would be diminished. These cells would produce lower IL-8 levels and may avoid eliciting a proinflammatory immune response better than cells infected by a population of predominant lactosyl LOS-expressing GC. A previous study in our lab indicated LnNT LOS-expressing GC are more invasive into cervical epithelial cells indicating they can disseminate from the initial site of colonization (266). Therefore, in this example, altered expression of a single GC surface structure could change the level of symptoms produced during infection, which could influence the ability of GC to invade and migrate to secondary tissues.

In order to quantify GC invasion, I developed the β-lactamase reporter assay to measure the number of epithelial cells that internalize GC at the single cell level and also employed gentamicin and tannic acid-based protection assays. The level of GC invasion

into cervical epithelial cells may also influence the outcome of infection. Greater GC invasion into host tissues could propagate increased GC dissemination to additional anatomical sites and protect more GC from killing by phagocytes. While Opa represents a major invasin on the GC cell surface (176, 190), reports indicate other GC surface structures can contribute to invasion. The work described here indicate that GC can invade epithelial cells using Opa-independent mechanisms. Furthermore, GC not expressing Opa invaded a greater number of cells than Opa-expressing GC, which raises questions about Opa's role as a primary invasin. While Opa may play a prominent role in establishing intimate adhesion between GC and some host cell types, its role in invasion may have been overestimated by the use of the gentamicin resistance assay. Regardless, the existence of Opa-independent invasion pathways demonstrates that GC express several different cell surface invasins that can orchestrate invasion mechanisms. GC viability was also shown to be necessary for invasion. Thus, in addition the physical interactions between GC ligands and cell receptors, invasion requires gonococcal responses to host cell cross-talk to generate invasion-promoting actions. Despite their multiple invasins and invasion strategies, my data also shows that invasive GC only enter a subpopulation of infected cells. Thus, cervical epithelial cells may possess mechanisms to resist invasion. Alternatively, GC may need to initiate enough interactions with a given host cell, possibly through microcolony formation, to generate a threshold level of signaling to trigger a bacterial internalization response in nonphagocytic cells. Thus, determining the signaling profiles and cellular response indicators that characterize an invasion-susceptible cell versus an invasion-resistant cell will be important focal points of future explorations. The β-lactamase reporter assay will serve as a useful technology

since it can be used to separate invasion-susceptible cells from invasion-resistant cells for further investigation.

The degree of intracellular survival of invasive GC can further influence disease outcomes. I developed a tannic acid-based survival assay to identify three intracellular fates of various invasive GC subpopulations: bacterial death, bacterial survival and transcytosis to subepithelial compartments, and bacterial escape to return to the extracellular milieu. The ability of GC to survive within phagocytes remains controversial. Thus, intracellular killing by epithelial cells may represent a primary mechanisms of GC clearance or at least serve an additional mechanism to complement phagocytic killing.

Some GC are capable of surviving after internalization by cervical epithelial cells and they may represent a critical subpopulation for disseminated disease and chronic persistence in the human population. GC that establish an intracellular niche can avoid eliciting proinflammatory responses that could lead to bacterial clearance. My data reveal that GC maintain a low-level of persistence in epithelial cells and their lack of proliferation may be a critical adaptation in the GC intracellular life cycle for evading immune recognition. These GC would also be protected from extracellular immune defenses by the epithelial barrier. These factors could contribute to the ability of these bacteria to disseminate with minimal immune confrontation. Data from this study also indicate intracellular GC can escape from host cells via an exocytotic pathway. Escaping GC possess the added dimension of spreading to neighboring epithelial cells after re-emergence to further compromise the epithelial barrier. These GC also represent a subpopulation ideally positioned from transmission to a new host due to their transient

extracellular location. Overall, I propose that intracellular GC are an important contributor to the high frequency of asymptomatic disease in women because they can persist at a low-level in the female reproductive tract and serve as a reservoir of GC disease.

GC establish infection by colonizing a localized host tissue site. Those GC that possess the virulence factors to spread into surrounding cells and progress into deeper tissues can cause divergent and more severe disease sequelae. Thus, determining the mechanisms of GC invasion, intracellular survival, and escape in cervical epithelial cells has important implications in our understanding of GC disease in women, including how to devise new treatment and prevention strategies for those infections that lead to morbid complications.

The work in this study has advanced our understanding of the invasion and post-invasion stages of GC pathogenesis. I would like to proposal the following updated model of GC-epithelial cell interactions (Fig. 32). GC are able to associate with most epithelial cells in an infected population, yet only invade into a subset of these cells. The GC ligand-cell receptor interactions and downstream signaling pathways most likely differ between invasion susceptible and resistant cells. GC invade the susceptible subpopulation of epithelial cells via multiple entry pathways using one or more surface invasins and through additional cross-talk interactions with host cells that requires GC viability. The invasin(s) implemented by GC for entry appear to depend on the cell type encountered during infection. Invasion into ME180 cells can be Opa-independent and Opa expression reduced the invaded host cell subpopulation, but in other cell types, such as Chang epithelial cells, Opa facilitates invasion. In any case, GC trigger invasion by

eliciting overlapping signaling events to kinases, including MAPK, linked to actin cytoskeletal reorganization. The unique extended ERK activation by GC prior to invasion implicates ERK as an important GC invasion-associated kinase that may be activated through a GC-induced ErbB1 signaling pathway. Furthermore, GC trigger IL-8 production in epithelial cells in part through JNK signaling. GC that diminish JNK activation in epithelial cells and thereby reduce IL-8 production could downgrade the innate immune response and help produce an asymptomatic infection. Once inside epithelial cells, GC can realize one of at least three intracellular fates. They can be killed by intracellular killing mechanisms that may involve phagolysosome maturation or bacterial starvation. GC that do survive can transcytose to subepithelial compartments where they can disseminate or possibly reinvade nearby cells through the basolateral membrane. In addition, surviving GC can escape into the extracellular lumen via a host exocytotic pathway where they can be transmitted to a subsequent host or reinvade neighboring cells to spread infection. Cycles of invasion and escape and a low-level of intracellular persistence in epithelial cells may help GC avoid immune recognition to promote asymptomatic infection.

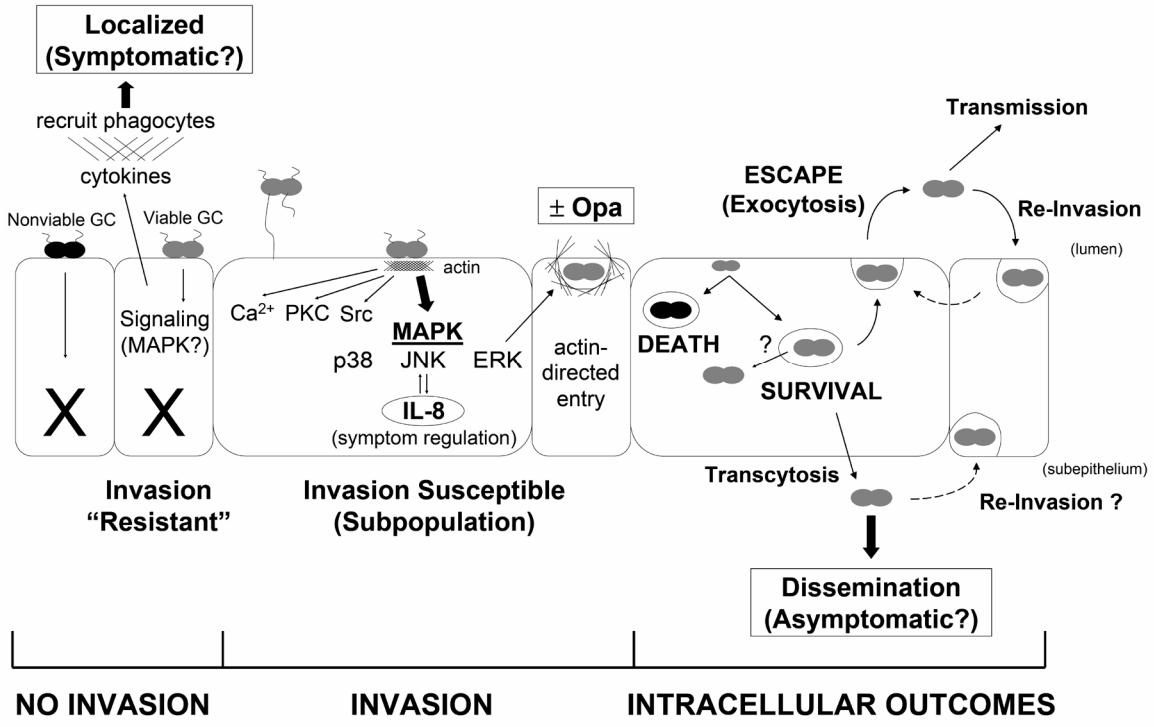

Figure 32—Working model for GC infection of the cervical epithelium. GC can adhere to most infected cervical epithelial cells and trigger invasion into a subpopulation of cells. Entry into epithelial cells may protect GC from phagocytes to help them avoid immune recognition and prevent symptom development. Invasion can be Opa-independent, but requires pili expression, bacterial viability, F-actin recruitment, and cross-talk with host cells that includes signaling to kinases, such as the MAPK ERK. GC can also regulate the JNK signaling pathway to manipulate IL-8-driven immune responses. Internalized GC realize one of three possible intracellular fates: death, survival, and escape. Surviving bacteria can transcytose to the subepithelium and disseminate or reinvade neighboring cells to spread infection. Escaping bacteria can be transmitted to new hosts or also reinvade nearby cells. These mechanisms of persistence in host tissue may contribute to the high frequency of asymptomatic infections in women. Nonviable GC = black diplococci and viable GC = gray diplococci.

References

1. 2007. Update to CDC's sexually transmitted diseases treatment guidelines, 2006: fluoroquinolones no longer recommended for treatment of gonococcal infections. MMWR Morb. Mortal. Wkly. Rep. **56:**332-336.

2. **Agerer, F., S. Waeckerle, and C. R. Hauck.** 2004. Microscopic quantification of bacterial invasion by a novel antibody-independent staining method. J. Microbiol. Methods **59:**23-32.

3. **Akira, S., K. Takeda, and T. Kaisho.** 2001. Toll-like receptors: critical proteins linking innate and acquired immunity. Nat. Immunol. **2:**675-680.

4. **Andrade, L. O., and N. W. Andrews.** 2004. Lysosomal fusion is essential for the retention of *Trypanosoma cruzi* inside host cells. J. Exp. Med. **200:**1135-1143.

5. **Apicella, M. A., M. Ketterer, F. K. Lee, D. Zhou, P. A. Rice, and M. S. Blake.** 1996. The pathogenesis of gonococcal urethritis in men: confocal and immunoelectron microscopic analysis of urethral exudates from men infected with *Neisseria gonorrhoeae.* J. Infect. Dis. **173:**636-646.

6. **Apicella, M. A., M. Shero, G. A. Jarvis, J. M. Griffiss, R. E. Mandrell, and H. Schneider.** 1987. Phenotypic variation in epitope expression of the *Neisseria gonorrhoeae* lipooligosaccharide. Infect. Immun. **55:**1755-1761.

7. **Archibald, F. S., and M. N. Duong.** 1986. Superoxide dismutase and oxygen toxicity defenses in the genus *Neisseria*. Infect. Immun. **51:**631-641.

8. **Armant, M. A., and M. J. Fenton.** 2002. Toll-like receptors: a family of pattern-recognition receptors in mammals. Genome Biol. **3:**reviews 3011.1-3011.6.

9. **Aspholm-Hurtig, M., G. Dailide, M. Lahmann, A. Kalia, D. Ilver, N. Roche, S. Vikstrom, R. Sjostrom, S. Linden, A. Backstrom, C. Lundberg, A. Arnqvist, J. Mahdavi, U. J. Nilsson, B. Velapatino, R. H. Gilman, M. Gerhard, T. Alarcon, M. Lopez-Brea, T. Nakazawa, J. G. Fox, P. Correa, M. G. Dominguez-Bello, G. I. Perez-Perez, M. J. Blaser, S. Normark, I. Carlstedt, S. Oscarson, S. Teneberg, D. E. Berg, and T. Boren.** 2004. Functional adaptation of BabA, the *H. pylori* ABO blood group antigen binding adhesin. Science **305:**519-522.

10. **Ayala, B. P., B. Vasquez, S. Clary, J. A. Tainer, K. Rodland, and M. So.** 2001. The pilus-induced Ca^{2+} flux triggers lysosome exocytosis and increases the amount of LAMP-1 accessible to *Neisseria* IgA1 protease. Cell. Microbiol. **3:**265-275.

11. **Ayala, P., L. Lin, S. Hopper, M. Fukuda, and M. So.** 1998. Infection of epithelial cells by pathogenic Neisseriae reduces the levels of multiple lysosomal constituents. Infect. Immun. **66:**5001-5007.

12. **Ayala, P., B. Vasquez, L. Wetzler, and M. So.** 2002. *Neisseria gonorrhoeae* porin P1.B induces endosome exocytosis and a redistribution of LAMP-1 to the plasma membrane. Infect. Immun. **70:**5965-5971.

13. **Ayala, P., J. S. Wilbur, L. M. Wetzler, J. A. Tainer, A. Snyder, and M. So.** 2005. The pilus and porin of *Neisseria gonorrhoeae* cooperatively induce Ca^{2+} transients in infected epithelial cells. Cell. Microbiol. **7:**1736-1748.

14. **Battistoni, A., F. Pacello, S. Folcarelli, M. Ajello, G. Donnarumma, R. Greco, M. G. Ammendolia, D. Touati, G. Rotilio, and P. Valenti.** 2000. Increased expression of periplasmic Cu,Zn superoxide dismutase enhances survival of *Escherichia coli* invasive strains within nonphagocytic cells. Infect. Immun. **68:**30-37.

15. **Bennett, B. L., D. T. Sasaki, B. W. Murray, E. C. O'Leary, S. T. Sakata, W. Xu, J. C. Leisten, A. Motiwala, S. Pierce, Y. Satoh, S. S. Bhagwat, A. M. Manning, and D. W. Anderson.** 2001. SP600125, an anthrapyrazolone inhibitor of Jun N-terminal kinase. Proc. Natl. Acad. Sci. USA **98:**13681-13686.

16. **Benz, R.** 1988. Structure and function of porins from gram-negative bacteria. Annu. Rev. Microbiol. **42:**359-393.

17. **Bergman, P., L. Johansson, V. Asp, L. Plant, G. H. Gudmundsson, A. B. Jonsson, and B. Agerberth.** 2005. *Neisseria gonorrhoeae* downregulates expression of the human antimicrobial peptide LL-37. Cell. Microbiol. **7:**1009-1017.

18. **Bhat, K. S., C. P. Gibbs, O. Barrera, S. G. Morrison, F. Jahnig, A. Stern, E. M. Kupsch, T. F. Meyer, and J. Swanson.** 1992. The opacity proteins of *Neisseria gonorrhoeae* strain MS11 are encoded by a family of 11 complete genes. Mol. Microbiol. **6:**1073-1076.

19. **Bhat, K. S., C. P. Gibbs, O. Barrera, S. G. Morrison, F. Jahnig, A. Stern, E. M. Kupsch, T. F. Meyer, and J. Swanson.** 1991. The opacity proteins of *Neisseria gonorrhoeae* strain MS11 are encoded by a family of 11 complete genes. Mol. Microbiol. **5:**1889-1901.

20. **Billker, O., A. Popp, V. Brinkmann, G. Wenig, J. Schneider, E. Caron, and T. F. Meyer.** 2002. Distinct mechanisms of internalization of *Neisseria gonorrhoeae* by members of the CEACAM receptor family involving Rac1- and Cdc42-dependent and -independent pathways. EMBO J. **21:**560-571.

21. **Binker, M. G., L. I. Cosen-Binker, M. R. Terebiznik, G. V. Mallo, S. E. McCaw, E. L. Eskelinen, M. Willenborg, J. H. Brumell, P. Saftig, S. Grinstein, and S. D. Gray-Owen.** 2007. Arrested maturation of *Neisseria*-containing phagosomes in the absence of the lysosome-associated membrane proteins, LAMP-1 and LAMP-2. Cell. Microbiol. **9:**2153-2166.

22. **Binnicker, M. J., R. D. Williams, and M. A. Apicella.** 2004. Gonococcal porin IB activates NF-kappaB in human urethral epithelium and increases the expression of host antiapoptotic factors. Infect. Immun. **72:**6408-6417.

23. **Binnicker, M. J., R. D. Williams, and M. A. Apicella.** 2003. Infection of human urethral epithelium with *Neisseria gonorrhoeae* elicits an upregulation of host anti-apoptotic factors and protects cells from staurosporine-induced apoptosis. Cell. Microbiol. **5:**549-560.

24. **Blake, M. S., C. M. Blake, M. A. Apicella, and R. E. Mandrell.** 1995. Gonococcal opacity: lectin-like interactions between Opa proteins and lipooligosaccharide. Infect. Immun. **63:**1434-1439.

25. **Blake, M. S., and E. C. Gotschlich.** 1984. Purification and partial characterization of the opacity-associated proteins of *Neisseria gonorrhoeae*. J. Exp. Med. **159:**452-462.

26. **Booth, J. W., D. Telio, E. H. Liao, S. E. McCaw, T. Matsuo, S. Grinstein, and S. D. Gray-Owen.** 2003. Phosphatidylinositol 3-kinases in carcinoembryonic antigen-related cellular adhesion molecule-mediated internalization of *Neisseria gonorrhoeae*. J. Biol. Chem. **278:**14037-14045.

27. **Boren, T., P. Falk, K. A. Roth, G. Larson, and S. Normark.** 1993. Attachment of *Helicobacter pylori* to human gastric epithelium mediated by blood group antigens. Science **262:**1892-1895.

28. **Bos, M. P., D. Kao, D. M. Hogan, C. C. Grant, and R. J. Belland.** 2002. Carcinoembryonic antigen family receptor recognition by gonococcal Opa proteins requires distinct combinations of hypervariable Opa protein domains. Infect. Immun. **70:**1715-1723.

29. **Boslego, J. W., E. C. Tramont, R. C. Chung, D. G. McChesney, J. Ciak, J. C. Sadoff, M. V. Piziak, J. D. Brown, C. C. Brinton, Jr., S. W. Wood, and et al.** 1991. Efficacy trial of a parenteral gonococcal pilus vaccine in men. Vaccine **9:**154-162.

30. **Boughan, P. K., R. H. Argent, M. Body-Malapel, J. H. Park, K. E. Ewings, A. G. Bowie, S. J. Ong, S. J. Cook, O. E. Sorensen, B. A. Manzo, N. Inohara, N. J. Klein, G. Nunez, J. C. Atherton, and M. Bajaj-Elliott.** 2006. Nucleotide-binding oligomerization domain-1 and epidermal growth factor receptor: critical

regulators of beta-defensins during *Helicobacter pylori* infection. J. Biol. Chem. **281:**11637-11648.

31. **Boyle, M. D.** 1995. Variation of multifunctional surface binding proteins--a virulence strategy for group A streptococci? J. Theor. Biol. **173:**415-426.

32. **Brinton, C. C., J. Bryan, J.A. Dillon, N. Guerina, L.J. Jacobson, A. Labik, S. Lee, A. Levine, S. Lim, J. McMichael, et al.** 1978. Uses of pili in gonorrhea control: role of pili in disease, purification and properties of gonococcal pili, and progress in the development of a gonococcal pilus vaccine for gonorrhea., p. 155-178. *In* J. G.F. Brooks, E.C. Gotschlich, K.K. Holmes, and W.D. Sawyer (ed.), Immunobiology of *Neisseria gonorrhoeae*. American Society for Microbiology, Washington D. C.

33. **Burch, C. L., R. J. Danaher, and D. C. Stein.** 1997. Antigenic variation in *Neisseria gonorrhoeae*: production of multiple lipooligosaccharides. J. Bacteriol. **179:**982-986.

34. **Carson, S. D., P. E. Klebba, S. M. Newton, and P. F. Sparling.** 1999. Ferric enterobactin binding and utilization by *Neisseria gonorrhoeae*. J. Bacteriol. **181:**2895-2901.

35. **Castrilli, G., D. Tatone, M. G. Diodoro, S. Rosini, M. Piantelli, and P. Musiani.** 1997. Interleukin 1 alpha and interleukin 6 promote the in vitro growth of both normal and neoplastic human cervical epithelial cells. Br. J. Cancer **75:**855-859.

36. **Caswell, C. C., E. Lukomska, N. S. Seo, M. Hook, and S. Lukomski.** 2007. Scl1-dependent internalization of group A *Streptococcus* via direct interactions with the alpha-2-beta-1 integrin enhances pathogen survival and re-emergence. Mol. Microbiol. **64:**1319-1331.

37. **CDC.** 2002. Sexually transmitted diseases treatment guidelines 2002. MMWR Recomm. Rep. **51:**1-78.

38. **Chen, J. C., P. Bavoil, and V. L. Clark.** 1991. Enhancement of the invasive ability of *Neisseria gonorrhoeae* by contact with HecIB, an adenocarcinoma endometrial cell line. Mol. Microbiol. **5:**1531-1538.

39. **Chen, L. M., S. Hobbie, and J. E. Galan.** 1996. Requirement of CDC42 for *Salmonella*-induced cytoskeletal and nuclear responses. Science **274:**2115-2118.

40. **Chen, T., F. Grunert, A. Medina-Marino, and E. C. Gotschlich.** 1997. Several carcinoembryonic antigens (CD66) serve as receptors for gonococcal opacity proteins. J. Exp. Med. **185:**1557-1564.

41. **Chen, Z., T. B. Gibson, F. Robinson, L. Silvestro, G. Pearson, B. Xu, A. Wright, C. Vanderbilt, and M. H. Cobb.** 2001. MAP kinases. Chem. Rev. **101:**2449-2476.

42. **Christodoulides, M., J. S. Everson, B. L. Liu, P. R. Lambden, P. J. Watt, E. J. Thomas, and J. E. Heckels.** 2000. Interaction of primary human endometrial cells with *Neisseria gonorrhoeae* expressing green fluorescent protein. Mol. Microbiol. **35:**32-43.

43. **Ciechanover, A., A. L. Schwartz, A. Dautry-Varsat, and H. F. Lodish.** 1983. Kinetics of internalization and recycling of transferrin and the transferrin receptor in a human hepatoma cell line. Effect of lysosomotropic agents. J. Biol. Chem. **258:**9681-9689.

44. **Clemens, D. L., and M. A. Horwitz.** 1995. Characterization of the *Mycobacterium tuberculosis* phagosome and evidence that phagosomal maturation is inhibited. J. Exp. Med. **181:**257-270.

45. **Cohen, M. S., J. G. Cannon, A. E. Jerse, L. M. Charniga, S. F. Isbey, and L. G. Whicker.** 1994. Human experimentation with *Neisseria gonorrhoeae*: rationale, methods, and implications for the biology of infection and vaccine development. J. Infect. Dis. **169:**532-537.

46. **Cooper, J. A.** 1987. Effects of cytochalasin and phalloidin on actin. J. Cell. Biol. **105:**1473-1478.

47. **Corfield, A. P., N. Myerscough, R. Longman, P. Sylvester, S. Arul, and M. Pignatelli.** 2000. Mucins and mucosal protection in the gastrointestinal tract: new prospects for mucins in the pathology of gastrointestinal disease. Gut **47:**589-594.

48. **Cornelissen, C. N., G. D. Biswas, J. Tsai, D. K. Paruchuri, S. A. Thompson, and P. F. Sparling.** 1992. Gonococcal transferrin-binding protein 1 is required for transferrin utilization and is homologous to TonB-dependent outer membrane receptors. J. Bacteriol. **174:**5788-5797.

49. **Cornelissen, C. N., and P. F. Sparling.** 1994. Iron piracy: acquisition of transferrin-bound iron by bacterial pathogens. Mol. Microbiol. **14:**843-850.

50. **Cossart, P., and P. J. Sansonetti.** 2004. Bacterial invasion: the paradigms of enteroinvasive pathogens. Science **304:**242-248.

51. **Criss, A. K., and H. S. Seifert.** 2006. Gonococci exit apically and basally from polarized epithelial cells and exhibit dynamic changes in type-IV pili. Cell. Microbiol. **8:**1430-1443.

52. **Cucurull, E., and L. R. Espinoza.** 1998. Gonococcal arthritis. Rheum. Dis. Clin. North Am. **24:**305-322.

53. **Danaher, R. J., J. C. Levin, D. Arking, C. L. Burch, R. Sandlin, and D. C. Stein.** 1995. Genetic basis of *Neisseria gonorrhoeae* lipooligosaccharide antigenic variation. J. Bacteriol. **177:**7275-7279.

54. **Datta, S. R., A. Brunet, and M. E. Greenberg.** 1999. Cellular survival: a play in three Akts. Genes Dev. **13:**2905-2927.

55. **Dautry-Varsat, A., A. Ciechanover, and H. F. Lodish.** 1983. pH and the recycling of transferrin during receptor-mediated endocytosis. Proc. Natl. Acad. Sci. USA **80:**2258-2262.

56. **Davies, J., L. Gorini, and B. D. Davis.** 1965. Misreading of RNA codewords induced by aminoglycoside antibiotics. Mol. Pharmacol. **1:**93-106.

57. **Deghmane, A. E., M. Larribe, D. Giorgini, D. Sabino, and M. K. Taha.** 2003. Differential expression of genes that harbor a common regulatory element in *Neisseria meningitidis* upon contact with target cells. Infect. Immun. **71:**2897-2901.

58. **Deghmane, A. E., S. Petit, A. Topilko, Y. Pereira, D. Giorgini, M. Larribe, and M. K. Taha.** 2000. Intimate adhesion of *Neisseria meningitidis* to human epithelial cells is under the control of the *crgA* gene, a novel LysR-type transcriptional regulator. EMBO J. **19:**1068-1078.

59. **Dehio, C., E. Freissler, C. Lanz, O. G. Gomez-Duarte, G. David, and T. F. Meyer.** 1998. Ligation of cell surface heparan sulfate proteoglycans by antibody-coated beads stimulates phagocytic uptake into epithelial cells: a model for cellular invasion by *Neisseria gonorrhoeae*. Exp. Cell Res. **242:**528-539.

60. **Dehio, C., S. D. Gray-Owen, and T. F. Meyer.** 2000. Host cell invasion by pathogenic Neisseriae. Subcell. Biochem. **33:**61-96.

61. **Dehio, M., O. G. Gomez-Duarte, C. Dehio, and T. F. Meyer.** 1998. Vitronectin-dependent invasion of epithelial cells by *Neisseria gonorrhoeae* involves alpha-V integrin receptors. FEBS Lett. **424:**84-88.

62. **Draper, D. L., E. A. Donegan, J. F. James, R. L. Sweet, and G. F. Brooks.** 1980. In vitro modeling of acute salpingitis caused by *Neisseria gonorrhoeae.* Am. J. Obstet. Gynecol. **138:**996-1002.

63. **Draper, D. L., E. A. Donegan, J. F. James, R. L. Sweet, and G. F. Brooks.** 1980. Scanning electron microscopy of attachment of *Neisseria gonorrhoeae*

colony phenotypes to surfaces of human genital epithelia. Am. J. Obstet. Gynecol. **138:**818-826.

64. **Drickamer, K.** 1988. Two distinct classes of carbohydrate-recognition domains in animal lectins. J. Biol. Chem. **263:**9557-9560.

65. **Du, Y., and C. G. Arvidson.** 2006. RpoH mediates the expression of some, but not all, genes induced in *Neisseria gonorrhoeae* adherent to epithelial cells. Infect. Immun. **74:**2767-2776.

66. **Duensing, T. D., and J. P. van Putten.** 1997. Vitronectin mediates internalization of *Neisseria gonorrhoeae* by Chinese hamster ovary cells. Infect. Immun. **65:**964-970.

67. **Duensing, T. D., J. S. Wing, and J. P. van Putten.** 1999. Sulfated polysaccharide-directed recruitment of mammalian host proteins: a novel strategy in microbial pathogenesis. Infect. Immun. **67:**4463-4468.

68. **Edwards, J. L., and M. A. Apicella.** 2005. I-domain-containing integrins serve as pilus receptors for *Neisseria gonorrhoeae* adherence to human epithelial cells. Cell. Microbiol. **7:**1197-1211.

69. **Edwards, J. L., and M. A. Apicella.** 2004. The molecular mechanisms used by *Neisseria gonorrhoeae* to initiate infection differ between men and women. Clin. Microbiol. Rev. **17:**965-981.

70. **Edwards, J. L., and M. A. Apicella.** 2006. *Neisseria gonorrhoeae* PLD directly interacts with Akt kinase upon infection of primary, human, cervical epithelial cells. Cell. Microbiol. **8:**1253-1271.

71. **Edwards, J. L., and M. A. Apicella.** 2002. The role of lipooligosaccharide in *Neisseria gonorrhoeae* pathogenesis of cervical epithelia: lipid A serves as a C3 acceptor molecule. Cell. Microbiol. **4:**585-598.

72. **Edwards, J. L., E. J. Brown, S. Uk-Nham, J. G. Cannon, M. S. Blake, and M. A. Apicella.** 2002. A co-operative interaction between *Neisseria gonorrhoeae* and complement receptor 3 mediates infection of primary cervical epithelial cells. Cell. Microbiol. **4:**571-584.

73. **Edwards, J. L., J. Q. Shao, K. A. Ault, and M. A. Apicella.** 2000. *Neisseria gonorrhoeae* elicits membrane ruffling and cytoskeletal rearrangements upon infection of primary human endocervical and ectocervical cells. Infect. Immun. **68:**5354-5363.

74. **Eitel, J., T. Heise, U. Thiesen, and P. Dersch.** 2005. Cell invasion and IL-8 production pathways initiated by YadA of *Yersinia pseudotuberculosis* require

common signaling molecules (FAK, c-Src, Ras) and distinct cell factors. Cell. Microbiol. **7:**63-77.

75. **Ellington, J. K., A. Elhofy, K. L. Bost, and M. C. Hudson.** 2001. Involvement of mitogen-activated protein kinase pathways in *Staphylococcus aureus* invasion of normal osteoblasts. Infect. Immun. **69:**5235-5242.

76. **Engel, J., H. Fasold, F. W. Hulla, F. Waechter, and A. Wegner.** 1977. The polymerization reaction of muscle actin. Mol. Cell. Biochem. **18:**3-13.

77. **Evans, D. J., I. A. Maltseva, J. Wu, and S. M. Fleiszig.** 2002. *Pseudomonas aeruginosa* internalization by corneal epithelial cells involves MEK and ERK signal transduction proteins. FEMS Microbiol. Lett. **213:**73-79.

78. **Fichorova, R. N., P. J. Desai, F. C. Gibson, 3rd, and C. A. Genco.** 2001. Distinct proinflammatory host responses to *Neisseria gonorrhoeae* infection in immortalized human cervical and vaginal epithelial cells. Infect. Immun. **69:**5840-5848.

79. **Finlay, B. B., and P. Cossart.** 1997. Exploitation of mammalian host cell functions by bacterial pathogens. Science **276:**718-725.

80. **Fisette, P. L., S. Ram, J. M. Andersen, W. Guo, and R. R. Ingalls.** 2003. The Lip lipoprotein from *Neisseria gonorrhoeae* stimulates cytokine release and NF-kappaB activation in epithelial cells in a Toll-like receptor 2-dependent manner. J. Biol. Chem. **278:**46252-46260.

81. **Freissler, E., A. Meyer auf der Heyde, G. David, T. F. Meyer, and C. Dehio.** 2000. Syndecan-1 and syndecan-4 can mediate the invasion of Opa_{HSPG}-expressing *Neisseria gonorrhoeae* into epithelial cells. Cell. Microbiol. **2:**69-82.

82. **Garcia-del Portillo, F., and B. B. Finlay.** 1994. *Salmonella* invasion of nonphagocytic cells induces formation of macropinosomes in the host cell. Infect. Immun. **62:**4641-4645.

83. **Geoffroy, M. C., S. Floquet, A. Metais, X. Nassif, and V. Pelicic.** 2003. Large-scale analysis of the meningococcus genome by gene disruption: resistance to complement-mediated lysis. Genome Res. **13:**391-398.

84. **Giardina, P. C., R. Williams, D. Lubaroff, and M. A. Apicella.** 1998. *Neisseria gonorrhoeae* induces focal polymerization of actin in primary human urethral epithelium. Infect. Immun. **66:**3416-3419.

85. **Gibson, B. W., J. W. Webb, R. Yamasaki, S. J. Fisher, A. L. Burlingame, R. E. Mandrell, H. Schneider, and J. M. Griffiss.** 1989. Structure and

heterogeneity of the oligosaccharides from the lipopolysaccharides of a pyocin-resistant *Neisseria gonorrhoeae.* Proc. Natl. Acad. Sci .USA **86:**17-21.

86. **Gill, D. B., D. Spitzer, M. Koomey, J. E. Heuser, and J. P. Atkinson.** 2005. Release of host-derived membrane vesicles following pilus-mediated adhesion of *Neisseria gonorrhoeae*. Cell. Microbiol. **7:**1672-1683.

87. **Girardin, S. E., I. G. Boneca, L. A. Carneiro, A. Antignac, M. Jehanno, J. Viala, K. Tedin, M. K. Taha, A. Labigne, U. Zahringer, A. J. Coyle, P. S. DiStefano, J. Bertin, P. J. Sansonetti, and D. J. Philpott.** 2003. Nod1 detects a unique muropeptide from gram-negative bacterial peptidoglycan. Science **300:**1584-1587.

88. **Goetz, M., A. Bubert, G. Wang, I. Chico-Calero, J. A. Vazquez-Boland, M. Beck, J. Slaghuis, A. A. Szalay, and W. Goebel.** 2001. Microinjection and growth of bacteria in the cytosol of mammalian host cells. Proc. Natl. Acad. Sci. USA **98:**12221-12226.

89. **Gomez-Duarte, O. G., M. Dehio, C. A. Guzman, G. S. Chhatwal, C. Dehio, and T. F. Meyer.** 1997. Binding of vitronectin to Opa-expressing *Neisseria gonorrhoeae* mediates invasion of HeLa cells. Infect. Immun. **65:**3857-3866.

90. **Goncharova, E. A., A. V. Vorotnikov, E. O. Gracheva, C. L. Wang, R. A. Panettieri, Jr., V. V. Stepanova, and V. A. Tkachuk.** 2002. Activation of p38 MAP-kinase and caldesmon phosphorylation are essential for urokinase-induced human smooth muscle cell migration. Biol. Chem. **383:**115-126.

91. **Gorby, G. L., E. N. Robinson, Jr., L. R. Barley, C. M. Clemens, and Z. A. McGee.** 1988. Microbial invasion: a covert activity? Can. J. Microbiol. **34:**507-512.

92. **Gotschlich, E. C.** 1994. Genetic locus for the biosynthesis of the variable portion of *Neisseria gonorrhoeae* lipooligosaccharide. J. Exp. Med. **180:**2181-2190.

93. **Grassme, H., E. Gulbins, B. Brenner, K. Ferlinz, K. Sandhoff, K. Harzer, F. Lang, and T. F. Meyer.** 1997. Acidic sphingomyelinase mediates entry of *N. gonorrhoeae* into nonphagocytic cells. Cell **91:**605-615.

94. **Grassme, H. U., R. M. Ireland, and J. P. van Putten.** 1996. Gonococcal opacity protein promotes bacterial entry-associated rearrangements of the epithelial cell actin cytoskeleton. Infect. Immun. **64:**1621-1630.

95. **Gray-Owen, S. D., C. Dehio, A. Haude, F. Grunert, and T. F. Meyer.** 1997. CD66 carcinoembryonic antigens mediate interactions between Opa-expressing *Neisseria gonorrhoeae* and human polymorphonuclear phagocytes. EMBO J. **16:**3435-3445.

96. **Grifantini, R., E. Bartolini, A. Muzzi, M. Draghi, E. Frigimelica, J. Berger, F. Randazzo, and G. Grandi.** 2002. Gene expression profile in *Neisseria meningitidis* and *Neisseria lactamica* upon host-cell contact: from basic research to vaccine development. Ann. N. Y. Acad. Sci. **975:**202-216.

97. **Grifantini, R., E. Bartolini, A. Muzzi, M. Draghi, E. Frigimelica, J. Berger, G. Ratti, R. Petracca, G. Galli, M. Agnusdei, M. M. Giuliani, L. Santini, B. Brunelli, H. Tettelin, R. Rappuoli, F. Randazzo, and G. Grandi.** 2002. Previously unrecognized vaccine candidates against group B meningococcus identified by DNA microarrays. Nat. Biotechnol. **20:**914-921.

98. **Griffiss, J. M., C. J. Lammel, J. Wang, N. P. Dekker, and G. F. Brooks.** 1999. *Neisseria gonorrhoeae* coordinately uses pili and Opa to activate HEC-1-B cell microvilli, which causes engulfment of the gonococci. Infect. Immun. **67:**3469-3480.

99. **Griffiss, J. M., H. Schneider, R. E. Mandrell, R. Yamasaki, G. A. Jarvis, J. J. Kim, B. W. Gibson, R. Hamadeh, and M. A. Apicella.** 1988. Lipooligosaccharides: the principal glycolipids of the neisserial outer membrane. Rev. Infect. Dis. **10:**S287-S295.

100. **Gruenberg, J., and F. R. Maxfield.** 1995. Membrane transport in the endocytic pathway. Curr. Opin. Cell. Biol. **7:**552-563.

101. **Grundhofer, P., R. Niemetz, G. Schilling, and G. G. Gross.** 2001. Biosynthesis and subcellular distribution of hydrolyzable tannins. Phytochemistry **57:**915-927.

102. **Guay, J., H. Lambert, G. Gingras-Breton, J. N. Lavoie, J. Huot, and J. Landry.** 1997. Regulation of actin filament dynamics by p38 MAP kinase-mediated phosphorylation of heat shock protein 27. J. Cell Sci. **110:**357-368.

103. **Gunn, J. S., and D. C. Stein.** 1996. Use of a non-selective transformation technique to construct a multiply restriction/modification-deficient mutant of *Neisseria gonorrhoeae.* Mol. Gen. Genet. **251:**509-517.

104. **Hagen, T. A., and C. N. Cornelissen.** 2006. *Neisseria gonorrhoeae* requires expression of TonB and the putative transporter TdfF to replicate within cervical epithelial cells. Mol. Microbiol. **62:**1144-1157.

105. **Hardt, W. D., L. M. Chen, K. E. Schuebel, X. R. Bustelo, and J. E. Galan.** 1998. *S. typhimurium* encodes an activator of Rho GTPases that induces membrane ruffling and nuclear responses in host cells. Cell **93:**815-826.

106. **Harvey, H. A., M. P. Jennings, C. A. Campbell, R. Williams, and M. A. Apicella.** 2001. Receptor-mediated endocytosis of *Neisseria gonorrhoeae* into

primary human urethral epithelial cells: the role of the asialoglycoprotein receptor. Mol. Microbiol. **42:**659-672.

107. **Harvey, H. A., M. R. Ketterer, A. Preston, D. Lubaroff, R. Williams, and M. A. Apicella.** 1997. Ultrastructural analysis of primary human urethral epithelial cell cultures infected with *Neisseria gonorrhoeae*. Infect. Immun. **65:**2420-2427.

108. **Harvey, H. A., D. M. Post, and M. A. Apicella.** 2002. Immortalization of human urethral epithelial cells: a model for the study of the pathogenesis of and the inflammatory cytokine response to *Neisseria gonorrhoeae* infection. Infect. Immun. **70:**5808-5815.

109. **Hassett, D. J., and M. S. Cohen.** 1989. Bacterial adaptation to oxidative stress: implications for pathogenesis and interaction with phagocytic cells. FASEB J. **3:**2574-2582.

110. **Hauck, C. R., H. Grassme, J. Bock, V. Jendrossek, K. Ferlinz, T. F. Meyer, and E. Gulbins.** 2000. Acid sphingomyelinase is involved in CEACAM receptor-mediated phagocytosis of *Neisseria gonorrhoeae*. FEBS Lett. **478:**260-266.

111. **Hauck, C. R., and T. F. Meyer.** 1997. The lysosomal/phagosomal membrane protein h-LAMP-1 is a target of the IgA1 protease of *Neisseria gonorrhoeae*. FEBS Lett **405:**86-90.

112. **Hauck, C. R., and T. F. Meyer.** 2003. 'Small' talk: Opa proteins as mediators of *Neisseria*-host-cell communication. Curr. Opin. Microbiol. **6:**43-49.

113. **Hauck, C. R., T. F. Meyer, F. Lang, and E. Gulbins.** 1998. CD66-mediated phagocytosis of Opa^{52} *Neisseria gonorrhoeae* requires a Src-like tyrosine kinase- and Rac1-dependent signaling pathway. EMBO J. **17:**443-454.

114. **Hayward, R. D., and V. Koronakis.** 1999. Direct nucleation and bundling of actin by the SipC protein of invasive *Salmonella*. EMBO J. **18:**4926-4934.

115. **Hedges, S. R., M. S. Mayo, J. Mestecky, E. W. Hook, 3rd, and M. W. Russell.** 1999. Limited local and systemic antibody responses to *Neisseria gonorrhoeae* during uncomplicated genital infections. Infect. Immun. **67:**3937-3946.

116. **Hernandez, L. D., K. Hueffer, M. R. Wenk, and J. E. Galan.** 2004. *Salmonella* modulates vesicular traffic by altering phosphoinositide metabolism. Science **304:**1805-1807.

117. **Higashi, D. L., S. W. Lee, A. Snyder, N. J. Weyand, A. Bakke, and M. So.** 2007. Dynamics of *N. gonorrhoeae* attachment: microcolony development, cortical plaque formation and cytoprotection. Infect. Immun. **75:**4743-4753.

118. **Hitchcock, P. J., and T. M. Brown.** 1983. Morphological heterogeneity among *Salmonella* lipopolysaccharide chemotypes in silver-stained polyacrylamide gels. J. Bacteriol. **154:**269-277.

119. **Hook III, E. W., and H. H. Handsfield.** 1999. Gonococcal infections in the adult, p. 433-466. *In* P. A. M. K.K. Holmes, P.F. Sparling, P. Wiesner (ed.), Sexual Transmitted Diseases. McGraw-Hill, New York, NY.

120. **Hopper, S., J. S. Wilbur, B. L. Vasquez, J. Larson, S. Clary, I. J. Mehr, H. S. Seifert, and M. So.** 2000. Isolation of *Neisseria gonorrhoeae* mutants that show enhanced trafficking across polarized T84 epithelial monolayers. Infect. Immun. **68:**896-905.

121. **Hornef, M. W., M. J. Wick, M. Rhen, and S. Normark.** 2002. Bacterial strategies for overcoming host innate and adaptive immune responses. Nat. Immunol. **3:**1033-1040.

122. **Householder, T. C., E. M. Fozo, J. A. Cardinale, and V. L. Clark.** 2000. Gonococcal nitric oxide reductase is encoded by a single gene, *norB*, which is required for anaerobic growth and is induced by nitric oxide. Infect. Immun. **68:**5241-5246.

123. **Howie, H. L., M. Glogauer, and M. So.** 2005. The *N. gonorrhoeae* type-IV pilus stimulates mechanosensitive pathways and cytoprotection through a pilT-dependent mechanism. PLoS Biol. **3:**e100.

124. **Hu, L., J. P. McDaniel, and D. J. Kopecko.** 2006. Signal transduction events involved in human epithelial cell invasion by *Campylobacter jejuni* 81-176. Microb. Pathog. **40:**91-100.

125. **Huang, C., C. H. Borchers, M. D. Schaller, and K. Jacobson.** 2004. Phosphorylation of paxillin by p38 MAPK is involved in the neurite extension of PC-12 cells. J. Cell Biol. **164:**593-602.

126. **Huang, C., K. Jacobson, and M. D. Schaller.** 2004. MAP kinases and cell migration. J. Cell Sci. **117:**4619-4628.

127. **Huang, C., Z. Rajfur, C. Borchers, M. D. Schaller, and K. Jacobson.** 2003. JNK phosphorylates paxillin and regulates cell migration. Nature **424:**219-223.

128. **Hubbard, S. R., and J. H. Till.** 2000. Protein tyrosine kinase structure and function. Annu. Rev. Biochem. **69:**373-398.

129. **Igietseme, J. U., I. M. Uriri, M. Chow, E. Abe, and R. G. Rank.** 1997. Inhibition of intracellular multiplication of human strains of *Chlamydia trachomatis* by nitric oxide. Biochem. Biophys. Res. Commun. **232:**595-601.

130. **Imlay, J. A., and S. Linn.** 1988. DNA damage and oxygen radical toxicity. Science **240:**1302-1309.

131. **Inohara, N., and G. Nunez.** 2001. The NOD: a signaling module that regulates apoptosis and host defense against pathogens. Oncogene **20:**6473-6481.

132. **Isberg, R. R., and S. Falkow.** 1985. A single genetic locus encoded by *Yersinia pseudotuberculosis* permits invasion of cultured animal cells by *Escherichia coli* K-12. Nature **317:**262-264.

133. **Ison, C. A.** 1990. Laboratory methods in genitourinary medicine. Methods of diagnosing gonorrhea. Genitourin. Med. **66:**453-459.

134. **Janeway, C. A., Jr., and R. Medzhitov.** 2002. Innate immune recognition. Annu. Rev. Immunol. **20:**197-216.

135. **Jarvis, G. A., J. Li, and V. S. K.** 1999. Invasion of human mucosal epithelial cells by *Neisseria gonorrhoeae* upregulates expression of intercellular adhesion molecule 1 (ICAM-1). Infect Immun. **67:**1149-1156.

136. **Jasper, H., V. Benes, C. Schwager, S. Sauer, S. Clauder-Munster, W. Ansorge, and D. Bohmann.** 2001. The genomic response of the *Drosophila* embryo to JNK signaling. Dev. Cell. **1:**579-586.

137. **Jerse, A. E.** 1999. Experimental gonococcal genital tract infection and opacity protein expression in estradiol-treated mice. Infect. Immun. **67:**5699-5708.

138. **Jerse, A. E., M. S. Cohen, P. M. Drown, L. G. Whicker, S. F. Isbey, H. S. Seifert, and J. G. Cannon.** 1994. Multiple gonococcal opacity proteins are expressed during experimental urethral infection in the male. J. Exp. Med. **179:**911-920.

139. **Joh, D., E. R. Wann, B. Kreikemeyer, P. Speziale, and M. Hook.** 1999. Role of fibronectin-binding MSCRAMMs in bacterial adherence and entry into mammalian cells. Matrix Biol. **18:**211-223.

140. **Johannsen, D. B., D. M. Johnston, H. O. Koymen, M. S. Cohen, and J. G. Cannon.** 1999. A *Neisseria gonorrhoeae* immunoglobulin A1 protease mutant is infectious in the human challenge model of urethral infection. Infect. Immun. **67:**3009-3013.

141. **John, C. M., G. A. Jarvis, K. V. Swanson, H. Leffler, M. D. Cooper, M. E. Huflejt, and J. M. Griffiss.** 2002. Galectin-3 binds lactosaminylated lipooligosaccharides from *Neisseria gonorrhoeae* and is selectively expressed by mucosal epithelial cells that are infected. Cell. Microbiol. **4:**649-662.

142. **John, C. M., H. Schneider, and J. M. Griffiss.** 1999. *Neisseria gonorrhoeae* that infect men have lipooligosaccharides with terminal N-acetyllactosamine repeats. J. Biol. Chem. **274:**1017-1025.

143. **Johnston, K. H., K. K. Holmes, and E. C. Gotschlich.** 1976. The serological classification of *Neisseria gonorrhoeae*. I. Isolation of the outer membrane complex responsible for serotypic specificity. J. Exp. Med. **143:**741-758.

144. **Jonsson, A. B., D. Ilver, P. Falk, J. Pepose, and S. Normark.** 1994. Sequence changes in the pilus subunit lead to tropism variation of *Neisseria gonorrhoeae* to human tissue. Mol. Microbiol. **13:**403-416.

145. **Judd, R. C.** 1989. Protein I: structure, function, and genetics. Clin. Microbiol. Rev. **2 Suppl:**S41-S48.

146. **Kallstrom, H., M. S. Islam, P. O. Berggren, and A. B. Jonsson.** 1998. Cell signaling by the type-IV pili of pathogenic *Neisseria*. J. Biol. Chem. **273:**21777-21782.

147. **Kallstrom, H., M. K. Liszewski, J. P. Atkinson, and A. B. Jonsson.** 1997. Membrane cofactor protein (MCP or CD46) is a cellular pilus receptor for pathogenic *Neisseria*. Mol. Microbiol. **25:**639-647.

148. **Kaul, R., S. L. Rowland-Jones, G. Gillespie, J. Kimani, T. Dong, P. Kiama, J. N. Simonsen, J. J. Bwayo, A. J. McMichael, and F. A. Plummer.** 2002. Gonococcal cervicitis is associated with reduced systemic CD8+ T cell responses in human immunodeficiency virus type 1-infected and exposed, uninfected sex workers. J. Infect. Dis. **185:**1525-1529.

149. **Keilhack, H., T. Tenev, E. Nyakatura, J. Godovac-Zimmermann, L. Nielsen, K. Seedorf, and F. D. Bohmer.** 1998. Phosphotyrosine 1173 mediates binding of the protein-tyrosine phosphatase SHP-1 to the epidermal growth factor receptor and attenuation of receptor signaling. J. Biol. Chem. **273:**24839-24846.

150. **Kenny, B., R. DeVinney, M. Stein, D. J. Reinscheid, E. A. Frey, and B. B. Finlay.** 1997. Enteropathogenic *E. coli* (EPEC) transfers its receptor for intimate adherence into mammalian cells. Cell **91:**511-520.

151. **Kim, J. M., H. Y. Jung, J. Y. Lee, J. Youn, C. H. Lee, and K. H. Kim.** 2005. Mitogen-activated protein kinase and activator protein-1 dependent signals are essential for *Bacteroides fragilis* enterotoxin-induced enteritis. Eur. J. Immunol. **35:**2648-2657.

152. **Kirchner, M., D. Heuer, and T. F. Meyer.** 2005. CD46-independent binding of neisserial type-IV pili and the major pilus adhesin, PilC, to human epithelial cells. Infect. Immun. **73:**3072-3082.

153. **Kirchner, M., and T. F. Meyer.** 2005. The PilC adhesin of the *Neisseria* type-IV pilus-binding specificities and new insights into the nature of the host cell receptor. Mol. Microbiol. **56:**945-957.

154. **Klauser, T., J. Pohlner, and T. F. Meyer.** 1990. Extracellular transport of cholera toxin B subunit using *Neisseria* IgA protease beta-domain: conformation-dependent outer membrane translocation. EMBO J. **9:**1991-1999.

155. **Klemke, R. L., S. Cai, A. L. Giannini, P. J. Gallagher, P. de Lanerolle, and D. A. Cheresh.** 1997. Regulation of cell motility by mitogen-activated protein kinase. J. Cell Biol. **137:**481-492.

156. **Knapp, J. S., and V. L. Clark.** 1984. Anaerobic growth of *Neisseria gonorrhoeae* coupled to nitrite reduction. Infect. Immun. **46:**176-181.

157. **Kohler, H., S. P. Rodrigues, and B. A. McCormick.** 2002. *Shigella flexneri* interactions with the basolateral membrane domain of polarized model intestinal epithelium: role of lipopolysaccharide in cell invasion and in activation of the mitogen-activated protein kinase ERK. Infect. Immun. **70:**1150-1158.

158. **Konkel, M. E., S. F. Hayes, L. A. Joens, and W. Cieplak, Jr.** 1992. Characteristics of the internalization and intracellular survival of *Campylobacter jejuni* in human epithelial cell cultures. Microb. Pathog. **13:**357-370.

159. **Ku, H., and K. E. Meier.** 2000. Phosphorylation of paxillin via the ERK mitogen-activated protein kinase cascade in EL4 thymoma cells. J. Biol. Chem. **275:**11333-11340.

160. **Kuhlewein, C., C. Rechner, T. F. Meyer, and T. Rudel.** 2006. Low-phosphate-dependent invasion resembles a general way for *Neisseria gonorrhoeae* to enter host cells. Infect. Immun. **74:**4266-4273.

161. **Kundu, A. K., M. Nagaoka, E. H. Chowdhury, S. Hirose, T. Sasagawa, and T. Akaike.** 2003. IGF-1 induces growth, survival and morphological change of primary hepatocytes on a galactose-bared polymer through both MAPK and beta-catenin pathways. Cell. Struct. Funct. **28:**255-263.

162. **Kupsch, E. M., B. Knepper, T. Kuroki, I. Heuer, and T. F. Meyer.** 1993. Variable opacity (Opa) outer membrane proteins account for the cell tropisms displayed by *Neisseria gonorrhoeae* for human leukocytes and epithelial cells. EMBO J. **12:**641-650.

163. **Lattemann, C. T., J. Maurer, E. Gerland, and T. F. Meyer.** 2000. Autodisplay: functional display of active beta-lactamase on the surface of *Escherichia coli* by the AIDA-I autotransporter. J. Bacteriol. **182:**3726-3733.

164. **Lee, B. C., and A. B. Schryvers.** 1988. Specificity of the lactoferrin and transferrin receptors in *Neisseria gonorrhoeae*. Mol. Microbiol. **2:**827-829.

165. **Lee, R. T.** 1991. Ligand structural requirements for recognition and binding by the hepatic asialoglycoprotein receptor. Targeted Diagn. Ther. **4:**65-86.

166. **Lee, S. W., R. A. Bonnah, D. L. Higashi, J. P. Atkinson, S. L. Milgram, and M. So.** 2002. CD46 is phosphorylated at tyrosine 354 upon infection of epithelial cells by *Neisseria gonorrhoeae*. J. Cell. Biol. **156:**951-957.

167. **Lee, S. W., D. L. Higashi, A. Snyder, A. J. Merz, L. Potter, and M. So.** 2005. PilT is required for PI(3,4,5)P3-mediated crosstalk between *Neisseria gonorrhoeae* and epithelial cells. Cell. Microbiol. **7:**1271-1284.

168. **Leuzzi, R., L. Serino, M. Scarselli, S. Savino, M. R. Fontana, E. Monaci, A. Taddei, G. Fischer, R. Rappuoli, and M. Pizza.** 2005. Ng-MIP, a surface-exposed lipoprotein of *Neisseria gonorrhoeae*, has a peptidyl-prolyl cis/trans isomerase (PPIase) activity and is involved in persistence in macrophages. Mol. Microbiol. **58:**669-681.

169. **Levine, W. C., V. Pope, A. Bhoomkar, P. Tambe, J. S. Lewis, A. A. Zaidi, C. E. Farshy, S. Mitchell, and D. F. Talkington.** 1998. Increase in endocervical CD4 lymphocytes among women with nonulcerative sexually transmitted diseases. J. Infect. Dis. **177:**167-174.

170. **Li, C. K., R. Seth, T. Gray, R. Bayston, Y. R. Mahida, and D. Wakelin.** 1998. Production of proinflammatory cytokines and inflammatory mediators in human intestinal epithelial cells after invasion by *Trichinella spiralis*. Infect. Immun. **66:**2200-2206.

171. **Lievin-Le Moal, V., and A. L. Servin.** 2006. The front line of enteric host defense against unwelcome intrusion of harmful microorganisms: mucins, antimicrobial peptides, and microbiota. Clin. Microbiol. Rev. **19:**315-337.

172. **Lin, J. S., S. P. Donegan, T. C. Heeren, M. Greenberg, E. E. Flaherty, R. Haivanis, X. H. Su, D. Dean, W. J. Newhall, J. S. Knapp, S. K. Sarafian, R. J. Rice, S. A. Morse, and P. A. Rice.** 1998. Transmission of *Chlamydia trachomatis* and *Neisseria gonorrhoeae* among men with urethritis and their female sex partners. J. Infect. Dis. **178:**1707-1712.

173. **Lin, L., P. Ayala, J. Larson, M. Mulks, M. Fukuda, S. R. Carlsson, C. Enns, and M. So.** 1997. The *Neisseria* type 2 IgA1 protease cleaves LAMP-1 and

promotes survival of bacteria within epithelial cells. Mol. Microbiol. **24:**1083-1094.

174. **Liu, J., and A. Lin.** 2005. Role of JNK activation in apoptosis: a double-edged sword. Cell Res. **15:**36-42.

175. **Lorenzen, D. R., D. Gunther, J. Pandit, T. Rudel, E. Brandt, and T. F. Meyer.** 2000. *Neisseria gonorrhoeae* porin modifies the oxidative burst of human professional phagocytes. Infect. Immun. **68:**6215-6222.

176. **Makino, S., J. P. van Putten, and T. F. Meyer.** 1991. Phase variation of the opacity outer membrane protein controls invasion by *Neisseria gonorrhoeae* into human epithelial cells. EMBO J. **10:**1307-1315.

177. **Martini, F. H.** 2001. The Tissue Level of Organization, p. 106-117, Fundamentals of Anatomy and Physiology, 5th ed, vol. Chapter 4. Benjamin Cummings.

178. **Maurer, J., J. Jose, and T. F. Meyer.** 1997. Autodisplay: one-component system for efficient surface display and release of soluble recombinant proteins from *Escherichia coli*. J. Bacteriol. **179:**794-804.

179. **McCaw, S. E., E. H. Liao, and S. D. Gray-Owen.** 2004. Engulfment of *Neisseria gonorrhoeae*: revealing distinct processes of bacterial entry by individual carcinoembryonic antigen-related cellular adhesion molecule family receptors. Infect. Immun. **72:**2742-2752.

180. **McCaw, S. E., J. Schneider, E. H. Liao, W. Zimmermann, and S. D. Gray-Owen.** 2003. Immunoreceptor tyrosine-based activation motif phosphorylation during engulfment of *Neisseria gonorrhoeae* by the neutrophil-restricted CEACAM3 (CD66d) receptor. Mol. Microbiol. **49:**623-637.

181. **McGee, Z. A., A. P. Johnson, and D. Taylor-Robinson.** 1981. Pathogenic mechanisms of *Neisseria gonorrhoeae*: observations on damage to human fallopian tubes in organ culture by gonococci of colony type 1 or type 4. J. Infect. Dis. **143:**413-422.

182. **McGee, Z. A., D. S. Stephens, L. H. Hoffman, W. F. Schlech, 3rd, and R. G. Horn.** 1983. Mechanisms of mucosal invasion by pathogenic *Neisseria.* Rev. Infect. Dis. **5 Suppl 4:**S708-S714.

183. **McKenna, W. R., P. A. Mickelsen, P. F. Sparling, and D. W. Dyer.** 1988. Iron uptake from lactoferrin and transferrin by *Neisseria gonorrhoeae*. Infect. Immun. **56:**785-791.

184. **Mellies, J., J. Jose, and T. F. Meyer.** 1997. The *Neisseria gonorrhoeae* gene *aniA* encodes an inducible nitrite reductase. Mol. Gen. Genet. **256:**525-532.

185. **Merz, A. J., C. A. Enns, and M. So.** 1999. Type-IV pili of pathogenic Neisseriae elicit cortical plaque formation in epithelial cells. Mol. Microbiol. **32:**1316-1332.

186. **Merz, A. J., D. B. Rifenbery, C. G. Arvidson, and M. So.** 1996. Traversal of a polarized epithelium by pathogenic Neisseriae: facilitation by type-IV pili and maintenance of epithelial barrier function. Mol. Med. **2:**745-754.

187. **Merz, A. J., and M. So.** 1997. Attachment of piliated, Opa^- and Opc^- gonococci and meningococci to epithelial cells elicits cortical actin rearrangements and clustering of tyrosine-phosphorylated proteins. Infect. Immun. **65:**4341-4349.

188. **Merz, A. J., and M. So.** 2000. Interactions of pathogenic Neisseriae with epithelial cell membranes. Annu. Rev. Cell Dev. Biol. **16:**423-457.

189. **Merz, A. J., M. So, and M. P. Sheetz.** 2000. Pilus retraction powers bacterial twitching motility. Nature **407:**98-102.

190. **Meyer, T. F.** 1991. Evasion mechanisms of pathogenic Neisseriae. Behring Inst. Mitt. **88:**194-199.

191. **Meyer, T. F.** 1999. Pathogenic Neisseriae: complexity of pathogen-host cell interplay. Clin. Infect. Dis. **28:**433-441.

192. **Meyer, T. F.** 1998. Pathogenic *Neisseria*--interplay between pro- and eukaryotic worlds. Folia Microbiol. (Praha) **43:**311-319.

193. **Meyer, T. F., E. Billyard, R. Haas, S. Storzbach, and M. So.** 1984. Pilus genes of *Neisseria gonorrhoeae*: chromosomal organization and DNA sequence. Proc. Natl. Acad. Sci. USA **81:**6110-6114.

194. **Meyer, T. F., N. Mlawer, and M. So.** 1982. Pilus expression in *Neisseria gonorrhoeae* involves chromosomal rearrangement. Cell **30:**45-52.

195. **Meyer, T. F., and J. P. van Putten.** 1989. Genetic mechanisms and biological implications of phase variation in pathogenic Neisseriae. Clin. Microbiol. Rev. **2 Suppl:**S139-S145.

196. **Minor, S. Y., A. Banerjee, and E. C. Gotschlich.** 2000. Effect of alpha-oligosaccharide phenotype of *Neisseria gonorrhoeae* strain MS11 on invasion of Chang conjunctival, HEC-1-B endometrial, and ME-180 cervical cells. Infect. Immun. **68:**6526-6534.

197. **Mitchell, J. A., M. J. Paul-Clark, G. W. Clarke, S. K. McMaster, and N. Cartwright.** 2007. Critical role of toll-like receptors and nucleotide oligomerisation domain in the regulation of health and disease. J. Endocrinol. **193:**323-330.

198. **Mitsuno, Y., H. Yoshida, S. Maeda, K. Ogura, Y. Hirata, T. Kawabe, Y. Shiratori, and M. Omata.** 2001. *Helicobacter pylori* induced transactivation of SRE and AP-1 through the ERK signaling pathway in gastric cancer cells. Gut **49:**18-22.

199. **Morales, P., P. Reyes, M. Vargas, M. Rios, M. Imarai, H. Cardenas, H. Croxatto, P. Orihuela, R. Vargas, J. Fuhrer, J. E. Heckels, M. Christodoulides, and L. Velasquez.** 2006. Infection of human fallopian tube epithelial cells with *Neisseria gonorrhoeae* protects cells from tumor necrosis factor alpha-induced apoptosis. Infect. Immun. **74:**3643-3650.

200. **Morelle, S., E. Carbonnelle, and X. Nassif.** 2003. The REP2 repeats of the genome of *Neisseria meningitidis* are associated with genes coordinately regulated during bacterial cell interaction. J. Bacteriol. **185:**2618-2627.

201. **Morris, J. F., and D. V. Pow.** 1988. Capturing and quantifying the exocytotic event. J. Exp. Biol. **139:**81-103.

202. **Morse, S. A.** 1978. The biology of the gonococcus. CRC Crit. Rev. Microbiol. **7:**93-189.

203. **Mosleh, I. M., H. J. Boxberger, M. J. Sessler, and T. F. Meyer.** 1997. Experimental infection of native human ureteral tissue with *Neisseria gonorrhoeae*: adhesion, invasion, intracellular fate, exocytosis, and passage through a stratified epithelium. Infect. Immun. **65:**3391-3398.

204. **Muenzner, P., O. Billker, T. F. Meyer, and M. Naumann.** 2002. Nuclear factor-kappa B directs carcinoembryonic antigen-related cellular adhesion molecule 1 receptor expression in *Neisseria gonorrhoeae*-infected epithelial cells. J. Biol. Chem. **277:**7438-7446.

205. **Muenzner, P., M. Naumann, T. F. Meyer, and S. D. Gray-Owen.** 2001. Pathogenic *Neisseria* trigger expression of their carcinoembryonic antigen-related cellular adhesion molecule 1 (CEACAM1; previously CD66a) receptor on primary endothelial cells by activating the immediate early response transcription factor, nuclear factor-kappaB. J. Biol. Chem. **276:**24331-24340.

206. **Muller, A., D. Gunther, F. Dux, M. Naumann, T. F. Meyer, and T. Rudel.** 1999. Neisserial porin (PorB) causes rapid calcium influx in target cells and induces apoptosis by the activation of cysteine proteases. EMBO J. **18:**339-352.

207. **Nakagawa, I., A. Amano, N. Mizushima, A. Yamamoto, H. Yamaguchi, T. Kamimoto, A. Nara, J. Funao, M. Nakata, K. Tsuda, S. Hamada, and T. Yoshimori.** 2004. Autophagy defends cells against invading group A *Streptococcus*. Science **306:**1037-1040.

208. **Nakashima, S.** 2002. Protein kinase C alpha (PKC alpha): regulation and biological function. J. Biochem. (Tokyo) **132:**669-675.

209. **Naumann, M., T. Rudel, and T. F. Meyer.** 1999. Host cell interactions and signaling with *Neisseria gonorrhoeae*. Curr. Opin. Microbiol. **2:**62-70.

210. **Naumann, M., T. Rudel, B. Wieland, C. Bartsch, and T. F. Meyer.** 1998. Coordinate activation of activator protein 1 and inflammatory cytokines in response to *Neisseria gonorrhoeae* epithelial cell contact involves stress response kinases. J. Exp. Med. **188:**1277-1286.

211. **Naumann, M., S. Wessler, and T. F. Meyer.** 1997. *Neisseria gonorrhoeae* epithelial cell interaction leads to the activation of the transcription factors nuclear factor kappaB and activator protein 1 and the induction of inflammatory cytokines. J. Exp. Med. **186:**247-258.

212. **Nguyen, D. H., A. D. Catling, D. J. Webb, M. Sankovic, L. A. Walker, A. V. Somlyo, M. J. Weber, and S. L. Gonias.** 1999. Myosin light chain kinase functions downstream of Ras/ERK to promote migration of urokinase-type plasminogen activator-stimulated cells in an integrin-selective manner. J. Cell Biol. **146:**149-164.

213. **Nusbaum, M. R., R. R. Wallace, L. M. Slatt, and E. C. Kondrad.** 2004. Sexually transmitted infections and increased risk of co-infection with human immunodeficiency virus. J. Am. Osteopath. Assoc. **104:**527-535.

214. **O'Callaghan, C. H., A. Morris, S. M. Kirby, and A. H. Shingler.** 1972. Novel method for detection of beta-lactamases by using a chromogenic cephalosporin substrate. Antimicrob. Agents Chemother. **1:**283-288.

215. **Otto, I. M., T. Raabe, U. E. Rennefahrt, P. Bork, U. R. Rapp, and E. Kerkhoff.** 2000. The p150-Spir protein provides a link between c-Jun N-terminal kinase function and actin reorganization. Curr. Biol. **10:**345-348.

216. **Paladino, S., T. Pocard, M. A. Catino, and C. Zurzolo.** 2006. GPI-anchored proteins are directly targeted to the apical surface in fully polarized MDCK cells. J. Cell. Biol. **172:**1023-1034.

217. **Parsons, N. J., J. R. Andrade, P. V. Patel, J. A. Cole, and H. Smith.** 1989. Sialylation of lipopolysaccharide and loss of absorption of bactericidal antibody

during conversion of gonococci to serum resistance by cytidine 5'-monophospho-N-acetyl neuraminic acid. Microb. Pathog. **7:**63-72.

218. **Patrone, J. B., S. E. Bish, and D. C. Stein.** 2006. TNF-alpha-independent IL-8 expression: alterations in bacterial challenge dose cause differential human monocytic cytokine response. J. Immunol. **177:**1314-1322.

219. **Pesci, E. C., D. L. Cottle, and C. L. Pickett.** 1994. Genetic, enzymatic, and pathogenic studies of the iron superoxide dismutase of *Campylobacter jejuni*. Infect. Immun. **62:**2687-2694.

220. **Philpott, D. J., S. E. Girardin, and P. J. Sansonetti.** 2001. Innate immune responses of epithelial cells following infection with bacterial pathogens. Curr. Opin. Immunol. **13:**410-416.

221. **Pierce, K. L., L. M. Luttrell, and R. J. Lefkowitz.** 2001. New mechanisms in heptahelical receptor signaling to mitogen activated protein kinase cascades. Oncogene **20:**1532-1539.

222. **Pils, S., T. Schmitter, F. Neske, and C. R. Hauck.** 2006. Quantification of bacterial invasion into adherent cells by flow cytometry. J. Microbiol. Methods **65:**301-310.

223. **Pizarro-Cerda, J., and P. Cossart.** 2006. Bacterial adhesion and entry into host cells. Cell **124:**715-727.

224. **Plaut, A. G., J. V. Gilbert, M. S. Artenstein, and J. D. Capra.** 1975. *Neisseria gonorrhoeae* and *Neisseria meningitidis*: extracellular enzyme cleaves human immunoglobulin A. Science **190:**1103-1105.

225. **Pohlner, J., R. Halter, K. Beyreuther, and T. F. Meyer.** 1987. Gene structure and extracellular secretion of *Neisseria gonorrhoeae* IgA protease. Nature **325:**458-462.

226. **Polishchuk, R., A. Di Pentima, and J. Lippincott-Schwartz.** 2004. Delivery of raft-associated, GPI-anchored proteins to the apical surface of polarized MDCK cells by a transcytotic pathway. Nat. Cell Biol. **6:**297-307.

227. **Popp, A., O. Billker, and T. Rudel.** 2001. Signal transduction pathways induced by virulence factors of *Neisseria gonorrhoeae*. Int. J. Med. Microbiol. **291:**307-314.

228. **Porat, N., M. A. Apicella, and M. S. Blake.** 1995. A lipooligosaccharide-binding site on HepG2 cells similar to the gonococcal opacity-associated surface protein Opa. Infect. Immun. **63:**2164-2172.

229. **Porat, N., M. A. Apicella, and M. S. Blake.** 1995. *Neisseria gonorrhoeae* utilizes and enhances the biosynthesis of the asialoglycoprotein receptor expressed on the surface of the hepatic HepG2 cell line. Infect. Immun. **63:**1498-1506.

230. **Pridmore, R. D.** 1987. New and versatile cloning vectors with kanamycin-resistance marker. Gene **56:**309-312.

231. **Pujol, C., E. Eugene, M. Marceau, and X. Nassif.** 1999. The meningococcal PilT protein is required for induction of intimate attachment to epithelial cells following pilus-mediated adhesion. Proc. Natl. Acad. Sci. USA **96:**4017-4022.

232. **Quayle, A. J.** 2002. The innate and early immune response to pathogen challenge in the female genital tract and the pivotal role of epithelial cells. J. Reprod. Immunol. **57:**61-79.

233. **Ram, S., D. P. McQuillen, S. Gulati, C. Elkins, M. K. Pangburn, and P. A. Rice.** 1998. Binding of complement factor H to loop 5 of porin protein 1A: a molecular mechanism of serum resistance of nonsialylated *Neisseria gonorrhoeae*. J. Exp. Med. **188:**671-680.

234. **Ramsey, K. H., H. Schneider, A. S. Cross, J. W. Boslego, D. L. Hoover, T. L. Staley, R. A. Kuschner, and C. D. Deal.** 1995. Inflammatory cytokines produced in response to experimental human gonorrhea. J. Infect. Dis. **172:**186-191.

235. **Ramsey, K. H., H. Schneider, R. A. Kuschner, A. F. Trofa, A. S. Cross, and C. D. Deal.** 1994. Inflammatory cytokine response to experimental human infection with *Neisseria gonorrhoeae*. Ann. N. Y. Acad. Sci. **730:**322-325.

236. **Rasmussen, H., P. Barrett, J. Smallwood, W. Bollag, and C. Isales.** 1990. Calcium ion as intracellular messenger and cellular toxin. Environ. Health Perspect. **84:**17-25.

237. **Rasmussen, H., C. M. Isales, R. Calle, D. Throckmorton, M. Anderson, J. Gasalla-Herraiz, and R. McCarthy.** 1995. Diacylglycerol production, Ca^{2+} influx, and protein kinase C activation in sustained cellular responses. Endocr. Rev. **16:**649-681.

238. **Ratledge, C., and L. G. Dover.** 2000. Iron metabolism in pathogenic bacteria. Annu. Rev. Microbiol. **54:**881-941.

239. **Rest, R. F., and W. M. Shafer.** 1989. Interactions of *Neisseria gonorrhoeae* with human neutrophils. Clin. Microbiol. Rev. **2 Suppl:**S83-S91.

240. **Roux, P. P., and J. Blenis.** 2004. ERK and p38 MAPK-activated protein kinases: a family of protein kinases with diverse biological functions. Microbiol. Mol. Biol. Rev. **68:**320-344.

241. **Rudel, T., I. Scheurerpflug, and T. F. Meyer.** 1995. *Neisseria* PilC protein identified as type-4 pilus tip-located adhesin. Nature **373:**357-359.

242. **Rudel, T., A. Schmid, R. Benz, H. A. Kolb, F. Lang, and T. F. Meyer.** 1996. Modulation of *Neisseria* porin (PorB) by cytosolic ATP/GTP of target cells: parallels between pathogen accommodation and mitochondrial endosymbiosis. Cell **85:**391-402.

243. **Rudel, T., J. P. van Putten, C. P. Gibbs, R. Haas, and T. F. Meyer.** 1992. Interaction of two variable proteins (PilE and PilC) required for pilus-mediated adherence of *Neisseria gonorrhoeae* to human epithelial cells. Mol. Microbiol. **6:**3439-3450.

244. **Sambrook, J. and D. W. Russell.** 2001. Molecular Cloning: A Laboratory Manual, 3rd ed, vol. 1. Cold Spring Harbor Press, Cold Spring Harbor, NY.

245. **Sanchez, A., M. J. Feito, and J. M. Rojo.** 2004. CD46-mediated costimulation induces a Th1-biased response and enhances early TCR/CD3 signaling in human CD4+ T lymphocytes. Eur. J. Immunol. **34:**2439-2448.

246. **Sandlin, R. C., M. A. Apicella, and D. C. Stein.** 1993. Cloning of a gonococcal DNA sequence that complements the lipooligosaccharide defects of *Neisseria gonorrhoeae* 1291d and 1291e. Infect. Immun. **61:**3360-3368.

247. **Savkovic, S. D., A. Ramaswamy, A. Koutsouris, and G. Hecht.** 2001. EPEC-activated ERK1/2 participate in inflammatory response but not tight junction barrier disruption. Am. J. Physiol. Gastrointest. Liver Physiol. **281:**G890-G898.

248. **Schliwa, M.** 1982. Action of cytochalasin D on cytoskeletal networks. J. Cell. Biol. **92:**79-91.

249. **Schmid, Y., G. A. Grassl, O. T. Buhler, M. Skurnik, I. B. Autenrieth, and E. Bohn.** 2004. *Yersinia enterocolitica* adhesin A induces production of interleukin-8 in epithelial cells. Infect. Immun. **72:**6780-6789.

250. **Schmidt, K. A., H. Schneider, J. A. Lindstrom, J. W. Boslego, R. A. Warren, L. Van de Verg, C. D. Deal, J. B. McClain, and J. M. Griffiss.** 2001. Experimental gonococcal urethritis and reinfection with homologous gonococci in male volunteers. Sex. Transm. Dis. **28:**555-564.

251. **Schmitter, T., S. Pils, S. Weibel, F. Agerer, L. Peterson, A. Buntru, K. Kopp, and C. R. Hauck.** 2007. Opa proteins of pathogenic Neisseriae initiate Src

kinase-dependent or lipid raft-mediated uptake via distinct human carcinoembryonic antigen-related cell adhesion molecule isoforms. Infect. Immun. **75:**4116-4126.

252. **Schneider, H., A. S. Cross, R. A. Kuschner, D. N. Taylor, J. C. Sadoff, J. W. Boslego, and C. D. Deal.** 1995. Experimental human gonococcal urethritis: 250 *Neisseria gonorrhoeae* MS11mkC are infective. J. Infect. Dis **172:**180-185.

253. **Schneider, H., J. M. Griffiss, J. W. Boslego, P. J. Hitchcock, K. M. Zahos, and M. A. Apicella.** 1991. Expression of paragloboside-like lipooligosaccharides may be a necessary component of gonococcal pathogenesis in men. J. Exp. Med. **174:**1601-1605.

254. **Schneider, H., T. L. Hale, W. D. Zollinger, R. C. Seid, C. A. Hammack, and J. M. Griffiss.** 1984. Heterogeneity of molecular size and antigenic expression within lipooligosaccharides of individual strains of *Neisseria gonorrhoeae* and *Neisseria meningitidis*. Infect. Immun. **45:**544-549.

255. **Schryvers, A. B., and B. C. Lee.** 1989. Comparative analysis of the transferrin and lactoferrin binding proteins in the family Neisseriaceae. Can. J. Microbiol. **35:**409-415.

256. **Schwarz-Linek, U., M. Hook, and J. R. Potts.** 2004. The molecular basis of fibronectin-mediated bacterial adherence to host cells. Mol. Microbiol. **52:**631-641.

257. **Segal, E., E. Billyard, M. So, S. Storzbach, and T. F. Meyer.** 1985. Role of chromosomal rearrangement in *N. gonorrhoeae* pilus phase variation. Cell **40:**293-300.

258. **Seib, K. L., H. J. Wu, S. P. Kidd, M. A. Apicella, M. P. Jennings, and A. G. McEwan.** 2006. Defenses against oxidative stress in *Neisseria gonorrhoeae*: a system tailored for a challenging environment. Microbiol. Mol. Biol. Rev. **70:**344-361.

259. **Sen, P., S. Mukherjee, D. Ray, and S. Raha.** 2003. Involvement of the Akt/PKB signaling pathway with disease processes. Mol. Cell. Biochem. **253:**241-246.

260. **Serino, L., B. Nesta, R. Leuzzi, M. R. Fontana, E. Monaci, B. T. Mocca, E. Cartocci, V. Masignani, A. E. Jerse, R. Rappuoli, and M. Pizza.** 2007. Identification of a new OmpA-like protein in *Neisseria gonorrhoeae* involved in the binding to human epithelial cells and in vivo colonization. Mol. Microbiol. **64:**1391-1403.

261. **Shaw, J. H., and S. Falkow.** 1988. Model for invasion of human tissue culture cells by *Neisseria gonorrhoeae.* Infect. Immun. **56:**1625-1632.

262. **Silva, O., E. Ferreira, M. Vaz Pato, M. Canica, and E. T. Gomes.** 2002. In vitro anti-*Neisseria gonorrhoeae* activity of *Terminalia macroptera* leaves. FEMS Microbiol. Lett. **217:**271-274.

263. **Singh, S., D. W. Powell, M. J. Rane, T. H. Millard, J. O. Trent, W. M. Pierce, J. B. Klein, L. M. Machesky, and K. R. McLeish.** 2003. Identification of the p16-Arc subunit of the Arp 2/3 complex as a substrate of MAPK-activated protein kinase 2 by proteomic analysis. J. Biol. Chem. **278:**36410-36417.

264. **Sokolova, O., N. Heppel, R. Jagerhuber, K. S. Kim, M. Frosch, M. Eigenthaler, and A. Schubert-Unkmeir.** 2004. Interaction of *Neisseria meningitidis* with human brain microvascular endothelial cells: role of MAP- and tyrosine kinases in invasion and inflammatory cytokine release. Cell. Microbiol. **6:**1153-1166.

265. **Soler-Garcia, A. A., and A. E. Jerse.** 2007. *Neisseria gonorrhoeae* catalase is not required for experimental genital tract infection despite the induction of a localized neutrophil response. Infect. Immun. **75:**2225-2233.

266. **Song, W., L. Ma, R. Chen, and D. C. Stein.** 2000. Role of lipooligosaccharide in Opa-independent invasion of *Neisseria gonorrhoeae* into human epithelial cells. J. Exp. Med. **191:**949-960.

267. **Spector, I., N. R. Shochet, Y. Kashman, and A. Groweiss.** 1983. Latrunculins: novel marine toxins that disrupt microfilament organization in cultured cells. Science **219:**493-495.

268. **Spence, J. M., and V. L. Clark.** 2000. Role of ribosomal protein L12 in gonococcal invasion of Hec1B cells. Infect. Immun. **68:**5002-5010.

269. **Spence, J. M., R. E. Tyler, R. A. Domaoal, and V. L. Clark.** 2002. L12 enhances gonococcal transcytosis of polarized Hec1B cells via the lutropin receptor. Microb. Pathog. **32:**117-125.

270. **Spence, M. R.** 1983. Gonorrhea. Clin. Obstet. Gynecol. **26:**111-124.

271. **Stein, D. C., F. E. Young, F. C. Tenover, and V. L. Clark.** 1983. Characterization of a chimeric beta-lactamase plasmid of *Neisseria gonorrhoeae* which can function in *Escherichia coli.* Mol. Gen. Genet. **189:**77-84.

272. **Stephens, D. S.** 1989. Gonococcal and meningococcal pathogenesis as defined by human cell, cell culture, and organ culture assays. Clin. Microbiol. Rev. **2 Suppl:**S104-S111.

273. **Stern, A., M. Brown, P. Nickel, and T. F. Meyer.** 1986. Opacity genes in *Neisseria gonorrhoeae*: control of phase and antigenic variation. Cell **47:**61-71.

274. **Swanson, J.** 1973. Studies on gonococcus infection. IV. Pili: their role in attachment of gonococci to tissue culture cells. J. Exp. Med. **137:**571-589.

275. **Swanson, K. V., G. A. Jarvis, G. F. Brooks, B. J. Barham, M. D. Cooper, and J. M. Griffiss.** 2001. CEACAM is not necessary for *Neisseria gonorrhoeae* to adhere to and invade female genital epithelial cells. Cell. Microbiol. **3:**681-691.

276. **Sykes, J. A., J. Whitescarver, P. Jernstrom, J. F. Nolan, and P. Byatt.** 1970. Some properties of a new epithelial cell line of human origin. J. Natl. Cancer Inst. **45:**107-122.

277. **Tan, X., R. Pearce-Pratt, and D. M. Phillips.** 1993. Productive infection of a cervical epithelial cell line with human immunodeficiency virus: implications for sexual transmission. J. Virol. **67:**6447-6452.

278. **Tang, P., C. L. Sutherland, M. R. Gold, and B. B. Finlay.** 1998. *Listeria monocytogenes* invasion of epithelial cells requires the MEK-1/ERK-2 mitogen-activated protein kinase pathway. Infect. Immun. **66:**1106-1112.

279. **Tayek, J. A., and G. L. Blackburn.** 1984. Goals of nutritional support in acute infections. Am. J. Med. **76:**81-90.

280. **Thomas, S. M., and J. S. Brugge.** 1997. Cellular functions regulated by Src family kinases. Annu. Rev. Cell Dev. Biol. **13:**513-609.

281. **Timmerman, M. M., J. Q. Shao, and M. A. Apicella.** 2005. Ultrastructural analysis of the pathogenesis of *Neisseria gonorrhoeae* endometrial infection. Cell. Microbiol. **7:**627-636.

282. **Totsukawa, G., Y. Wu, Y. Sasaki, D. J. Hartshorne, Y. Yamakita, S. Yamashiro, and F. Matsumura.** 2004. Distinct roles of MLCK and ROCK in the regulation of membrane protrusions and focal adhesion dynamics during cell migration of fibroblasts. J. Cell Biol. **164:**427-439.

283. **Tsai, C. M., and C. E. Frasch.** 1982. A sensitive silver stain for detecting lipopolysaccharides in polyacrylamide gels. Anal. Biochem. **119:**115-119.

284. **Turner, P. C., C. E. Thomas, C. Elkins, S. Clary, and P. F. Sparling.** 1998. *Neisseria gonorrhoeae* heme biosynthetic mutants utilize heme and hemoglobin as a heme source but fail to grow within epithelial cells. Infect. Immun. **66:**5215-5223.

285. **Turner, S., E. Reid, H. Smith, and J. Cole.** 2003. A novel cytochrome c peroxidase from *Neisseria gonorrhoeae*: a lipoprotein from a Gram-negative bacterium. Biochem. J. **373:**865-873.

286. **Vadlamudi, R. K., F. Li, L. Adam, D. Nguyen, Y. Ohta, T. P. Stossel, and R. Kumar.** 2002. Filamin is essential in actin cytoskeletal assembly mediated by p21-activated kinase 1. Nat. Cell Biol. **4:**681-690.

287. **van Putten, J. P.** 1993. Phase variation of lipopolysaccharide directs interconversion of invasive and immuno-resistant phenotypes of *Neisseria gonorrhoeae.* EMBO J. **12:**4043-4051.

288. **van Putten, J. P., T. D. Duensing, and J. Carlson.** 1998. Gonococcal invasion of epithelial cells driven by P.IA, a bacterial ion channel with GTP binding properties. J. Exp. Med. **188:**941-952.

289. **van Putten, J. P., T. D. Duensing, and R. L. Cole.** 1998. Entry of $OpaA^{+}$ gonococci into Hep-2 cells requires concerted action of glycosaminoglycans, fibronectin and integrin receptors. Mol. Microbiol. **29:**369-379.

290. **van Putten, J. P., and S. M. Paul.** 1995. Binding of syndecan-like cell surface proteoglycan receptors is required for *Neisseria gonorrhoeae* entry into human mucosal cells. EMBO J. **14:**2144-2154.

291. **Veale, D. R., M. Goldner, C. W. Penn, J. Ward, and H. Smith.** 1979. The intracellular survival and growth of gonococci in human phagocytes. J. Gen. Microbiol. **113:**383-393.

292. **Virji, M., K. Makepeace, D. J. Ferguson, and S. M. Watt.** 1996. Carcinoembryonic antigens (CD66) on epithelial cells and neutrophils are receptors for Opa proteins of pathogenic Neisseriae. Mol. Microbiol. **22:**941-950.

293. **Wang, J., S. D. Gray-Owen, A. Knorre, T. F. Meyer, and C. Dehio.** 1998. Opa binding to cellular CD66 receptors mediates the transcellular traversal of *Neisseria gonorrhoeae* across polarized T84 epithelial cell monolayers. Mol. Microbiol. **30:**657-671.

294. **Wang, J. A., T. F. Meyer, and T. Rudel.** 2007. Cytoskeleton and motor proteins are required for the transcytosis of *Neisseria gonorrhoeae* through polarized epithelial cells. Int. J. Med. Microbiol. (not archived).

295. **Ward, M. E., and P. J. Watt.** 1972. Adherence of *Neisseria gonorrhoeae* to urethral mucosal cells: an electron-microscopic study of human gonorrhea. J. Infect. Dis. **126:**601-605.

296. **Watson, R. O., and J. E. Galan.** 2005. Signal transduction in *Campylobacter jejuni*-induced cytokine production. Cell. Microbiol. **7:**655-665.

297. **Weel, J. F., C. T. Hopman, and J. P. van Putten.** 1991. Bacterial entry and intracellular processing of *Neisseria gonorrhoeae* in epithelial cells: immunomorphological evidence for alterations in the major outer membrane protein P.IB. J. Exp. Med. **174:**705-715.

298. **Weel, J. F., and J. P. van Putten.** 1991. Fate of the major outer membrane protein P.IA in early and late events of gonococcal infection of epithelial cells. Res. Microbiol. **142:**985-993.

299. **Westphal, O., K. Jann, and K. Himmelspach.** 1983. Chemistry and immunochemistry of bacterial lipopolysaccharides as cell wall antigens and endotoxins. Prog. Allergy **33:**9-39.

300. **White, L. A., and D. S. Kellogg, Jr.** 1965. *Neisseria gonorrhoeae* identification in direct smears by a fluorescent antibody-counterstain method. Appl. Microbiol. **13:**171-174.

301. **Whiteway, J., P. Koziarz, J. Veall, N. Sandhu, P. Kumar, B. Hoecher, and I. B. Lambert.** 1998. Oxygen-insensitive nitroreductases: analysis of the roles of *nfsA* and *nfsB* in development of resistance to 5-nitrofuran derivatives in *Escherichia coli*. J. Bacteriol. **180:**5529-5539.

302. **Wiesenfeld, H. C., S. L. Hillier, M. A. Krohn, A. J. Amortegui, R. P. Heine, D. V. Landers, and R. L. Sweet.** 2002. Lower genital tract infection and endometritis: insight into subclinical pelvic inflammatory disease. Obstet. Gynecol. **100:**456-463.

303. **Williams, J. M., G. C. Chen, L. Zhu, and R. F. Rest.** 1998. Using the yeast two-hybrid system to identify human epithelial cell proteins that bind gonococcal Opa proteins: intracellular gonococci bind pyruvate kinase via their Opa proteins and require host pyruvate for growth. Mol. Microbiol. **27:**171-186.

304. **Witt, K., D. R. Veale, H. Finch, C. W. Penn, D. Sen, and H. Smith.** 1976. Resistance of *Neisseria gonorrhoeae* grown in vivo to ingestion and digestion by phagocytes of human blood. J. Gen. Microbiol. **96:**341-350.

305. **Woo, M. S., Y. Ohta, I. Rabinovitz, T. P. Stossel, and J. Blenis.** 2004. Ribosomal S6 kinase (RSK) regulates phosphorylation of filamin A on an important regulatory site. Mol. Cell Biol. **24:**3025-3035.

306. **Workowski, K. A., and S. M. Berman.** 2006. Sexually transmitted diseases treatment guidelines, 2006. MMWR Recomm. Rep. **55:**1-94.

307. **Wu, H. J., K. L. Seib, J. L. Edwards, M. A. Apicella, A. G. McEwan, and M. P. Jennings.** 2005. Azurin of pathogenic *Neisseria* spp. is involved in defense against hydrogen peroxide and survival within cervical epithelial cells. Infect. Immun. **73:**8444-8448.

308. **Wu, H. J., K. L. Seib, Y. N. Srikhanta, S. P. Kidd, J. L. Edwards, T. L. Maguire, S. M. Grimmond, M. A. Apicella, A. G. McEwan, and M. P. Jennings.** 2006. PerR controls Mn-dependent resistance to oxidative stress in *Neisseria gonorrhoeae*. Mol. Microbiol. **60:**401-416.

309. **Zheng, H. Y., T. M. Alcorn, and M. S. Cohen.** 1994. Effects of H_2O_2-producing lactobacilli on *Neisseria gonorrhoeae* growth and catalase activity. J. Infect. Dis. **170:**1209-1215.

310. **Zheng, H. Y., D. J. Hassett, K. Bean, and M. S. Cohen.** 1992. Regulation of catalase in *Neisseria gonorrhoeae*. Effects of oxidant stress and exposure to human neutrophils. J. Clin. Invest. **90:**1000-1006.

311. **Zhong, B., P. Tien, and H. B. Shu.** 2006. Innate immune responses: crosstalk of signaling and regulation of gene transcription. Virology **352:**14-21.

312. **Zlokarnik, G., P. A. Negulescu, T. E. Knapp, L. Mere, N. Burres, L. Feng, M. Whitney, K. Roemer, and R. Y. Tsien.** 1998. Quantitation of transcription and clonal selection of single living cells with beta-lactamase as reporter. Science **279:**84-88.